FACILITATING MULTI-ELECTRON REACTIVITY AT LOW-COORDINATE COBALT COMPLEXES USING REDOX-ACTIVE LIGANDS

A Thesis
Presented to
The Academic Faculty

by

Aubrey L. Smith

In Partial Fulfillment
of the Requirements for the Degree
Doctorate in the
School of Chemistry and Biochemistry

Georgia Institute of Technology
December, 2011

FACILITATING MULTI-ELECTRON REACTIVITY AT LOW-COORDINATE COBALT COMPLEXES USING REDOX-ACTIVE LIGANDS

Approved by:

Dr. Jake D. Soper, Advisor
School of Chemistry and Biochemistry
Georgia Institute of Technology

Dr. L. Andrew Lyon
School of Chemistry and Biochemistry
Georgia Institute of Technology

Dr. E. Kent Barefield
School of Chemistry and Biochemistry
Georgia Institute of Technology

Dr. Christopher W. Jones
School of Chemical and Biomolecular Engineering
Georgia Institute of Technology

Dr. Z. John Zhang
School of Chemistry and Biochemistry
Georgia Institute of Technology

Date Approved: August 16, 2011

ACKNOWLEDGEMENTS

Throughout this journey, the list is long of those who deserve acknowledgement and thanks. First, great appreciation goes to my advisor, Professor Jake D. Soper, for five years of advice, guidance and support. I hope I am a better chemist for all you have taught me. Words cannot express the recognition which “the group” deserves. My friendship formed with Clarence Rolle, Michael Bayless, and Cameron Lippert made each day more enjoyable and successful. Many thanks for your support which ranged from scientific advice and collaboration to comic relief and a shoulder to lean on. To my life-long friend, Kris Hammitt, countless thanks for always making me laugh, standing beside me throughout the years, and giving me valuable outside perspective on the real priorities in life. My sister, Ashley Smith, deserves immeasurable gratitude for always listening to all my “boring chemistry”. I count myself lucky that you are not only my sister but became my best friend. My parents Terry and Beverly Smith built a solid and valuable foundation on which I could grow. They then trusted me to find my own way through life. For this I became who I am and will spend the rest of my life trying to express my appreciation. And finally to my husband, Dean Shahriari, my most heartfelt thanks goes to you for always being there for me on good days and bad, for keeping me focused on the end goal, reminding me I could succeed when I doubted myself, and for helping me be the person and make the life I want to have. You each helped me reach my goals and without you, I would not have completed this process and presented this body of work today.

TABLE OF CONTENTS

LIST OF TABLES

LIST OF FIGURES

LIST OF SYMBOLS AND ABBREVIATIONS

NMR	Nuclear magnetic resonance
EPR	Electron paramagnetic resonance
UV-vis	Ultraviolet-visible
FTIR	Fourier transform infrared spectroscopy
MS	Mass spectrometery
FAB	Fast atom bombardment
ESI	Electrospray ionization
EI	Electron impact
GC	Gas chromatography
LC	Liquid chromatography
CV	Cyclic voltammetry
L	Ligand
ap^{2-}	Amidodphenolate
isq^{1-}	Iminosemiquinonate
ibq	Imidobenzoquinone
cat^{2-}	Catecholate
sq^{1-}	Semiquninonate
q	Quinone
triphos	Bis(diphenylphosphineoethyl)phenylphosphine
dppe	Bis(diphenylphosphino)ethane

Tp^{1-}	Trispyrazolylborate
Me	Methyl
Et	Ethyl
nPr	n-propyl
iPr	Isopropyl
tBu	Tertbutyl
Pn	Pentyl
Hx	Hexyl
Oc	Octyl
Fc	Ferrocene
THF	Tetrahydrofuran
MeOH	Methanol
DMSO	Dimethyl sulfoxide
SCE	Saturated calomel electrode
TMS	Tetramethylsilane
^{o}C	degrees Celcius
ppm	parts per million
λ	wavelength
K	Kelvin
V	Volts
M	Molar
Å	Angstrom

s	second
MHz	megahertz
mL	milliliters
μL	microliters
δ	Chemical shift
^{1}H	Proton
ε	Molar absorbtivity
z	Effective charge
DFT	Density functional theory
MO	Molecular orbital
HOMO	Highest occupied molecular orbital
LUMO	Lowest unoccupied molecular orbital
ET	Electron transfer
CT	Charge transfer
LLCT	Ligand-to-ligand charge transfer
MLCT	Metal-to-ligand charge transfer
obs	Observed
equiv	equivalent

Summary

Herein, I describe a detailed investigation or the preparation and reactive chemistry of cobalt complexes containing redox-active ligands. In the first part of this study, I have prepared an electron transfer series of complexes in three oxidation states (Figure 6.1): $[Co^{III}(ap^{Ar})_2]^-$, $Co^{III}(isq^{Ar})(ap^{Ar})$, and $[Co^{III}(CH_3CN)(isq^{Ar})_2]^+$. Characterization according to the bond lengths within the ligands of all three of these complexes show that the metal center remains cobalt(III) through the redox changes and indicates that the oxidation state changes occur with gain or loss of electrons from the ligand set.

In a proof-of-concept study, I show that ligand-derived electrons can be use to make cobalt-halide bonds. With this examination, I demonstrate that while $Co^{III}(isq)(ap)$ reacts with halide radicals to form a new cobalt-halide bond in a single electron reaction, $[Co^{III}(ap)_2]^-$ undergoes a multi-electron reaction with sources of "Cl^+". Both reactions result in the previously reported and characterized $Co^{III}(Cl)(isq)_2$ indicating that the electrons used to form the new bond are derived from the ligand set. Mechanistic studies of the net two electron reaction with $[Co^{III}(ap)_2]^-$ showed no evidence of the reaction proceeding through sequential radical steps but suggest a single, two electron step is responsible for the bond-formation. Similarly, $[Co^{III}(ap)_2]^-$ reacts with alkyl halides. The product of the reaction can be isolated and fully characterized and was found to be best assigned as $Co^{III}(R)(isq)_2$. This assignment indicates that the new cobalt-carbon bond is formed with two electrons formally deriving from the ligand set and with no change in oxidation state at the metal center. Mechanistic investigations of the pseudo-oxidative addition suggest the reaction is S_N2-like.

This activation of alkyl halides represents a step often difficult in cross-coupling reactions facilitated by traditional palladium catalysts. Reaction of $Co^{III}(R)(isq)_2$ with RZnX forms a new carbon-carbon bond. Similarly, the two electron oxidized complex $[Co^{III}(CH_3CN)(isq)_2]^+$ reacts with organozinc reagents to couple two carbon nucleophiles and form a new carbon-carbon bond. Both reactions proceed with both sp^2 and sp^3 carbon nucleophiles. When followed substoichiometrically, the homocoupling reaction can be observed to form the five-coordinate organometallic complex isolated from the reaction of $[Co^{III}(ap)_2]^-$ with alkyl halides. This indicates that after the first alkyl or aryl is installed on the $[Co^{III}(CH_3CN)(isq)_2]^+$, the homocoupling and cross-coupling reactions proceed by the same method.

However, both reactions have low yields. The yield of the cross-coupling reaction is decreased by increased steric bulk around the metal center created by substituents on the ligand. Investigation of the homocoupling reaction indicates that while the added steric congestion surrounding the metal center disfavors the addition of the first alkyl fragment, the addition of the second alkyl fragment and subsequent rapid elimination of the coupling product is almost completely inhibited. This result also implies that the coupling of the two alkyl fragments is entirely inner-sphere requiring installation of both for coupling organic fragments on the same cobalt center prior to coupling to form the new carbon-carbon bond.

In a complementary study, use of bidentate or tridentate stabilizing ligands in combination with one redox-active catechol-derived or amidophenol-derived ligand was investigated. With the synthesis of (triphos)Co^{II}(cat) and the one electron oxidized $[(triphos)Co^{II}(sq)]^+$ I found that the electronic structure of the cation had been previously

mis-assigned. Oxidation occurs at the ligand and not the metal. Reaction of (triphos)Co^{II}(cat) with a "Cl^{+}" reagent generated a new material which I tentatively describe as (triphos)Co^{III}(Cl)(sq). This implies that the two electrons used to create the new cobalt-halide bond are derived from both the ligand and the metal, one from each. I believe the complex is unreactive with organic halides due to the steric bulk surrounding the metal center. Attempts to prepare similar cobalt complexes containing tridentate or bidentate phosphine ligands or a tridentate pyrazol ligand in combination with a catechol-derived or amidophenol-derived ligand were unsuccessful because they produced materials prone to ligand redistribution.

The sum of these studies shows that the amidophenol ligands can act as an electron reservoir and facilitate reactivity at the metal center. I have also shown that this combination can create a proclivity to facilitate multi-electron reactions at the metal that is naturally prone to radical reactions. Throughout the course of both of these studies, steric crowding at the metal center is a problem disfavoring the facilitated reactivity. The factor limiting use of the catalysis is steric crowding.

Background and introduction

1.1. Carbon-carbon coupling reactions

One of the most powerful tools a synthetic chemist relies on every day is the ability to assemble complex molecules from simple precursors. To accomplish this goal, bonds within precursors must be broken and new bonds must be formed to join the reactants. Bond forming reactions make up some of the tools used for synthesis of natural products, small molecule design, and new material development. Over the past half century, an extensive number of ways to selectively assemble carbon-carbon bonds have been examined.[1,2] If reactions are not facilitated in a selective and controlled manor, the costs of resources and time needed to isolate desired products can be huge. Side products, isomers and enantiomers formed in the synthetic process create the need for isolation and purification of the material before its use.

Two particular types of coupling reactions have been examined extensively. First, the reaction of organic halides with carbon nucleophiles is commonly used in the assembly of complex molecules.[1,3-8] Carbon nucleophiles can be derived from several sources including organolithiums (LiR), Grignard reagents (RMgX) and organozinc reagents (RZnX). The use of an organozinc as the carbanion source to couple with organic halides is known as Negishi-coupling[8] and this choice of carbanion source provides several benefits.[9] Organozinc reagents are not as strongly nucleophilic as other organometallic sources and are therefore tolerant of a variety of functional groups. However, the decreased nucleophilicity makes them less reactive with certain catalysts as well. These reactions were first reported catalyzed by nickel and later, more

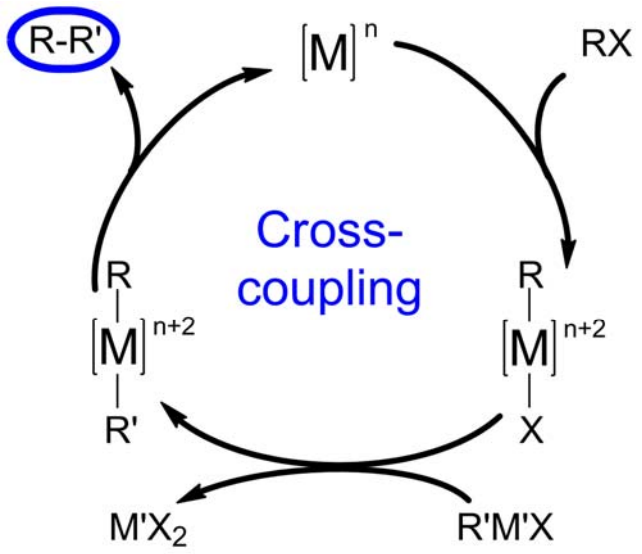

Scheme 1.1

efficiently, by palladium.[6,8,10] Negishi-type coupling occurs through, first, oxidative addition of the organic halide at the metal center, followed by transmetallation of the carbanion and completed with reductive elimination of the product (Scheme 1.1).[11] However, alkyl halides are often unsuitable reactants with these methods as the oxidative addition reaction is slow and palladium is known to β-hydride eliminate after addition of the sp^3 carbon to the metal center.[12] Ligand selection or use of alkyl halides without β-hydrogen atoms can minimize this degradation pathway.[7,11] Extensive mechanistic studies have been done to understand the unique nature of the reactions on palladium.[1,3,6] These suggest that the reaction occurs by two electron steps and proceeds without observation of radical intermediate species.

Oxidative coupling reactions are another useful carbon-carbon bond-forming method.[1,13-15] These reactions can join two carbon nucleophiles such as carbanions and, with the use of a sacrificial oxidant, complete the catalytic coupling cycle. The first step

in this reaction is transmetallation from RMX installing the first organic fragment on the metal. This is followed by a second transmetallation, a reductive elimination and finally a two electron oxidation of the catalyst to reset the process (Scheme 1.2).[14] Selection of the oxidant can be very important as reaction of the organic nucleophiles directly with the oxidant can lead to unwanted side products.[14] Readily available oxygen from the air is considered an ideal oxidant requiring no prior processing and resulting in safer waste products than other available sacrificial oxidants.[12]

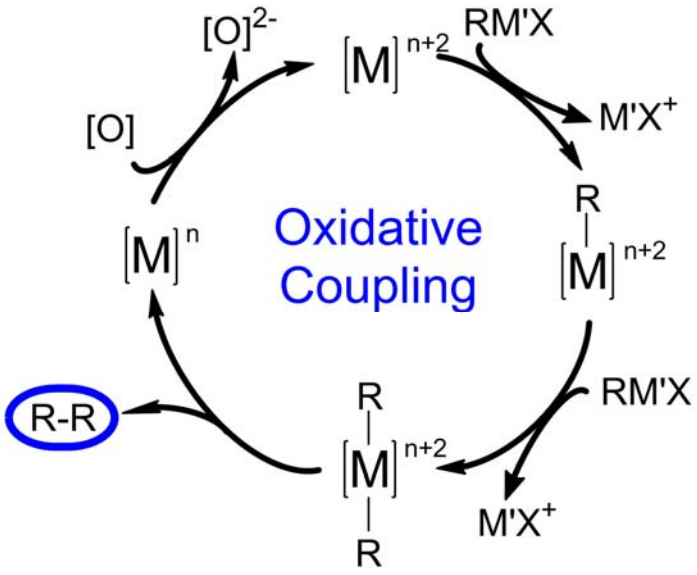

Scheme 1.2

Development of new catalysts able to address some of these limitations for these coupling reactions has been the focus of much effort throughout the past decades. Use of first row transition metal salts for these reactions is becoming more prevalent in the literature.[3,5,16-18] However, catalytic conditions are generally optimized with the addition of co-catalysts. These are often used without a clear understanding of their role in the system and with little known about the active catalytic species. Mechanisms developed

from the palladium coupling systems are often applied to the metal salt systems, despite the established knowledge that first row transition metals react quite differently than second and third row metals. Without a clear understanding of how multi-electron reactivity can be facilitated by first row transition metals and investigation of the mechanism of these reactions, new catalyst design is limited by a factor of time and luck required to find an ideal system.

1.2. Design and characterization of redox-active ligands

Nature uses first row transition metals to facilitate various the bond-making and bond-breaking reactions needed to sustain life.[19] Some of these reactions are facilitated by metalloproteins that often require coenzymes and co-catalysts to control the desired reactivity and produce the correct product.[19,20] These support molecules are frequently a way to store and deliver electrons needed to facilitate reactions. It has been demonstrated in several systems that organic radicals in the active site facilitate the reactivity at the metal center.[19-21]

This strategy of using organic molecules to store and deliver electrons for reactivity at a first row transition metal center can be extended into small molecule catalyst design as well. For fifty years, ligands known as “non-innocent” have been studied to establish an understanding of how these ligands coordinate to metal centers in various oxidation states.[22-26] Non-innocent ligands are able to support oxidation state changes themselves, thus becoming a potential source of electrons and can even stabilize atypical metal electronic configurations. After the first report by Jørgenson of the non-innocent dithiolene ligand,[27] the field has been expanded to also include

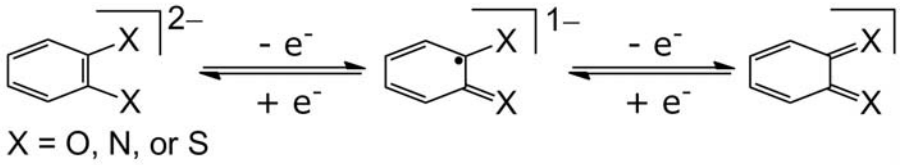

Scheme 1.3

catecholates, diimines and a variety of combinations of disubsituted benzene derivatives.[22,28] The majority of these complexes rely on S, N or O atoms to coordinate to the metal and all contain a π-electron system (Scheme 1.3). In certain complexes, these ligands can also actively participate in the reactivity of the complex, thus being classified as "redox-active".[22] This requires that the metal and ligand frontier orbitals have favorable mixing and similar energies to allow movement of the electrons through the complex. In recent studies, several of these complexes have been shown to contain ligands which are the site of the oxidation and reduction of the complex, as opposed to the oxidation state change occurring at the metal center.[29,30]

Within a stable complex, metals and ligands can exist in a cooperative balance of electron sharing though charge. The degree with which electrons are delocalized across metal and ligand orbitals is dependent on the overlap of the molecular orbitals of each atom.[31,32] This delocalization can be classified using the Robin-Day system,[33,34] defining Class I as a fully localized system in which a radical is contained within a particular orbital. Class III is fully delocalized with the radical spread equally through the complex. The degree with which the measurable characteristics of the ligands, such as bond lengths and charge transfer bands, change with modification of the oxidation state largely depends on the extent of delocalization.[34,35]

A basis for the characterization of these redox-active ligands and assignment of their oxidation state has taken decades to develop. Extensive research has been done with the ligands on a multitude of metals with a variety of spectroscopic techniques.[22,25,35] Assignment of the oxidation state of the metal and ligands within the complexes relies on a combination of spectroscopic techniques and is often supported by theoretical calculations. Electron paramagnetic resonance (EPR) can be a useful indicator of the electronics of the complex and can help determine if a radical is localized on either the metal or ligand. In systems not favorable for investigation by EPR or fully delocalized systems, structural data can give clues to the oxidation state of the ligands as well. Assignment of oxidation state of ligands using X-ray crystallographic data is a technique developed by both Pierpont and Wieghardt over decades.[24,25,36] After gathering data on electronic series of various complexes containing different ligands coordinated to different metals, general parameters for defining the oxidation state assignment of ligands have been established based on the observed bond lengths within the π-system.[24,36,35]

Several small molecules containing redox-active ligands have been recently shown to facilitate enzyme-like bond-breaking or bond-making reactions.[37-40] The degree to which electrons derived from the ligand set participate in the reactivity varies by system. The choice of metal and ligand are important to obtain a successful balance of delocalization allowing the electrons of the metal and ligand to mix while preserving a stable coordination complex. DFT calculations indicate that the HOMO of cobalt bis-dithiolate complexes are an ideal 50% ligand-50% metal mix.[35,41] This makes cobalt an ideal choice to have the desired molecular orbital overlap to facilitate reactivity with

participation from all ligands. However, dithiolate ligands are most reactive at the sulfur atom and are not ideal for use when targeting reactivity at the metal center.[22,35,42] Diimine and catecholate ligands have been extensively studied as ligands for cobalt complexes.[43-46] The more recently reported hybrid of these, the amidophenolate ligand, shows potential for favorable overlap with cobalt as well.[23,47] Several amidophenol-derived complexes have been reported and structurally characterized on a variety of metals.[45,48] Examples of the aminophenol-derived ligands facilitating bond-breaking and bond-making reactivity have also been reported.[49-51]

1.3. Project aim

Many bond-forming coupling reactions are performed at 4d and 5d metals but use of 3d metals has only recently been demonstrated.[1,5,17] However, first row transition metals have a natural proclivity to participate in one electron redox changes often making their use as coupling catalysts unselective and relying on radical type reactivity. With this project, we investigated the possibility of harnessing the usefulness of redox-active ligands for multi-electron reactivity at cobalt. We believed that through appropriate molecular orbital overlap between cobalt and amidophenolate or catecholate ligands, the electrons stored and delivered by these ligands could participate in bond-breaking and bond–making activity at the metal center. We expect that the stability afforded by these ligands would allow us to perform mechanistic investigations to understand the complexes and how their characteristics influence the reaction mechanism. All of these goals ultimately form the basis for development of new carbon-carbon coupling reactions using cobalt.

1.4. References

1. Diederich, F.; Stang, P. J.; Editors, *Metal-catalyzed Cross-coupling Reactions*. Wiley-VCH: 1998; p 517.

2. Molnar, A., Efficient, Selective, and Recyclable Palladium Catalysts in Carbon-Carbon Coupling Reactions. *Chem. Rev.* **2011,** *111*, 2251-2320.

3. Frisch, A. C.; Beller, M., Catalysts for cross-coupling reactions with non-activated alkyl halides. *Angew. Chem., Int. Ed.* **2005,** *44*, 674-688.

4. Adrio, J.; Carretero, J. C., Functionalized Grignard Reagents in Kumada Cross-Coupling Reactions. *ChemCatChem* **2010,** *2*, 1384-1386.

5. Sherry, B. D.; Fuerstner, A., The Promise and Challenge of Iron-Catalyzed Cross Coupling. *Acc. Chem. Res.* **2008,** *41*, 1500-1511.

6. Brennfuehrer, A.; Neumann, H.; Beller, M., Palladium-Catalyzed Carbonylation Reactions of Aryl Halides and Related Compounds. *Angew. Chem., Int. Ed.* **2009,** *48*, 4114-4133.

7. Terao, J.; Kambe, N., Cross-Coupling Reaction of Alkyl Halides with Grignard Reagents Catalyzed by Ni, Pd, or Cu Complexes with π-Carbon Ligand(s). *Acc. Chem. Res.* **2008,** *41*, 1545-1554.

8. Negishi, E.-i., Magical Power of Transition Metals: Past, Present, and Future. *Nobel Lecture* **2010**.

9. Erdik, E.; Editor, *Organozinc Reagents in Organic Synthesis*. CRC: 1996; p 464

10. Phapale, V. B.; Cardenas, D. J., Nickel-catalyzed Negishi cross-coupling reactions: scope and mechanisms. *Chem. Soc. Rev.* **2009,** *38*, 1598-1607.

11. Negishi, E.-i.; Hu, Q.; Huang, Z.; Wang, G.; Yin, N. In *Palladium- or nickel-catalyzed cross-coupling reactions with organozincs and related organometals*, John Wiley & Sons Ltd.: 2006; 457-553.

12. Liu, C.; Jin, L.; Lei, A., Transition-metal-catalyzed oxidative cross-coupling reactions. *Synlett* **2010**, 2527-2536.

13. Liu, C.; Zhang, H.; Shi, W.; Lei, A., Bond formations between two nucleophiles: Transition metal catalyzed oxidative cross-coupling reactions. *Chem. Rev.* **2011,** *111*, 1780-1824.

14. Shi, W.; Liu, C.; Lei, A., Transition-metal catalyzed oxidative cross-coupling reactions to form C-C bonds involving organometallic reagents as nucleophiles. *Chem. Soc. Rev.* **2011,** *40*, 2761-2776.

15. Zhao, Y.; Wang, H.; Hou, X.; Hu, Y.; Lei, A.; Zhang, H.; Zhu, L., Oxidative Cross-Coupling through Double Transmetallation: Surprisingly High Selectivity for Palladium-Catalyzed Cross-Coupling of Alkylzinc and Alkynylstannanes. *J. Am. Chem. Soc.* **2006,** *128*, 15048-15049.

16. Czaplik, W. M.; Mayer, M.; Cvengros, J.; Jacobi, v. W. A., Coming of Age: Sustainable Iron-Catalyzed Cross-Coupling Reactions. *ChemSusChem* **2009,** *2*, 396-417.

17. Cahiez, G.; Moyeux, A., Cobalt-Catalyzed Cross-Coupling Reactions. *Chem. Rev.* **2010,** *110*, 1435-1462.

18. Rudolph, A.; Lautens, M., Secondary alkyl halides in transition-metal-catalyzed cross-coupling reactions. *Angew. Chem., Int. Ed.* **2009,** *48*, 2656-2670.

19. Silverman, R. B., *The organic chemistry of enzyme-catalyzed reactions*. Academic Press: San Diego, CA, 2000.

20. Kruger, H. J., What can we learn from Nature about the reactivity of coordinatied phenoxyl radicals? - A bioinorganic success story. *Angew. Chem., Int. Ed.* **1999,** *38*, 672-631.

21. Whittaker, J. W., Free radicals catalysis by galactose oxidase. *Chem. Rev.* **2003,** *103*, 2347-2363.

22. Butin, K. P.; Beloglazkina, E. K.; Zyk, N. V., Metal complexes with non-innocent ligands. *Russ. Chem. Rev.* **2005,** *74*, 531-553.

23. Poddel'sky, A. I.; Cherkasov, V. K.; Abakumov, G. A., Transition metal complexes with bulky 4,6-di-tert-butyl-N-aryl(alkyl)-o-iminobenzoquinonato ligands: Structure, EPR and magnetism. *Coord. Chem. Rev.* **2009,** *253*, 291-324.

24. Pierpont, C. G.; Lange, C. W., The chemistry of transition metal complexes containing catechol and semiquinone ligands. *Prog. Inorg. Chem.* **1994,** *41*, 331-442.

25. Pierpont, C. G., Studies on charge distribution and valence tautomerism in transition metal complexes of catecholate and semiquinonate ligands. *Coord. Chem. Rev.* **2001,** *216-217*, 99-125.

26. Lu, C. C.; Bill, E.; Weyhermueller, T.; Bothe, E.; Wieghardt, K., Neutral bis(α-iminopyridine)metal complexes of the first-row transition ions (Cr, Mn, Fe, Co, Ni, Zn) and their monocationic analogues: mixed valency involving a redox noninnocent ligand system. *J. Am. Chem. Soc.* **2008,** *130*, 3181-3197.

27. Jorgensen, C. K., Difference between the four halide ligand, and discussion remarks on trigonal-bipyramidal complexes, on oxidation states, and on diagonal elements of one-electron energy. *Coord. Chem. Rev.* **1966**, 164.

28. Muresan, N.; Lu, C. C.; Ghosh, M.; Peters, J. C.; Abe, M.; Henling, L. M.; Weyhermoeller, T.; Bill, E.; Wieghardt, K., Bis(α-diimine)iron complexes: electronic structure determination by spectroscopy and broken symmetry density functional theoretical calculations. *Inorg. Chem.* **2008,** *47*, 4579-4590.

29. Khusniyarov, M. M.; Bill, E.; Weyhermueller, T.; Bothe, E.; Wieghardt, K., Hidden Noninnocence: Theoretical and Experimental Evidence for Redox Activity of a β-Diketiminate(1-) Ligand. *Angew. Chem., Int. Ed.* **2011,** *50*, 1652-1655.

30. Bowman, A. C.; Milsmann, C.; Hojilla, A. C. C.; Lobkovsky, E.; Wieghardt, K.; Chirik, P. J., Synthesis and Molecular and Electronic Structures of Reduced Bis(imino)pyridine Cobalt Dinitrogen Complexes: Ligand versus Metal Reduction. *J. Am. Chem. Soc.* **2010,** *132*, 1676-1684.

31. Demadis, K. D.; Hartshorn, C. M.; Meyer, T. J., The localized-to-delocalized transition in mixed-valence chemistry. *Chem. Rev.* **2001,** *101*, 2655-2685.

32. Evangelio, E.; Ruiz-Molina, D., Valence tautomerism: More actors than just electroactive ligands and metal ions. *C. R. Chim.* **2008,** *11*, 1137-1154.

33. Robin, M. B.; Day, P., Mixed valence chemistry. A survey and classification. *Advan. Inorg. Chem. Radiochem.* **1967,** *10*, 247-422.

34. Evangelio, E.; Ruiz-Molina, D., Valence tautomerism: New challenges for electroactive ligands. *Eur. J. Inorg. Chem.* **2005**, 2957-2971.

35. Ray, K.; Petrenko, T.; Wieghardt, K.; Neese, F., Joint spectroscopic and theoretical investigations of transition metal complexes involving non-innocent ligands. *J. Chem. Soc., Dalton Trans.* **2007**, 1552-1566.

36. Chun, H.; Verani, C. N.; Chaudhuri, P.; Bothe, E.; Bill, E.; Weyhermueller, T.; Wieghardt, K., Molecular and Electronic Structure of Octahedral o-Aminophenolato and o-Iminobenzosemiquinonato Complexes of V(V), Cr(III), Fe(III), and Co(III). Experimental Determination of Oxidation Levels of Ligands and Metal Ions. *Inorg. Chem.* **2001,** *40*, 4157-4166.

37. Rolle, C. J.; Hardcastle, K. I.; Soper, J. D., Reactions of tetrabromocatecholatomanganese(III) complexes with dioxygen. *Inorg. Chem.* **2008,** *47*, 1892-1894.

38. Barbaro, P.; Bianchini, C.; Linn, K.; Mealli, C.; Meli, A.; Vizza, F.; Laschi, F.; Zanello, P., Dioxygen uptake and transfer by cobalt(III), rhodium(III) and iridium(III) catecholate complexes. *Inorg. Chim. Acta* **1992,** *198-200*, 31-56.

39. Chaudhuri, P.; Hess, M.; Mueller, J.; Hildenbrand, K.; Bill, E.; Weyhermueller, T.; Wieghardt, K., Aerobic Oxidation of Primary Alcohols (Including Methanol) by Copper(II)- and Zinc(II)-Phenoxyl Radical Catalysts. *J. Am. Chem. Soc.* **1999,** *121*, 9599-9610.

40. Lippert, C. A.; Arnstein, S. A.; Sherrill, C. D.; Soper, J. D., Redox-Active Ligands Facilitate Bimetallic O2 Homolysis at Five-Coordinate Oxorhenium(V) Centers. *J. Am. Chem. Soc.* **2010,** *132*, 3879-3892.

41. Bill, E.; Bothe, E.; Chaudhuri, P.; Chlopek, K.; Herebian, D.; Kokatam, S.; Ray, K.; Weyhermueller, T.; Neese, F.; Wieghardt, K., Molecular and electronic structure of four- and five-coordinate cobalt complexes containing two o-phenylenediamine- or two o-aminophenol-type ligands at various oxidation levels: An experimental, density functional, and correlated ab initio study. *Chem. Eur. J.* **2005,** *11*, 204-224.

42. Ray, K.; Bill, E.; Weyhermuller, T.; Wieghardt, K., Redox-noninnocence of the S,S'-coordinated ligands in bis(benzene-1,2-dithiolato)iron complexes. *J. Am. Chem. Soc.* **2005,** *127*, 5641-54.

43. Adams, D. M.; Dei, A.; Rheingold, A. L.; Hendrickson, D. N., Bistability in the [CoII(semiquinonate)2] to [CoIII(catecholate)(semiquinonate)] valence-tautomeric conversion. *J. Am. Chem. Soc.* **1993,** *115*, 8221-8229.

44. Verani, C. N.; Gallert, S.; Bill, E.; Weyhermuller, T.; Wieghardt, K.; Chaudhuri, P., [Tris(o-iminosemiquinone)cobalt(III)] - a radical complex with an St = 3/2 ground state. *Chem. Comm.* **1999**, 1747-1748.

45. Herebian, D.; Ghosh, P.; Chun, H.; Bothe, E.; Weyhermuller, T.; Wieghardt, K., Cobalt(II)/(III) complexes containing o-iminothiobenzosemiquinonato(1-) and o-iminobenzosemiquinonato(1-) π-radical ligands. *Eur. J. Inorg. Chem.* **2002**, 1957-1967.

46. Shay, D. T.; Yap, G. P. A.; Zakharov, L. N.; Rheingold, A. L.; Theopold, K. H., Intramolecular C-H activation by an open-shell cobalt(III) imido complex. *Angew. Chem., Int. Ed.* **2005,** *44*, 1508-1510.

47. Abakumov, G. A.; Druzhkov, N. O.; Kurskii, Y. A.; Shavyrin, A. S., NMR study of products of thermal transformation of substituted N-aryl-o-quinoneimines. *Russ. Chem. Bull.* **2003,** *52*, 712-717.

48. Poddel'sky, A. I.; Cherkasov, V. K.; Fukin, G. K.; Bubnov, M. P.; Abakumova, L. G.; Abakumov, G. A., New four- and five-coordinated complexes of cobalt with sterically hindered o-iminobenzoquinone ligands: synthesis and structure. *Inorg. Chim. Acta* **2004,** *357*, 3632-3640.

49. Blackmore, K. J.; Ziller, J. W.; Heyduk, A. F., "Oxidative Addition" to a Zirconium(IV) Redox-Active Ligand Complex. *Inorg. Chem.* **2005,** *44*, 5559-5561.

50. Haneline, M. R.; Heyduk, A. F., C-C Bond-Forming Reductive Elimination from a Zirconium(IV) Redox-Active Ligand Complex. *J. Am. Chem. Soc.* **2006,** *128*, 8410-8411.

51. Boyer, J. L.; Cundari, T. R.; DeYonker, N. J.; Rauchfuss, T. B.; Wilson, S. R., Redox Activation of Alkene Ligands in Platinum Complexes with Non-innocent Ligands. *Inorg. Chem.* **2009,** *48*, 638-645.

Synthesis and characterization of square planar cobalt(III) complexes and their ligand-mediated Co-X bond-formating reactivity

2.1. Introduction

At the heart of many applications of chemistry, ranging from organic synthesis to energy production, lies the need to make and break bonds.[1-3] Multi-electron redox control is needed for selective bond-forming reactions because free radical reactions are typically unselective, leading to costly purification of products that wastes time and money. To develop a new catalyst with specific reactivity and products, it is often useful to understand the mechanistic details of the catalytic cycles and relevant stoichiometric reactions using well-defined complexes. Many selective carbon-carbon coupling reactions are facilitated by palladium catalysts due to the thermodynamic preference of the 5d metal to undergo two electron changes in oxidation state in concerted steps, thus facilitating the multi-electron reaction in a controlled step.[3-9] First row transition metals however are more prone to single electron oxidation state changes.

One approach to evoke multi-electron reactivity at first row transition metals metal centers involves combining the redox power of the metal with a non-innocent, or redox-active, ligand.[10-13] Some non-innocent ligands can act as reservoirs of electrons that participate in reactivity at metal centers. Recently, these redox-active ligands have been shown to facilitate redox reactions of small molecules by stabilizing unusual oxidation state of the metal.[14-24] We believe through careful ligand selection, this

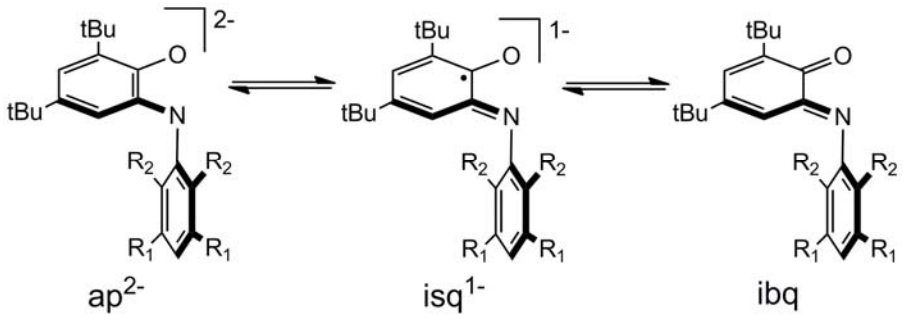

Figure 2.1. Electronic series of amidophenol-derived, redox-active ligand. Unsubstitued L^{Ph} in which R_1=R_2=H; L^{iPr} in which R_1=H and R_2=isopropyl; and L^{Cl} in which R_1=Cl and R_2=H.

chemistry can be extended to evoke bond-forming redox reactions at cobalt using electrons derived from both the metal and ligand set.

The bidentate amidophenol-derived ligands (H_2ap) used in this study coordinate to the metal center through an oxygen and a nitrogen (Figure 2.1).[10] This ligand can also be modified through substituents on the N-aryl ring that allow fine tuning of the sterics or the electronics of the ligand itself and thus alter the accessibility to open coordination sites of the metal or the redox potential of the resulting metallated complex. Recently, it has been shown that these ligands are able to facilitate two-electron, bond-forming reactions at d^0 and d^{10} metals in which the reactive electrons must be derived from the ligand set.[14,25] We chose to use cobalt because both the metal and ligand contain accessible electrons of similar energy.[26] We hope to gain understanding about how this electronic relationship affects the overall reactivity of the complex.

We began our examination with a previously reported low-coordinate cobalt complex containing two amidophenol-derived ligands. We believed from examiniation of the body of work investigating the characteristics of various redox active ligands and

metals that this combination of cobalt metal and amidophenol-derived ligand would give the molecular orbital overlap needed and would stabilize the complex with open coordination sites for bond-forming and bond-breaking reactivity.

Previous work reported on these complexes was sporadic and conclusions inconsistent between research groups. It was first reported by Wieghardt and coworkers that the unsubstituted ligand (H_2ap^{Ph}) could be reacted with $CoCl_2$ to form the coordinatively saturated $Co(L)_3$ complex.[27] Shortly thereafter, the same group reported synthesis of 5-coordinate complexes containing only two unsubstituted (R_1=R_2=H) amidophenol-derived ligands and stabilized by a coordinating halide (Cl or I) ligand.[28] The authors reported that substiochiometric quantities of the ligand were required to avoid formation of the tris $Co(L)_3$ complex. The ligand oxidation states of the 5-coordinate complexes were assigned as bis-iminosemiquinonate (isq^{1-}) by analysis of the bond lengths within the crystal structures of the molecule. This makes the assignment of the metal cobalt(III). The $Co^{III}(Cl)(isq^{Ph})_2$ complex was generated by halide exchange between $Co^{III}(I)(isq^{Ph})_2$ and $CHCl_3$.

Following this report, another group reported the synthesis of 4- and 5-coordinate complexes $Co(L)_2$ and $Co(X)(L)_2$ in which the ligand is substituted with methyls or isopropyls in the R_2 position (H_2ap^{Me} or H_2ap^{iPr}).[29] Consistent with the earlier report of the tendency of these species to form $Co(L)_3$, these authors report the need for steric bulk at the *ortho* positions of the N-phenyl to isolate the low-coordinate complexes. Interestingly, they conclude the paper with an argument that $Co(L)_3$ degrades to $Co(L)_2$ in solution. They also report that the 4-coordinate, neutral complex is best formulated as $Co^{II}(isq^{Ar})_2$ based on bond lengths obtained from X-ray crystal analysis as well as electron

paramagnetic resonance (EPR) indicating only one unpaired electron on the cobalt center.

In one later study by Wieghardt and coworkers, a 4-coordinate derivative containing two ligands with a trifluoromethyl group is substituted in only one of the *ortho*-positions of the N-phenyl (H_2ap^{CF3}) was prepared from reaction with $Co(ClO_4)_2 \bullet 6H_2O$.[26] The authors formulate this complex as $Co^{III}(isq^{CF3})(ap^{CF3})$ (ap=amidophenolate) from the bond-lengths from the X-ray crystallographic analysis. They also report the one electron reduced species $[CoCp^*_2][Co(L)_2]$ which they formulate as $[Co^{III}(ap)_2]^-$.

The sum of this literature led us to question whether steric bulk is required to stabilize these cobalt-amidophenolate complexes in a low-coordinate environment. Wieghardt's report that the reduction of the neutral to the monoanion is ligand centered encouraged us that reactions facilitated by the complex may also be ligand based. However, it was important to resolve the inconsistency in the literature as to the assignment of oxidation state of the neutral complex.. The reaction chemistry of these complexes is basically unexplored with only casual reports of addition of halides and a CH_2CN^- fragment at the cobalt center. This shows promise that these complexes may be suitable for bond-forming reactions at the metal center.

Reported in this chapter are our initial efforts to utilize amidophenolate ligands and cobalt(III) for bond-forming reactions at the metal center. Towards this goal, we have prepared and characterized new square planar cobalt complexes with amidophenolate ligands that were previously reported to be inaccessible.[30] X-ray crystallographic data is used to rationalize the electronic structures of these species, prompting a re-evaluation of the previously reported assignment for the related

complex.[29] Finally, control of ligand oxidation state is shown to facilitate one electron versus two electron selectivity in Co–Cl bond-forming reactions, establishing the ability of redox-active ligands to produce multi-electron reactivity at square planar cobalt(III).

2.2. Experimental Details

2.2.1. General considerations

Unless otherwise noted, all manipulations were performed under anaerobic conditions using standard vacuum line techniques, or in an inert atmosphere glove box under purified nitrogen. All NMR spectra were acquired on a Varian Mercury 300 spectrometer (300.323 MHz for ^{1}H) at ambient temperature. Chemical shifts are reported in parts per million (ppm) relative to TMS, with the residual solvent peak serving as an internal reference. Solution state magnetic moments were determined by Evans' NMR method. UV–visible absorption spectra were acquired using a Varian Cary 50 spectrophotometer. Unless otherwise specified, all electronic absorption spectra were recorded at ambient temperatures in 1 cm quartz cells. IR spectra were obtained using attenuated total reflection (ATR) with a diamond plate on a Thermo Scientific Nicolet 4700 Fourier-transform infrared spectrophotometer. All mass spectra were recorded in the Georgia Institute of Technology Bioanalytical Mass Spectrometry Facility. Fast-atom bombardment mass spectrometry (FAB-MS) was performed using a VG Instruments 70-SE spectrometer. Electrospray ionization mass spectrometry (ESI-MS) was carried out with acetonitrile (CH_3CN) or tetrahydrofuran (THF) solutions using as Micromass Quattro LC spectrometer. Cyclic voltammetric measurements were made using a CH Instruments CHI620C potentiostat in a three component cell consisting of a platinum

disk working electrode, a platinum wire auxiliary electrode, and a non-aqueous $AgNO_3$/Ag reference electrode. All electrochemical experiments were performed in CH_3CN with 0.1 M $[^nBu_4N][PF_6]$ as the supporting electrolyte. Electrochemical data are referenced and reported to Fc^+/Fc as an internal standard. Elemental analyses were performed by Atlantic Microlab, Inc., Norcross, GA. All analyses were performed in duplicate, and the reported compositions are the average of the two runs.

2.2.2. Methods and materials

Anhydrous acetonitrile (CH_3CN), tetrahydrofuran (THF), toluene, dichloromethane (CH_2Cl_2), and pentane solvents for air- and moisture-sensitive manipulations were purchased from Sigma–Aldrich, further dried by passage through columns of activated alumina, degassed by at least three freeze–pump–thaw cycles, and stored under N_2 prior to use. Methanol (MeOH) (anhydrous, 99.0%) was purchased from Honeywell Burdick & Jackson, and used as received. Deuterated acetonitrile (CD_3CN) was purchased from Cambridge Isotope Laboratories, degassed by three freeze–pump–thaw cycles, vacuum distilled from CaH_2, and stored under a dry N_2 atmosphere prior to use. The ligands 2,4-ditertbutyl-6-(2,6-diisopropylphenylimino)benzoquinone (ibq^{iPr}), 2,4-ditertbutyl-6-(phenylamino)phenol (H_2ap^{Ph}), 2,4-ditertbutyl-6-(3,5-dichlorophenylamino)phenol (H_2ap^{Cl}) and 2,4-ditertbutyl-6-(3,5-ditertbutylphenylamino)phenol (H_2ap^{tBu}) were prepared by literature method.[13,31] All characterization data matched those referenced. $Co(ClO_4)_2 \cdot 6H_2O$ and $Co_2(CO)_8$ were purchased from Strem Chemical, Inc. All other chemicals were purchased from Sigma–Aldrich and used as received.

2.2.3. Preparation of $Co^{III}(isq^{Ph})(ap^{Ph})$

In modification of a literature procedure,[26] $Co(ClO_4)_2 \cdot 6H_2O$ (0.365 g, 1.00 mmol) and H_2ap^{Ph} (0.596 g, 2.00 mmol) were combined in a 50 L round bottom flask with a stir bar and dissolved in 20 mL anhydrous methanol. Dropwise addition of Et_3N (560 µL, 4.02 mmol) with vigorous stirring immediately afforded a clear dark blue solution. The flask was fitted to a condenser and the reaction mixture was heated to reflux in air for 1 hour, then cooled to ambient temperature for 2 hour to deposit a dark blue precipitate. The solids were recovered by vacuum filtration, washed with cold anhydrous methanol (3 × 2.0 mL, ice cold), and dried *in vacuo* to yield $Co^{III}(isq^{Ph})(ap^{Ph})$ (0.368 g, 0.566 mmol, 57%). Crystalline solids suitable for single crystal X-ray diffraction were recovered by slow diffusion of pentane into saturated CH_2Cl_2 solution in the absence of light. UV–vis (THF) nm (ε, M^{-1} cm^{-1}): 280 (15 700), 675 (11 500), 900 (16 200). FAB-MS (*m*/*z*): 649 $[M]^+$. FTIR (ATR): 3062 (w), 3041 (w), 3026 (w), 2956 (m), 2900 (m), 2863 (m), 1579 (w), 1536 (w), 1481 (m), 1432 (m), 1356 (m), 1302 (m), 1260 (m), 1215 (w), 1183 (w), 1138 (s), 1104 (s), 1025 (m), 1002 (w), 922 (m), 910 (m), 881(w), 859 (m), 824 (w), 766 (w), 738 (s), 692 (s), 659 (s), 609 (w), 571 (m), 540 (m), 510 (s), 467 (m), 424 (m) cm^{-1}. The sample for elemental analysis was washed in methanol, as described above. The reported analysis is for $Co^{III}(isq^{Ph})(ap^{Ph}) \cdot 1.3MeOH$, and the presence of the methanol in the sample was confirmed by ^1H NMR spectroscopy. *Anal.* Calc. for $C_{41.3}H_{53.9}N_2CoO_{3.3}$: C, 71.74; H, 8.05; N, 4.05. Found C, 71.36; H, 7.62; N, 4.16%.

2.2.4. Preparation of $Co^{III}(isq^{iPr})(ap^{iPr})$

In modification of a literature procedure,[29] a five dram scintillation vial was charged with a solution of $Co_2(CO)_8$ (0.069 g, 0.203 mmol) in 10 mL toluene and a stir

bar. Slow addition of a solution of ibq^{iPr} (0.308 g, 0.811 mmol) in 5 mL toluene with vigorous stirring immediately afforded a blue solution. The solution was stirred for 1 hour at ambient temperature and the volume was reduced to 4 mL to precipitate dark blue solids. The solids were collected by vacuum filtration in air, washed with toluene (2 × 2.0 mL, ice cold) and dried *in vacuo* to give $Co^{III}(isq^{iPr})(ap^{iPr})$ (0.255g, 0.312mmol, 77%). Slow diffusion of toluene into a saturated THF solution afforded single crystals of $Co^{III}(isq^{iPr})(ap^{iPr})$ suitable for assignment of connectivity by X-ray diffraction. UV–vis (THF) nm (ε, M^{-1} cm^{-1}): 280 (15 500), 680 (10 400), 905 (15 400). FAB-MS (*m*/*z*): 817 $[M]^+$. FTIR (ATR): 3061 (w), 2959 (m), 2925 (m), 2902 (m), 2864 (m), 1535 (w), 1462 (w), 1357 (m), 1327 (w), 1298 (m), 1257 (w), 1230 (w), 1215 (w), 1181 (w), 1133 (s), 1097 (s), 1019 (m), 911 (w), 897 (m), 859 (m), 825 (w), 737 (m), 680 (w), 657 (s), 586 (w), 565 (w), 514 (s), 506 (s), 471 (m), 433 (m) cm^{-1}.

2.2.5. Preparation of $Co^{III}(isq^{Cl})(ap^{Cl})$

In a procedure directly analogous to that described above and modified from literature for $Co^{III}(isq^{Ph})(ap^{Ph})$, $Co(ClO_4)_2{\cdot}6H_2O$ (0.184 g, 0.50 mmol) and H_2ap^{Cl} (0.366 g, 1.00 mmol) were reacted with Et_3N (280 µL, 2.01 mmol) to yield $Co^{III}(isq^{Cl})(ap^{Cl})$ (0.088 g, 0.112 mmol, 22%). Slow diffusion of pentane into a saturated THF solution afforded single crystals of $Co^{III}(isq^{iPr})(ap^{iPr})$ suitable for analysis by X-ray diffraction. FAB-MS (*m*/*z*): 789 $[M]^+$. FTIR (ATR): 2950 (m), 2901 (m), 2865 (m), 1753 (w), 1570 (m), 1560 (m), 1538 (m), 1525 (m), 1461 (w), 1436 (m), 1422 (m), 1389 (w), 1376 (m), 1358 (m), 1304 (m), 1259 (m), 1218 (m), 1138 (s), 1096 (s), 1038 (m), 1025 (m), 1006 (m), 993

(m), 940 (m), 909 (m), 878 (w), 870 (w), 852 (m), 836 (w), 816 (m), 801 (m), 772 (m), 730 (m), 695 (m), 651 (m), 594 (w), 554 (w), 523 (w), 506 (w), 471 (w), 425 (w) cm^{-1}.

2.2.6. Preparation of $Na[Co^{III}(ap^{Ph})_2]$

A five dram scintillation vial was charged with sodium-mercury amalgam beads (5% Na, 0.250 g, 0.544 mmol) and $Co^{III}(isq^{Ph})(ap^{Ph})$ (0.350 g, 0.539 mol) and 10 mL CH_3CN. The reaction mixture was fitted with a Teflon-lined cap and stirred for 12 hour under N_2. During this time a color change was observed from dark blue to purple. The solution was collected by vacuum filtration and the solvent was removed *in vacuo* to afford $Na[Co^{III}(ap^{Ph})_2]$ (0.341 g, 0.504 mmol, 94%) as purple power. UV–vis (CH_3CN) nm (ε, M^{-1} cm^{-1}): 295 (20 000), 540 (4 910), 850 (10 600). ^1H NMR (300 MHz, CD_3CN, δ): 58.89 (2H), 35.62 (2H), 26.82 (4H), 8.29 (18H), −0.17 (18H), −7.43 (2H), −24.62 (4H) (all br s). The sample for elemental analysis was collected from a CH_3CN solution. The reported analysis is for $Na[Co^{III}(ap^{Ph})_2]\cdot 2CH_3CN$, and the presence of CH_3CN in the sample was confirmed by ^1H NMR spectroscopy. *Anal.* Calc. for $C_{44}H_{56}N_4CoO_2Na$: C, 70.01; H, 7.48; N, 7.42. Found: C, 70.31; H, 7.53; N, 7.00%. Crystals suitable for analysis by X-ray diffraction were obtained from a CH_3CN solution dissolved with added Ph_4PBr chilled at –20°C for two weeks.

2.2.7. Preparation of Na[Co^{III}(ap^{iPr})$_2$]

This complex was prepared using sodium-mercury amalgam beads (5% Na, 0.211 g, 0 459 mmol) and Co^{III}(isq^{iPr})(ap^{iPr}) (0.368 g, 0.449 mmol) in a procedure directly analogous to that described above for Na[Co^{III}(ap^{Ph})$_2$], to give Na[Co^{III}(ap^{iPr})$_2$] (0.351 g, 0.417 mmol, 93%). UV–vis (CH_3CN) nm (ε, M^{-1} cm^{-1}): 290 (15 200), 535 (4 430), 835 (9 810). ^{1}H NMR (300 MHz, CD_3CN, δ): 52.45 (br s, 2H), 34.18 (br s 2H), 24.71 (br d, J=8 Hz, 4H), 10.11 (br t, J=8 Hz, 2H), 7.94 (br s, 18H), 1.43 (br s, 12H), −0.32 (br s, 18H), −10.42 (br s, 4H), −13.91 (br s, 12H).

2.2.8. Preparation of Na[Co^{III}(ap^{Cl})$_2$]

This complex was prepared using sodium-mercury amalgam beads (20% Na, 0.022 g, 0.191 mmol) and Co^{III}(isq^{Cl})(ap^{Cl}) (0.126 g, 0.161 mmol) in a procedure directly analogous to that described above for Na[Co^{III}(ap^{Ph})$_2$] to give Na[Co^{III}(ap^{Cl})$_2$] (0.134 g, 0.166 mmol, 81%). UV–vis (CH_3CN) nm (ε, M^{-1} cm^{-1}): 550 (4 120), 855 (7 305). ^{1}H NMR (300 MHz, CD_3CN, δ): 36.75 (2H), 18.36 (2H), 8.68 (18H), -0.15 (18H), -10.05 (2H), -28.53 (4H).

2.2.9. Preparation of (Cp$_2$Co)[Co^{III}(ap^{iPr})$_2$]*

In an adaptation of a literature procedure,[26] Cp*$_2$Co (0.040 g, 0.121 mmol) and Co^{III}(isq^{iPr})(ap^{iPr}) (0.098 g, 0.119 mmol) were combined in a five dram scintillation vial and dissolved in 10 mL CH_3CN with vigorous stirring. The reaction mixture was fitted with a Teflon-lined cap and stirred for 3 h under N_2 to generate a dark-purple solution. The volume of the solution was reduced to 3 mL *in vacuo* and stored at −20^{o}C for 48 h to

yield $(Cp^*_2Co)[Co^{III}(ap^{iPr})_2]$ (0.111 g, 0.0965 mmol, 80%) as violet microcrystals. Crystals suitable for X-ray crystallographic analysis were grown at -20°C in concentrated CH_3CN solutions over weeks. Purity was determined by comparison of the UV–vis spectrum of the isolated product to that reported above for the sodium salt.

2.2.10. X-ray crystallography

Single crystals of $Co^{III}(ap^{Ph})(isq^{Ph})$ and $(Cp^*_2Co)[Co^{III}(ap^{iPr})_2]\cdot 2CH_3CN$ suitable for X-ray diffraction analysis were coated with Paratone N, suspended in a small fiber loop and placed in a cooled nitrogen gas stream at 173 K on a Bruker D8 APEX II CCD sealed tube diffractometer. Diffraction data for $Co^{III}(ap^{Ph})(isq^{Ph})$ was collected using graphite monochromated Cu Kα (λ = 1.54178 Å) radiation. Data for $(Ph_4P)[Co^{III}(ap^{Ph})_2]$ and $(Cp^*_2Co)[Co^{III}(ap^{iPr})_2]\cdot 2CH_3CN$ was obtained with graphite monochromated Mo Kα (λ = 0.71073 Å) radiation. All other data collection procedures, data processing and programs were the same for all three samples. Data were measured using a series of combinations of phi and omega scans with 10 s frame exposures and 0.5° frame widths. Data collection, indexing and initial cell refinements were all carried out using apex II software.[32] Frame integration and final cell refinements were done using saint software.[33] The final cell parameters were determined from least-squares refinement on 2789 reflections for $Co^{III}(ap^{Ph})(isq^{Ph})$, 18241 reflections for $(Ph_4P)[Co^{III}(ap^{Ph})_2]$ and 2968 reflections for $(Cp^*_2Co)[Co^{III}(ap^{iPr})_2]\cdot 2CH_3CN$. The structures were solved using direct methods and difference Fourier techniques using the shelxtl program package[34]. Hydrogen atoms were placed in their expected chemical positions using the HFIX command and were included in the final cycles of least-squares with isotropic U_{ij}'s

related to the atoms ridden upon. All non-hydrogen atoms were refined anisotropically. Details of data collection and structure refinement are provided in Table 2.1.

Table 2.1. Crystallographic data and structure parameters for $Co^{III}(ap^{Ph})(isq^{Ph})$, $(Ph_4P)[Co^{III}(ap^{Ph})_2]$ and $(Cp^*_2Co)[Co^{III}(ap^{iPr})_2]\bullet 2CH_3CN$.

Complex	**$Co^{III}(ap^{Ph})(isq^{Ph})$**	**(Ph_4P) $[Co^{III}(ap^{Ph})_2]$**	**(Cp^*_2Co) $[Co^{III}(ap^{iPr})_2]$ $\bullet$ $2CH_3CN$**
Empirical formula	$C_{40}H_{50}CoN_2O_2$	$C_{64}H_{70}CoN_2O_2P$	$C_{76}H_{110}Co_2N_4O_2$
Formula weight	649.75	989.12	1229.54
T (K)	173(2)	296(2)	173(2)
Crystal system	triclinic	triclinic	monoclinic
Space group	P1	P1	$P2_1/c$
Unit Cell dimensions			
a (Å)	5.8590(2)	14.217(3)	9.3811(1)
b (Å)	11.7285(4)	14.283(3)	17.0552(4)
c (Å)	13.6999(6)	16.218(4)	21.9136(5)
α (^{o})	110.421(2)	75.250(4)	90
β (^{o})	93.205(2)	77.662(4)	92.785(2)
γ (^{o})	93.739(2)	73.012(4)	90
V (Å^3)	877.26(6)	3010.9(12)	3501.96(14)
Z	1	2	2
D_{calc} (g/cm^3)	1.230	1.091	1.166
Absorption coefficient (mm^{-1})	4.102	0.352	0.520
Crystal Size (mm)	0.37x0.12x0.10	0.36x0.18x0.02	0.36x0.11x0.10
θ range for data collection (^{o})	4.29 to 66.89	1.31 to 30.51	1.51 to 27.15
Index ranges	$-6 \le h \le 6$	$-20 \le h \le 20$	$-10 \le h \le 12$
	$-13 \le k \le 13$	$-20 \le k \le 20$	$-18 \le k \le 21$
	$-15 \le l \le 12$	$-23 \le l \le 23$	$-27 \le l \le 28$
Reflections collected	5817	61223	23193
Reflections unique	2624	18241	7686
Goodness of fit on F^2	1.056	1.009	1.015
R [$I>2\sigma(I)$]	0.0338	0.0655	0.0542
wR^2 (all data)	0.0873	0.1956	0.1579

2.3. Results

2.3.1. Preparation and characterization of $Co^{III}(ap^{Ar})(isq^{Ar})$

Charge neutral, four-coordinate cobalt complexes were obtained by modifications of literature procedures: via stoichiometric reaction of $Co_2(CO)_8$ with ibq^{iPr} in toluene in an air free environment,[29] or by addition of $Co(ClO_4)_2 \cdot 6H_2O$ to H_2ap^{Ph} in basic MeOH with air (ibq^{iPr} = 2,4-di-tert-butyl-6-(2,6-diisopropylphenylimino)benzoquinone; H_2ap^{Ph} = 2,4-di-tert-butyl-6-(phenylamino)phenol).[26] A single crystal X-ray structure of the Ph derivative is provided in Figure 2.2.a. It contains cobalt bound to two coplanar ligands. The *N*-phenyl substituents are rotated out of the plane defined by the square planar cobalt core, with Co–N–C–C torsion angles of −107.63(19)° and 68.5(2)°. The cobalt lies

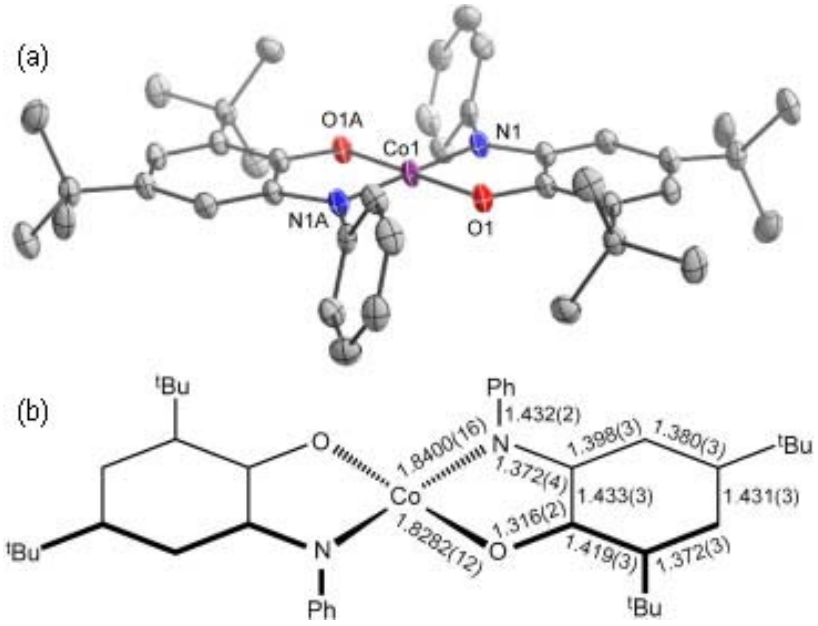

Figure 2.2. (a) Solid-state structure of $Co^{III}(ap^{Ph})(isq^{Ph})$ drawn with 50% probability ellipsoids. Hydrogen atoms omitted for clarity. Selected bonds angles (deg): O1-Co1-N1 85.58(6), O1-Co1-N1A 94.42(6). **(b)** Schematic of selected bond lengths (Å) in $Co^{III}(ap^{Ph})(isq^{Ph})$.

on an inversion center making the two aminophenol-derived ligands crystallographically identical. This symmetry may be a result of either crystallographic disorder of the molecule or Class III delocalization of the electrons of the ligand.[35] A determination of which is responsible for the inversion center in the structure cannot be determined. The C–O, C–N and C–C bond distances shown in Figure 2.2.b exhibit a small but significant quinoid distortion that is in good agreement with the mean of those typical for $[ap^{Ph}]^{2-}$ and $[isq^{Ph}]^{\bullet-}$,[36,26] suggesting that the complex is best formulated as $Co^{III}(ap^{Ph})(isq^{Ph})$ (isq^{Ph} = 2,4-di-tert-butyl-6-(phenylimino)semiquinonate). All of the bond distances are crystallographically indistinguishable from the previously reported structures of the ^{i}Pr analog[29] and a congener containing one *ortho*-triflouromethyl substituent on the *N*-aryl ring.[26] The solution magnetic moment of 2.18 μ_B for $Co^{III}(ap^{Ph})(isq^{Ph})$ at 25°C in THF is in agreement with a previously reported value for the trifluoromethyl analog.[26] This was proposed to result from intramolecular antiferromagnetic coupling between the intermediate spin S = 1 cobalt(III) ion and one iminobenzoseminonate radical ligand to yield an S = ½ ground state.

2.3.2. Preparation and characterization of $[Co^{III}(ap^{Ar})_2]^-$

Addition of 1 equivalent Cp^*_2Co or Na (as 5 or 20% Na–Hg amalgam) to the blue $Co^{III}(ap^{Ar})(isq^{Ar})$ complexes in CH_3CN under N_2 affords a dark-purple color change over hours at ambient temperature with stirring (Figure 2.3). Recrystallization of the isopropyl derivative from CH_3CN yielded single crystals of the cobaltocenium salt suitable for analysis by X-ray diffraction. As shown in Figure 2.4.a, the cobalt anion retains its square planar geometry. Two CH_3CN solvent molecules per anion are located in the crystal structure but are not bound to cobalt. As in the neutral species, the ligands in the anion are crystallographically indistinguishable, and the *N*-aryl rings are nearly orthogonal to the plane defined by the square planar cobalt center, with Co–N–C–C torsion angles of −91.0(3)° and 82.8(3)°. The aromatic C–C bond distances (Figure 2.4.b) are identical within 3σ (1.40 ± 0.01 Å). However, the ligand C–O and C–N bond

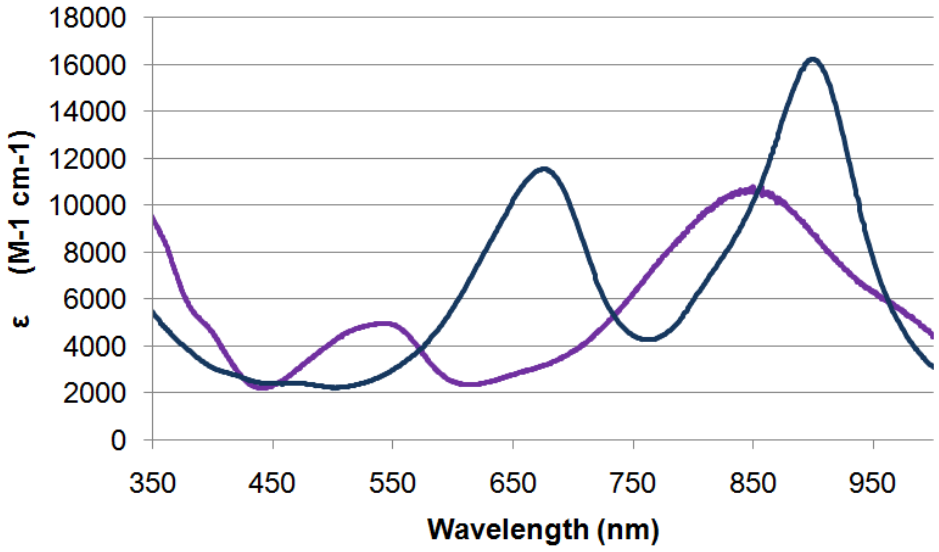

Figure 2.3. UV-vis absorption data for neutral $Co^{III}(isq^{Ar})(ap^{Ar})$ (blue spectrum) THF and $Na[Co^{III}(ap^{Ar})_2]$ (purple spectrum) in CH_3CN.

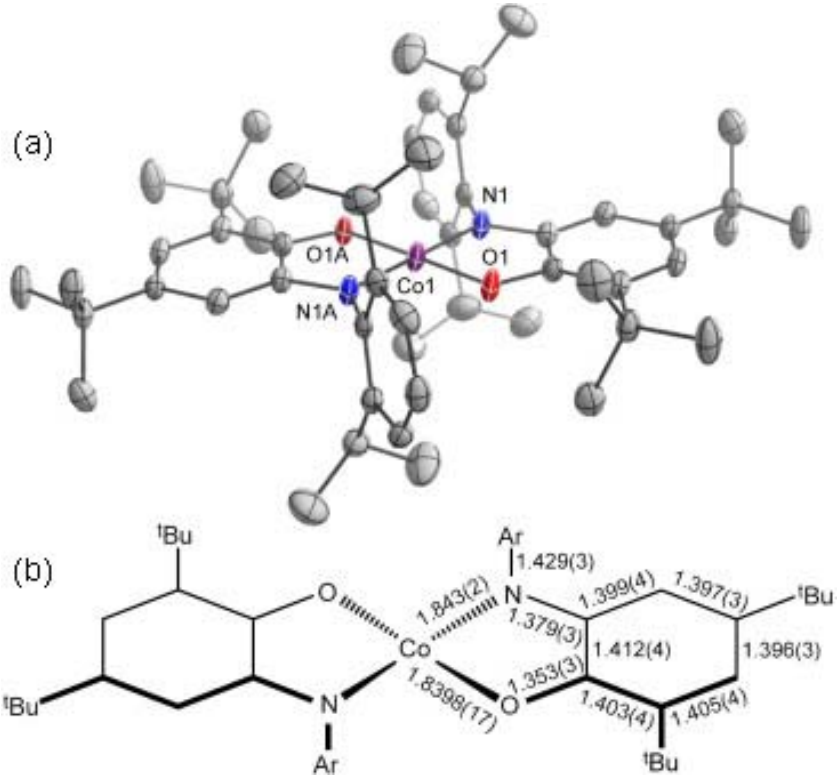

Figure 2.4. (a) Solid-state structure of the anion $(Cp^*_2Co)[Co^{III}(ap^{iPr})_2]\bullet 2CH_3CN$ drawn with 50% probability ellipsoids. Hydrogen atoms, CH_3CN solvate molecules and counteraction omitted for clarity. Selected bonds angles (deg): O1-Co1-N1 85.75(8), O1-Co1-N1A 94.25(8). **(b)** Schematic of selected bond lengths (Å) in $[Co^{III}(ap^{iPr})_2]^-$.

distances are elongated as compared to $Co^{III}(ap^{iPr})(isq^{iPr})$. This lengthening is indicative of the decrease in the double-bond character of the two bonds. The reduced complexes are therefore best formulated as $[Co^{III}(ap^{Ar})_2]^-$.[36,29] An X-ray crystal structure of the $(Ph_4P)[Co^{III}(ap^{Ph})_2]$ analog was also obtained (Figure 2.5.a). The C–O and C–N bond distances (Figure 2.5.b) are identical within 3σ to those of $(Cp^*_2Co)[Co^{III}(ap^{iPr})_2]$ and the aromatic C–C bond distances again have an average value of 1.40 Å. There is one C–C bond that is slightly elongated. This is believed to be a result of molecular packing in the

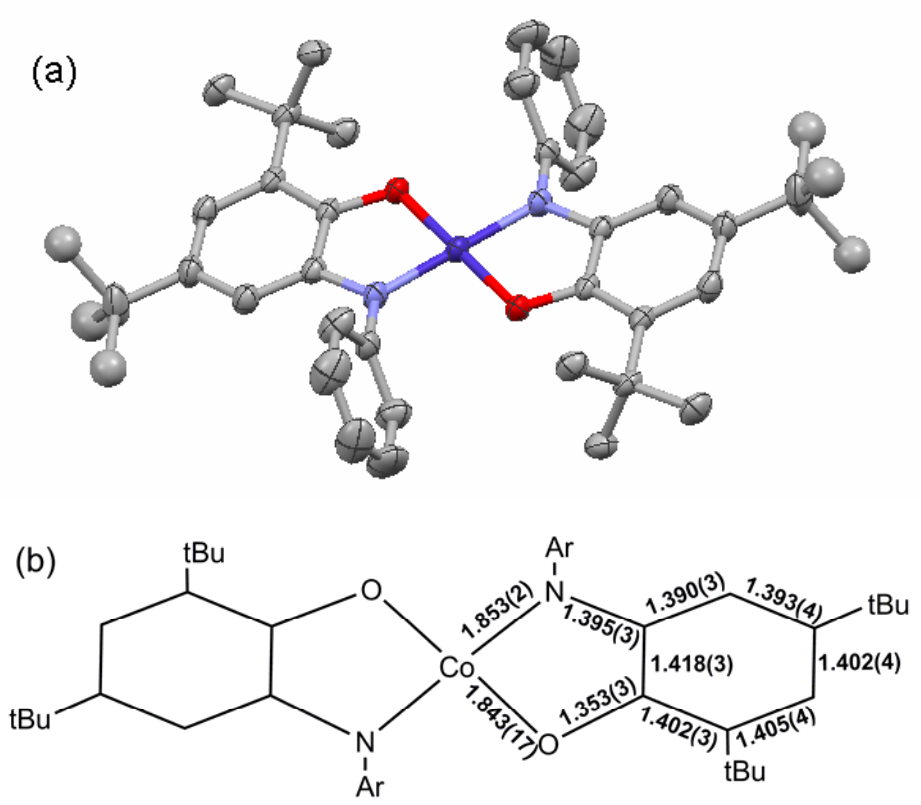

Figure 2.5. (a) Solid-state structure of the anion $(Ph_4P)[Co^{III}(ap^{Ph})_2]$ drawn with 50% probability ellipsoids. Hydrogen atoms and counteraction omitted for clarity. **(b)** Schematic of selected bond lengths (Å) in $[Co^{III}(ap^{Ph})_2]^-$.

crystal and not indicative of a different electronic assignment, given the sum of the other data.

$[Co^{III}(ap^{Ar})_2]^-$ complexes exhibit diagnostic broad, paramagnetically shifted ^1H NMR spectra (δ +59 to −24 ppm) at ambient temperatures. As determined by Evan's Method,[37,38] the solution magnetic moment of 2.77 μ_B for $[Co^{III}(ap^{Ph})_2]^-$ at 25°C in CH_3CN is consistent with two unpaired electrons as intermediate spin S=1 cobalt(III) in a square planar ligand field. Cyclic voltammograms of the $[Co^{III}(ap^{Ar})_2]^-$ complexes display two quasi-reversible one electron redox couples (Figure 2.6, Table 2.2). Because

$Co^{III}(ap^{Ph})(isq^{Ph})$ is not reduced by Cp^*_2Fe (with a reduction potential of −0.48 V versus Fc^+/Fc in CH_3CN),[39] the redox event at more negative potential is assigned to interconversion of $Co^{III}(ap^{Ar})(isq^{Ar})$ and $[Co^{III}(ap^{Ar})_2]^-$.

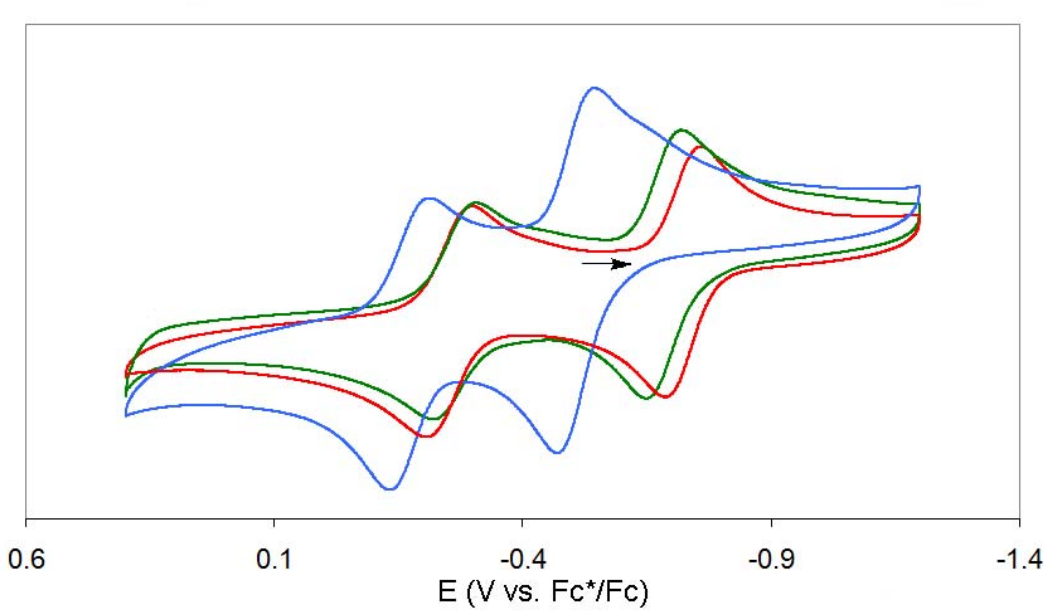

Figure 2.6. Cyclic voltammograms of 5mM $Na[Co^{III}(ap^{Ph})_2]$ (green line), $Na[Co^{III}(ap^{iPr})_2]$ (red line) and $Na[Co^{III}(ap^{Cl})_2]$ (blue line) in CH_3CN containing 0.1M $[^nBu_4N][PF_6]$ at a 10 mm Pt electrode. Scan rate: 0.5 v s^{-1}. Temperature: 25°C. The arrow represents the direction of the scan sweep for all three analogs.

Table 2.2. Electrochemical midpoint potentials of $[Co^{III}(ap^{Ar})_2]^-$ complexes.[a]

Complex	$[Co]^+/[Co]$	$[Co]/[Co]^-$
Ar = Phen	-0.350 V	-0.770 V
Ar = iPr	-0.339 V	-0.809 V
Ar = Cl	-0.173 V	-0.508 V

[a] As measured by cyclic voltammetry in CH_3CN solutions containing 0.1M $[^nBu_4N][PF_6]$ at a 10 mm Pt electrode with a scan rate: 0.5 v s^{-1} and performed at 25°C. Potentials are reported versus Fc^+/Fc.

2.3.3. Behavior of $[Co^{III}(ap^{Ar})_2]^-$ in various solvents

The purple $Na[Co^{III}(ap^{Ar})_2]$ complexes appear purple in CH_3CN, benzene, and DMSO in solutions ranging from saturated (*ca.* 1.5M) to 0.01 mM. However, in dilute THF the solutions appear blue (Figure 2.7) and must be approximately >0.01 M to remain purple. The color change is also observed in dilute solutions of pentane and toluene. This blue spectrum is very similar, but not identical, to that of the one electron oxidized neutral material (blue line of Figure 2.3). Crystals of $Na[Co^{III}(ap^{Ar})_2]$ grown out of THF:pentane solutions for X-ray diffraction study retain their monoanionic character and show no significant differences in the solid state to crystals grown from CH_3CN solutions There is also no coordination of the solvent molecules to the complex in either of the crystal structures.

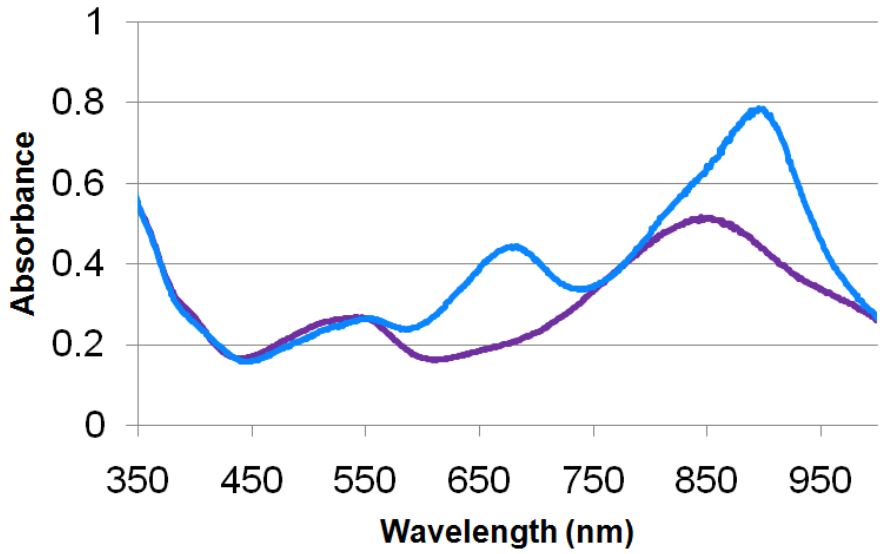

Figure 2.7. UV-vis absorption data for 0.05 mM solution of $Na[Co^{III}(ap^{Ar})_2]$ (purple spectrum) in CH_3CN and 0.05 mM solution of $Na[Co^{III}(ap^{Ar})_2]$ in THF (blue spectrum).

When a blue Na[$Co^{III}(ap^{Ar})_2$] THF solution is dried and taken back up into CH_3CN, the color change is reversible and the solution is again purple. If the blue THF solution is heated (60°C, 1 hour) prior to the solvent removal, the material becomes insoluble in CH_3CN and the color change appears irreversible. The degree to which the UV-vis spectra are changed is independent of the concentration of the solution over a 20x range (0.05 mM to 1.0 mM) in THF. In mixed solvent solutions, as the mole percent of CH_3CN is decreased relative to THF, the growth of the 670 and 900 nm peaks and the corresponding decrease in the 540 and 850 nm peaks are linear within error over three trials. A similar study using 2-methyl-THF showed similar results to the unsubstituted THF solvent. Change in the countercation slightly changes the behavior of the material. With the larger bis(triphenylphosphoranylidene)ammonium (PPN) countercation in place of the Na^+, the material is less sensitive upon dilution in THF, requiring a lower concentration of the complex before a change in the appearance or in the UV-vis spectrum is observed.

2.3.4. One-electron Co–Cl bond-forming reaction

Addition of 1 equivalent of CCl_4 or *N*-chlorosuccinimide (NCS) to the blue $Co^{III}(ap^{Ar})(isq^{Ar})$ complexes in THF gives a color change to blue-green in seconds at ambient temperature. Identical UV–vis spectra are obtained by exposure of CH_2Cl_2 solutions of the $Co^{III}(ap^{Ar})(isq^{Ar})$ materials to ambient fluorescent light, as was previously reported in literature.[29] The product of all the reactions is the previously reported square pyramidal $Co^{III}Cl(isq^{Ar})_2$ species containing two iminobenzoseminonate(1^-) radical ligands.[28,29,30] The assignment of the 5-cooridinate species previously reported was

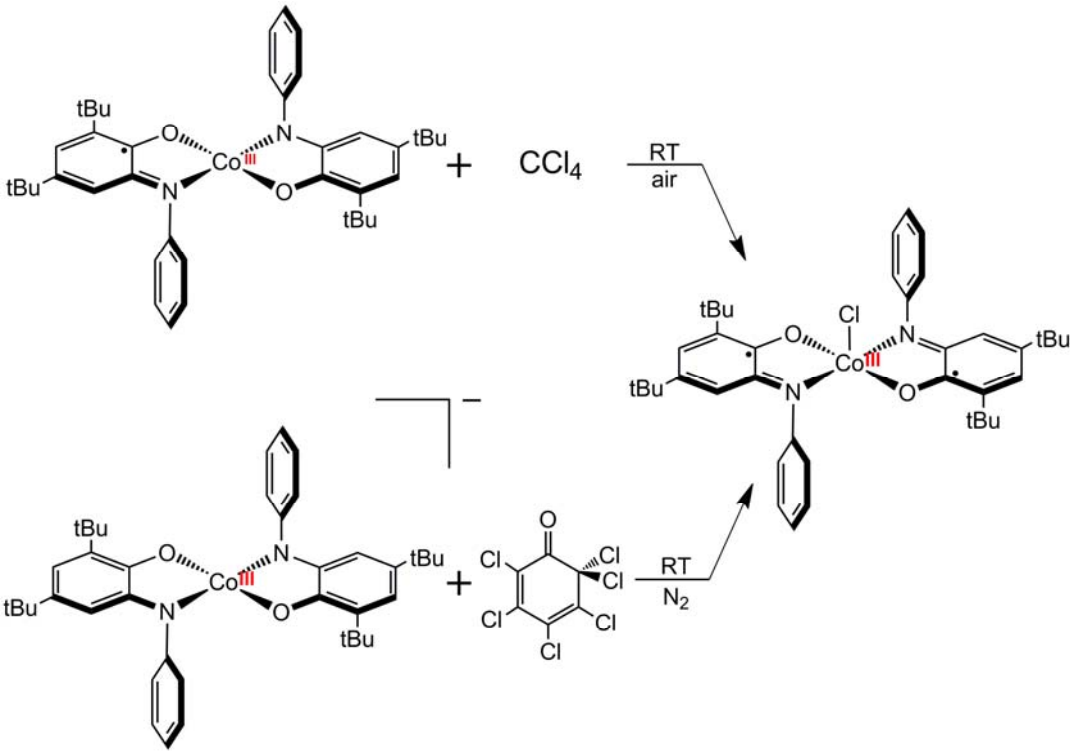

Scheme 2.1.

made based on X-ray crystallographic data. This assignment also supports the diamagnetic nature of $Co^{III}Cl(isq^{Ar})_2$ created by anti-ferromagnetic coupling of both ligand radicals to both unpaired electrons on the cobalt(III) center.

As illustrated in Scheme 2.1, quantitative conversion of $Co^{III}(ap^{Ar})(isq^{Ar})$ to $Co^{III}Cl(isq^{Ar})_2$ occurs by net addition of a chlorine radical. Because the Co–Cl bond-forming reactions are formally a reduction of $Cl^{\bullet}$ to Cl^{-}, they occur with one electron oxidation of the $Co^{III}(ap)(isq)$ fragment, which is ligand centered based on the characterization of both the starting material and the product. Addition of 1 equivalent of the radical inhibitor 2,6-di-*tert*-butyl-4-methylphenol (BHT) to THF solutions containing $Co^{III}(ap^{Ar})(isq^{Ar})$ results in a significant decrease in its rate of reaction with CCl_4. While

addition of 5 equivalents CCl_4 to $Co^{III}(ap^{Ph})(isq^{Ph})$ affords quantitative conversion to $Co^{III}Cl(isq^{Ph})_2$ in seconds, with added BHT the same reaction takes hours to reach completion. The origin of this inhibition is apparently a reaction of $Co^{III}(ap^{Ph})(isq^{Ph})$ with BHT. Accordingly, addition of 1 equivalent BHT to $Co^{III}(ap^{Ph})(isq^{Ph})$ in THF or CH_3CN under N_2 affords an immediate color change from blue to olive green. The dark green color is slowly discharged on addition of CCl_4 to afford $Co^{III}Cl(isq^{Ph})_2$.

2.3.5. Two-electron Co–Cl bond-forming reaction

Reaction of CH_3CN solutions of the $[Co^{III}(ap^{Ar})_2]^-$ complexes with 1 equivalent 2,3,4,5,6,6-hexachloro-2,4-cyclohexadien-1-one, which serves as a source of electrophilic Cl^+,[40] immediately gives $Co^{III}Cl(isq^{Ar})_2$ (Figure 2.8). The reaction is quantitative and proceeds without the accumulation of any observable intermediates at

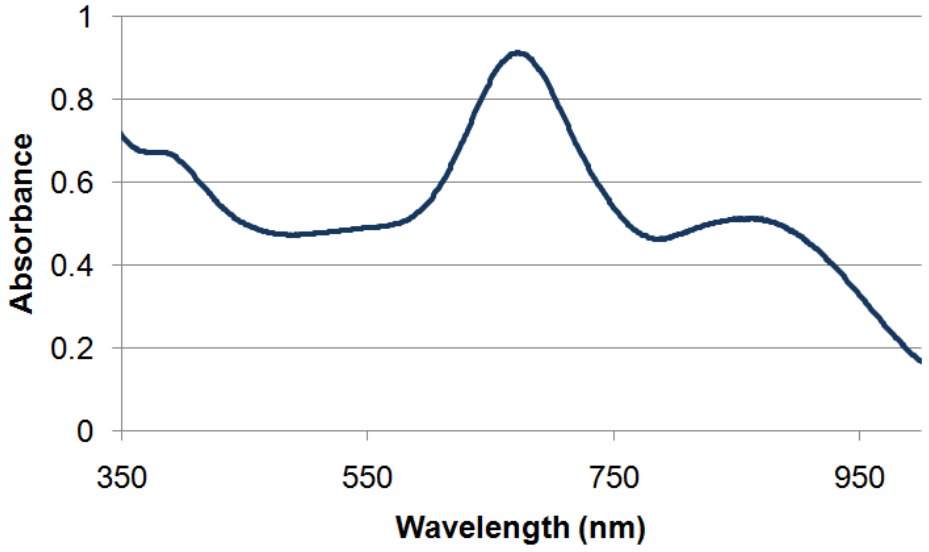

Figure 2.8. Sample UV-vis absorption of product of both reactions with cholride electrophiles. Spectrum matches that of previously reported $Co^{III}(Cl)(isq^{Ar})_2$.

298 K, as evidenced by UV–vis spectroscopy. The rate of $Co^{III}Cl(isq^{Ph})_2$ formation is unaffected by addition of 1 equivalent BHT to the reaction mixture. Control reactions confirm that $[Co^{III}(ap^{Ph})_2]^-$ does not react with added BHT. The bond-forming reaction with net Cl^+ is a two electron redox process as the electrophilic addition to $[Co^{III}(ap^{Ar})_2]^-$ formally reduces Cl^+ to Cl^- (Scheme 2.1). However, the two electron oxidation of the square planar cobalt(III) fragment is not metal-centered because the redox-active ligands each supply one electron for the reaction. Addition of 1 equivalent CCl_4 to CH_3CN solutions of $[Co^{III}(ap^{Ph})_2]^-$ gives no reaction over days at ambient temperature, as evidenced by UV–vis spectroscopy.

2.3.6. Two-electron Co–Br bond-forming reaction

Reaction of CH_3CN solutions of the $[Co^{III}(ap^{Ar})_2]^-$ complexes with 1 equivalent 2,4,4,6-tetrabromo-2,5-cyclohexadienone, which serves as a source of electrophilic Br^+,[40] immediately gives a color change to a similar blue material as the $Co^{III}Cl(isq)_2$ (Figure 2.9). While this material is unreported, given the similarities of the reactions and the UV-vis spectra, the product is believed to be $Co^{III}Br(isq)_2$. Crystals suitable for X-ray diffraction were of relatively little value as the $Co^{III}Cl(isq)_2$ and $Co^{III}I(isq)_2$ complexes have been previously investigated[26] and crystals of the new material were, therefore, not obtained.

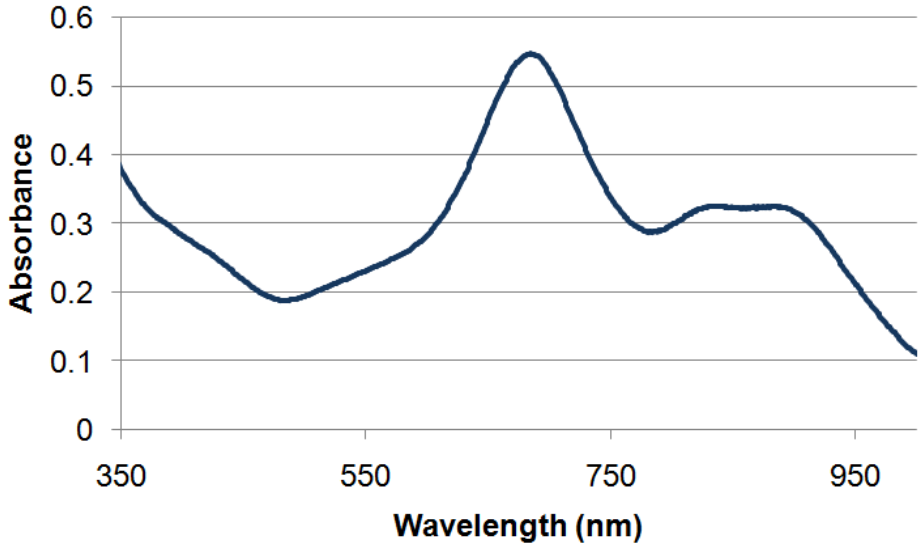

Figure 2.9. UV-vis absorption of product of reaction with Br^+ electrophile. Species tentatively assigned as $Co^{III}(Br)(isq^{Ar})_2$ due to reaction and product similarities with the analogous $Co^{III}(Cl)(isq^{Ar})_2$ complex.

2.4. Discussion

2.4.1. Structure and electronic assignment of four-coordinate complexes

The structural and electronic properties of the square planar cobalt electron-transfer pairs reported here are notable in several respects. First, our successful isolation of the $Co(L^{Ph})_2$ complexes demonstrates that, contrary to a previous report,[30] steric bulk at the *ortho*-positions of the ligand *N*-aryl group is not a prerequisite for stabilization of a four-coordinate cobalt complex. This ability to forego bulky ligands is essential for the development of reaction chemistry at these complexes. With all previously reported analogs, the substituents at the 2 or 6 position on the N-phenyl ring

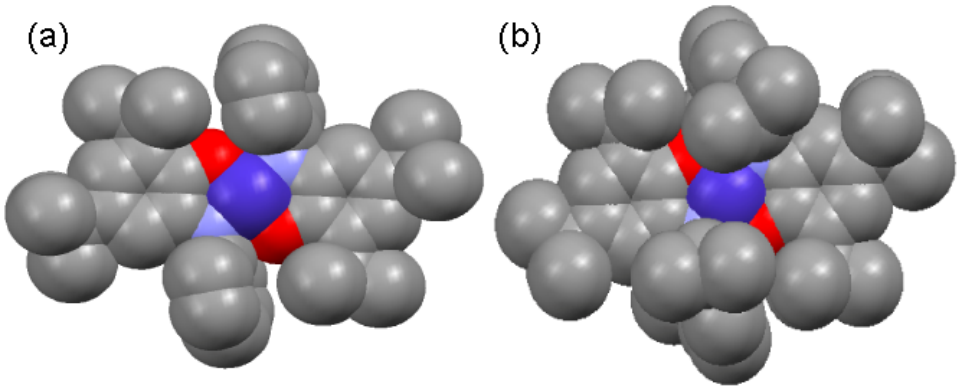

Figure 2.10. (a) Space-filling model of $[Co^{III}(ap^{Ph})_2]^-$ showing the accessible metal center (royal blue) **(b)** Space-filling model of $[Co^{III}(ap^{iPr})_2]^-$ showing the steric crowding at the metal center (royal blue) created by the isopropyl substituents on the N-phenyl ring in the 2 and 6 positions. Atomic dimensions are the atomic van der Waals radii. Hydrogen atoms are omitted. Co (royal blue), O (red), N (light blue), and C (gray).

creates steric crowding around the metal center (Figure 2.10) which hinders substrate access to the cobalt center.

Second, the X-ray crystallographic data for both the neutral *S*=½ and anionic *S*=1 complexes suggest that they are both best formulated as cobalt(III), so addition of an electron to $Co^{III}(ap^{Ar})(isq^{Ar})$ complexes occurs at redox-active ligand. This proposed charge distribution agrees with a recent assignment of a closely related electron-transfer pair containing an *ortho*-trifluoromethyl substituent on the ligand *N*-aryl group.[26]

It should be noted that an alternative electronic structure assignment has been proposed for the charge neutral *S*=½ complexes. Poddel'sky and coworkers argue that these materials may be better formulated as $Co^{II}(isq^{Ar})_2$ containing a low spin d^7 cobalt(II) ion ligated by two iminobenzoseminonate(1–) radicals. They propose that the two organic radicals couple antiferromagnetically.[29,36] The basis for this claim is previously

reported EPR spectra for two $Co^{III}(ap^{Ar})(isq^{Ar})$ complexes that exhibit features expected for an electron localized on the cobalt ion.[29,26] However, the cobalt(III) assignment proposed by Wieghardt and coworkers, in fact, invokes a metal-centered radical that is consistent with the observed EPR data.[26] Moreover, Poddel'sky and coworkers suggest that the unpaired electrons in an *S*=1 square planar cobalt(III) center would occupy MOs that derive from the metal $d_{x^2-y^2}$ and d_{z^2} orbitals,[36] but this is incorrect. Calculations on a very closely related system clearly show that the unpaired electrons are in orbitals of b_{2g} and b_{3g} symmetry that are primarily of metal d_{xz} and d_{yz} parentage.[26] In this scheme, overlap with the amidophenolate π-donor MOs raises the energy of the metal b_{2g} and b_{3g} orbitals and provides a pathway for facile intramolecular ligand-to-metal charge transfer. Because the ligand metrical parameters for $Co^{III}(ap^{Ph})(isq^{Ph})$ are indistinguishable from those of the previously reported ^{i}Pr congener,[29] we suggest that all of these complexes are better described as $Co^{III}(ap^{Ar})(isq^{Ar})$ in the ground state.

Use of the isopropyl substituted ligand alters the sterics surrounding the metal center. The isopropyl groups in the *ortho*-position on the N-phenyl point directly toward the cobalt above and below the plane of the amidophenol ligands. This substitution has little effect on the electronic redox-potentials as observed in the similar redox potentials of the material. However, substitution of two chlorides in the meta positions of each N-phenyl greatly affects the redox potentials, altering the events by 150 mV and 300 mV less reducing. These substitutions are made away from the cobalt and the large halide atoms do not alter access to the metal center.

2.4.2. Changes in $[Co^{III}(ap^{Ar})_2]^-$ in various solvents

Several possible explanations for the observed color changes evoked by the solvent differences can be proposed. The change in appearance of the $[Co^{III}(ap^{Ar})_2]^-$ material in THF, toluene, and pentane versus CH_3CN, benzene, and DMSO could be attributed to outer sphere electron transfer which oxidizes the material by one electron to the $Co^{III}(ap^{Ar})(isq^{Ar})$ species. However, given that this color change is reversible when the THF is removed and the material is redissolved in CH_3CN and that crystals grown out of THF:pentane solutions remain monoanionic, this is not believed to be the case. The UV-vis features are established to be largely ligand-to-ligand charge transfer bands (LLCT).[26] If a change in the solvent induces a change in the localization of the π orbital electrons or the mix of the metal and ligand molecular orbitals, this could significantly shift the electronic transitions within the complex. The UV-vis spectrum with λ_{max} identical to the neutral, mixed ligand complex could be mimicked by the fully reduced complex if instead of the assigned $[Co^{III}(ap^{Ar})_2]^-$ formulation, the material took on a more $[Co^{II}(ap^{Ar})(isq^{Ar})]^-$ character. Given that the four absorbance bands are LLCT and not MLCT, the change from cobalt(III) to cobalt(II) would play little part in the UV-vis spectra but the change from fully reduced to a mixed ligand set would be evident. Reports of a similar change in electron density having such a great effect on the appearance of the complex have been documented in related systems.[41,42]

Studies comparing THF and CH_3CN solutions with varying mole ratios of the two solvents demonstrate a linear relationship in the change in the spectra. Therefore, we cannot conclude that the behavior is a result of preferential binding of one solvent. Given that the counterion affects this behavior, it is speculated that the observed changes are

the result of aggregation. THF may interact with the molecule enough to disrupt this aggregation. However, this does not completely explain the observed color change as non-polar pentane would not interact with the molecule and toluene and benzene would be predicted to have similar dielectric constants. A full explanation of this behavior cannot be determined at this time.

2.4.3. Proof-of-principle bond-forming reactions at cobalt(III)

The ability of the redox-active ligands to accept and store electrons facilitates the preparation of coordinatively-unsaturated cobalt(III) complexes that can deliver multiple electrons at modest reduction potentials. This forms a basis for oxidative bond-forming reactions with electrophilic chlorine at cobalt(III) centers. Identical $Co^{III}Cl(isq^{Ar})_2$ products are obtained from reactions of $Co^{III}(ap^{Ar})(isq^{Ar})$ with sources of a net $Cl^{\bullet}$(via a one electron reaction) or by addition of electrophilic Cl^{+} to $[Co^{III}(ap^{Ar})_2]^{-}$ (via a two electron process). Both the radical addition and electrophilic addition reactions are formally oxidations of the metal fragments, but neither oxidizes the cobalt(III) center because the redox-active ligand manifold acts as a reservoir for electrons. As described above, facile transfer of electrons from the ligand to the metal derives from a high degree of covalency in the metal–ligand bonding that is a result of the close match of the frontier orbital energies of cobalt(III) and the aminophenol-derived ligands.[26] In this way, the ligand-mediated Co–Cl bond-forming reactions reported herein are very similar to recent reports of pseudo-oxidative addition reactions of X_2 to redox-active ligand complexes that rely on ligand centered changes in oxidation state to accommodate the transformation without a formal change in oxidation state at the metal center.[14,17,18,43]

2.4.4. Mechanistic implications of reactions with $[Co^{III}(ap^{Ar})_2]^-$

Two possible mechanistic pathways (Scheme 2.2) were considered for the electrophilic addition reactions at $[Co^{III}(ap^{Ar})_2]^-$: (a) direct nucleophilic attack of the cobalt(III) center on the Cl^+ electrophile, resulting in a two electron oxidation of the metal fragment; (b) initial outer-sphere one electron transfer (ET) to generate the radical pair, $Co^{III}(ap^{Ar})(isq^{Ar})$ and $Cl^{\bullet}$, followed by coupling with bond formation. The facile reactions of $Co^{III}(ap^{Ar})(isq^{Ar})$ with sources of chlorine radical $Cl^{\bullet}$ to generate $Co^{III}Cl(isq^{Ar})_2$ demonstrate that the stepwise mechanism (b) is viable, but experiments performed in the presence of the radical inhibitor support mechanism (a). Namely, the reactions of $Co^{III}(ap^{Ph})(isq^{Ph})$ with CCl_4 is retarded by addition of BHT, but the reaction of $[Co^{III}(ap^{Ph})_2]^-$ with 2,3,4,5,6,6-hexachloro-2,4-cyclohexadien-1-one as a Cl^+ source is unaffected with added BHT. Although the mechanism of this radical inhibition is ill

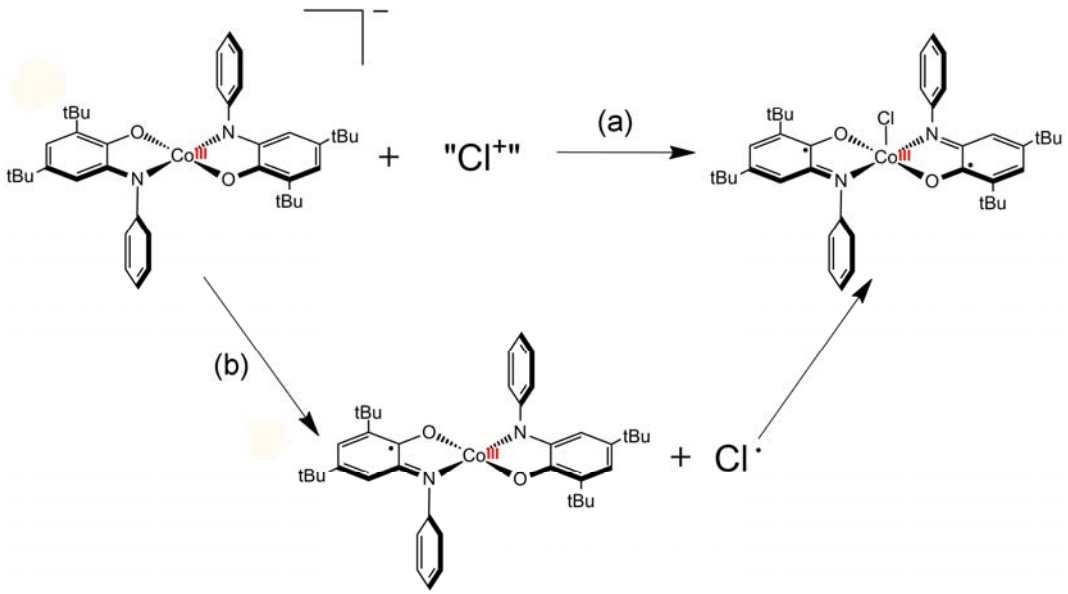

Scheme 2.2.

defined, control reactions demonstrate that $Co^{III}(ap^{Ph})(isq^{Ph})$ reacts rapidly with BHT under the reaction conditions. Accordingly, mechanisms that invoke formation of a long-lived $Co^{III}(ap^{Ph})(isq^{Ph})$ intermediate in the reaction of $[Co^{III}(ap^{Ph})_2]^-$ with net Cl^+ (including mechanism b) can likely be ruled out.

2.5. Conclusions

In this study, we have synthesized and characterized a series of square planar cobalt(III) complexes with redox-active amidophenol-derived ligands. Establishment that the redox event between the monoanion and neutral species is formally ligand based provides evidence that the redox active ligands may participate in reactions at the cobalt center. The electrochemistry also indicates a monocationic species is accessible at modest potentials. The two redox events of the complex occur within 0.5 V of each other and suggest that the complexes should be able to facilitate multi-electron changes in their oxidation state.

The proof-of-concept reactions with halide sources demonstrate that this redox potential can be used for bond-formation. Details of the reaction chemistry suggest that the *S*=½ $Co^{III}(ap^{Ar})(isq^{Ar})$ complexes behave as efficient radical scavengers but the $[Co^{III}(ap^{Ar})_2]^-$ complexes react as multi-electron nucleophiles and do not react efficiently with sources of net $Cl^{\bullet}$. This is somewhat surprising given the *S*=1 diradical ground state of the anionic complexes. The reactivity patterns of the $[Co^{III}(ap^{Ar})_2]^-$ species are therefore more reminiscent of the well-known cobaloxime(I) complexes that are closed-shell d^8 nucleophiles.[44] However, the $[Co^{III}(ap^{Ar})_2]^-$ complexes reported here are not strong outer-sphere reductants, being oxidized at potentials 200–400 mV less negative

than most cobalt(I) materials.[44,45] Control of single-electron versus multi-electron reactivity derives from management of ligand electron inventory. This ability to modulate the redox selectivity of the metal center to achieve two electron reactions under gentle conditions is predicated entirely on the redox-activity of the ligands and is a key design feature for the development of naturally abundant transition metals as catalysts for selective bond-making and bond-breaking reactions.

The redox-activity of the amidophenolate ligands exhibited in these complexes facilitates selective multi-electron reactions at square planar cobalt(III) centers. This demonstration of fundamental reactivity led us to investigate more useful bond-forming reactivity facilitated by these complexes (Chapter 4 and 5). In this study, we have demonstrated that modulation of the ligand oxidation state affords a unique mechanism to select for multi-electron redox reactivity over potentially competing one electron pathways.

2.6. References

1. Lewis, N. S.; Nocera, D. G., Powering the planet: chemical challenges in solar energy utilization. *Proc. Natl. Acad. Sci. U. S. A.* **2006,** *103*, 15729-15735.

2. Eisenberg, R.; Nocera, D. G., Preface: Overview of the Forum on Solar and Renewable Energy. *Inorg. Chem.* **2005,** *44*, 6799-6801.

3. Trost, B. M.; Fleming, I., *Comprehensive Organic Synthesis: Selectivity, Strategy, and Efficiency in Modern Organic Chemistry*. Pergamon Press: 1992; Vol. 9.

4. de Meijere, A.; Diederich, F., *Metal-catalyzed Cross-coupling Reactions, Second completely Revised and Enlarged Edition*. Wiley-VCH: 2004; Vol. 1.

5. Hartwig, J. F., Activation and Functionalization of C-H Bonds. Oxford University Press: 2004; Vol. 885, p 136.

6. Stahl, S.; Labinger, J. A.; Bercaw, J. E., Homogeneous oxidation of alkanes by electrophilic late transition metals. *Angew. Chem., Int. Ed.* **1998,** *37*, 2181-2192.

7. Stahl, S. S., Palladium oxidase catalysis. Selective oxidation of organic chemicals by direct dioxygen-coupled turnover. *Angew. Chem., Int. Ed.* **2004,** *43*, 3400-3420.

8. Goldberg, K. I.; Goldman, A. S., *Activation and Functionalization of C-H Bonds*. Oxford University Press: 2004.

9. (a) Labinger, J. A.; Bercaw, J. E., Understanding and exploiting C-H bond activation. *Nature* **2002,** *417*, 507-514; (b) Greenwood, N. N.; Earnshaw, A., *Chemistry of the Elements, second edition*. Butterworth Heinemann: 1997.

10. Poddel'sky, A. I.; Cherkasov, V. K.; Abakumov, G. A., Transition metal complexes with bulky 4,6-di-tert-butyl-N-aryl(alkyl)-o-iminobenzoquinonato ligands: Structure, EPR and magnetism. *Coord. Chem. Rev.* **2009,** *253*, 291-324.

11. Pierpont, C. G.; Lange, C. W., The chemistry of transition metal complexes containing catechol and semiquinone ligands. *Prog. Inorg. Chem.* **1994,** *41*, 331-442.

12. Pierpont, C. G., Studies on charge distribution and valence tautomerism in transition metal complexes of catecholate and semiquinonate ligands. *Coord. Chem. Rev.* **2001,** *216-217*, 99-125.

13. Chaudhuri, P.; Wieghardt, K., Phenoxyl radical complexes. *Prog. Inorg. Chem.* **2001,** *50*, 151-216.

14. Blackmore, K. J.; Ziller, J. W.; Heyduk, A. F., "Oxidative Addition" to a Zirconium(IV) Redox-Active Ligand Complex. *Inorg. Chem.* **2005,** *44*, 5559-5561.

15. Haneline, M. R.; Heyduk, A. F., C-C Bond-Forming Reductive Elimination from a Zirconium(IV) Redox-Active Ligand Complex. *J. Am. Chem. Soc.* **2006,** *128*, 8410-8411.

16. Zarkesh, R. A.; Heyduk, A. F., Reactivity of Diazoalkanes with Tantalum(V) Complexes of a Tridentate Amido-Bis(phenolate) Ligand. *Organometallics* **2009,** *28*, 6629-6631.

17. Ketterer, N. A.; Fan, H.; Blackmore, K. J.; Yang, X.; Ziller, J. W.; Baik, M.-H.; Heyduk, A. F., π.bul.-π.bul. Bonding Interactions Generated by Halogen Oxidation of Zirconium(IV) Redox-Active Ligand Complexes. *J. Am. Chem. Soc.* **2008,** *130*, 4364-4374.

18. Blackmore, K. J.; Sly, M. B.; Haneline, M. R.; Ziller, J. W.; Heyduk, A. F., Group IV Imino-Semiquinone Complexes Obtained by Oxidative Addition of Halogens. *Inorg. Chem.* **2008,** *47*, 10522-10532.

19. Nguyen, A. I.; Zarkesh, R. A.; Lacy, D. C.; Thorson, M. K.; Heyduk, A. F., Catalytic nitrene transfer by a zirconium(iv) redox-active ligand complex. *Chem. Sci.* **2011,** *2*, 166-169.

20. Bart, S. C.; Lobkovsky, E.; Bill, E.; Chirik, P. J., Synthesis and Hydrogenation of Bis(imino)pyridine Iron Imides. *J. Am. Chem. Soc.* **2006,** *128*, 5302-5303.

21. Bouwkamp, M. W.; Bowman, A. C.; Lobkovsky, E.; Chirik, P. J., Iron-Catalyzed [2π + 2π] Cycloaddition of α,ω-Dienes: The Importance of Redox-Active Supporting Ligands. *J. Am. Chem. Soc.* **2006,** *128*, 13340-13341.

22. Stanciu, C.; Jones, M. E.; Fanwick, P. E.; Abu-Omar, M. M., Multi-electron Activation of Dioxygen on Zirconium(IV) to Give an Unprecedented Bisperoxo Complex. *J. Am. Chem. Soc.* **2007,** *129*, 12400-12401.

23. Rolle, C. J.; Hardcastle, K. I.; Soper, J. D., Reactions of tetrabromocatecholatomanganese(III) complexes with dioxygen. *Inorg. Chem.* **2008,** *47*, 1892-1894.

24. Lu, C. C.; Weyhermueller, T.; Bill, E.; Wieghardt, K., Accessing the Different Redox States of α-Iminopyridines within Cobalt Complexes. *Inorg. Chem.* **2009,** *48*, 6055-6064.

25. Blackmore, K. J.; Lal, N.; Ziller, J. W.; Heyduk, A. F., Catalytic Reactivity of a Zirconium(IV) Redox-Active Ligand Complex with 1,2-Diphenylhydrazine. *J. Am. Chem. Soc.* **2008,** *130*, 2728-2729.

26. Bill, E.; Bothe, E.; Chaudhuri, P.; Chlopek, K.; Herebian, D.; Kokatam, S.; Ray, K.; Weyhermueller, T.; Neese, F.; Wieghardt, K., Molecular and electronic structure of four- and five-coordinate cobalt complexes containing two o-phenylenediamine- or two o-aminophenol-type ligands at various oxidation

levels: An experimental, density functional, and correlated ab initio study. *Chem. Eur. J.* **2005,** *11*, 204-224.

27. Verani, C. N.; Gallert, S.; Bill, E.; Weyhermuller, T.; Wieghardt, K.; Chaudhuri, P., [Tris(o-iminosemiquinone)cobalt(III)] - a radical complex with an St = 3/2 ground state. *Chem. Comm.* **1999**, 1747-1748.

28. Herebian, D.; Ghosh, P.; Chun, H.; Bothe, E.; Weyhermuller, T.; Wieghardt, K., Cobalt(II)/(III) complexes containing o-iminothiobenzosemiquinonato(1-) and o-iminobenzosemiquinonato(1-) π-radical ligands. *Eur. J. Inorg. Chem.* **2002**, 1957-1967.

29. Poddel'sky, A. I.; Cherkasov, V. K.; Fukin, G. K.; Bubnov, M. P.; Abakumova, L. G.; Abakumov, G. A., New four- and five-coordinated complexes of cobalt with sterically hindered o-iminobenzoquinone ligands: synthesis and structure. *Inorg. Chim. Acta* **2004,** *357*, 3632-3640.

30. Abakumov, G. A.; Cherkasov, V. K.; Bubnov, M. P.; Abakumova, L. G.; Ikorskii, V. N.; Romanenko, G. V.; Poddel'sky, A. I., Synthesis and structures of five-coordinate bis-o-iminobenzosemiquinone complexes M(ISQ-R)2X (X = Cl, Br, I, or SCN; M = CoIII, FeIII, or MnIII). *Russ. Chem. Bull.* **2006,** *55*, 44-52.

31. Abakumov, G. A.; Druzhkov, N. O.; Kurskii, Y. A.; Shavyrin, A. S., NMR study of products of thermal transformation of substituted N-aryl-o-quinoneimines. *Russ. Chem. Bull.* **2003,** *52*, 712-717.

32. Apex II, Analytical X-ray Systems, Brukers AXS, Inc., Madison, WI, 2005.

33. Saint Version 6.45A, Analytical X-ray Systems, Brukers AXS, Inc., Madison, WI, 2003.

34. Shelxtl Version 6.12, Analytical X-ray Systems, Bruker AXS, Inc., Madison, WI, 2002.

35. Demadis, K. D.; Hartshorn, C. M.; Meyer, T. J., The localized-to-delocalized transition in mixed-valence chemistry. *Chem. Rev.* **2001,** *101*, 2655-2685.

36. Poddelsky, A. I.; Vavilina, N. N.; Somov, N. V.; Cherkasov, V. K.; Abakumov, G. A., Triethylantimony(V) complexes with bidentate O,N-, O,O- and tridentate

O,N,O'-coordinating o-iminoquinonato/o-quinonato ligands: Synthesis, structure and some properties. *J. Organomet. Chem.* **2009,** *694*, 3462-3469.

37. Evans, D. F., The determination of the paramagnetic susceptibility of substances in solution by nuclear magnetic resonance. *J. Am. Chem. Soc.* **1959**, 2003-2005.

38. Live, D. H.; Chan, S. I., Bulk susceptibility corrections in nuclear magnetic resonance experiments using superconducting solenoids. *Anal. Chem.* **1970,** *42*, 791-792.

39. Connelly, N. G.; Geiger, W. E., Chemical Redox Agents for Organometallic Chemistry. *Chem. Rev.* **1996,** *96*, 877-910.

40. France, S.; Wack, H.; Taggi, A. E.; Hafez, A. M.; Wagerle, T. R.; Shah, M. H.; Dusich, C. L.; Lectka, T., Catalytic, asymmetric α-chlorination of acid halides. *J. Am. Chem. Soc.* **2004,** *126*, 4245-4255.

41. Adams, D. M.; Dei, A.; Rheingold, A. L.; Hendrickson, D. N., Bistability in the [CoII(semiquinonate)2] to [CoIII(catecholate)(semiquinonate)] valence-tautomeric conversion. *J. Am. Chem. Soc.* **1993,** *115*, 8221-8229.

42. Caneschi, A.; Cornia, A.; Dei, A., Valence Tautomerism in a Cobalt Complex of a Schiff Base Diquinone Ligand. *Inorg. Chem.* **1998,** *37*, 3419-3421.

43. Mukherjee, C.; Weyhermueller, T.; Bothe, E.; Chaudhuri, P., Oxidation of an o-Iminobenzosemiquinone Radical Ligand by Molecular Bromine: Structural, Spectroscopic, and Reactivity Studies of a Copper(II) o-Iminobenzoquinone Complex. *Inorg. Chem.* **2008,** *47*, 2740-2746.

44. Schrauzer, G. N.; Deutsch, E., Reactions of cobalt(I) supernucleophiles. The alkylation of vitamin B12s, cobaloximes(I), and related compounds. *J. Am. Chem. Soc.* **1969,** *91*, 3341-50.

45. Hu, X. L.; Brunschwig, B. S.; Peters, J. C., Electrocatalytic Hydrogen Evolution at Low Overpotentials by Cobalt Macrocyclic Glyoxime and Tetraimine Complexes. *J. Am. Chem. Soc.* **2007,** *129*, 8988-8998.

Pseudo-oxidative addition of alkyl halides to nucleophilic cobalt(III)

3.1. Introduction

The nucleophilicity of the $[Co^{III}(ap)_2]^-$ species presented in Chapter 2 resembles that of the coenzyme B12, commonly called cobalamin, and its related small molecule models. These enzymes are known for their ability to transfer carbon fragments from one molecule to another at four-coordinate cobalt metal centers.[1] The cobalamins utilize a metal-centered cobalt(I) to cobalt(III) oxidation. Well studied models of the active site, known as cobaloximes, have exhibited similar reactivity.[1,2] These small molecule models have been shown to activate alkyl halides and form stable cobalt-carbon bonds through an S_N2 reaction.[1,3] This two electron, bond-forming reaction occurs with a corresponding oxidation of the cobalt metal. Subsequent reaction of the alkylcobaloximes with organometallic reagents such as Grignard reagents (RMgX) results in isolation of stable dialkylcobaloxime or alkylarylcobaloxime species.[4] However, generation of the reactive cobalt(I) form of these cobaloximes requires severe reduction potentials, more negative by 200-400 mV,[1,5,6] than those observed with the $[Co^{III}(ap^{Ar})_2]^-$ complexes.[7] This suggests that all ligand-centered reactions at the $[Co^{III}(ap^{Ar})_2]^-$ complexes may allow access to both cobalamin-like oxidative reactions, as well as reductive chemistry that is typically inaccessible at cobalt(III).

The use of unactivated alkyl halides as reagents in cross-coupling reactions remains a challenge. Oxidative addition of the alkyl halide is often very slow and the metal-alkyl product formed is prone to rapid β-hydride elimination.[8] Reagents historically

have been selected that do not contain β-hydrogens or catalyst have been designed with ligands able to block the degradation pathway.[8] However, work over the past 15 years has developed systems able to form new carbon-carbon bonds from alkyl halide precursors, often by avoiding the problematic oxidative addition reaction entirely.[9-12] The ability of cobaloxime to activate alkyl halides and form stable products is limited in that the alkylcobaloximes usually react further through radical pathways, relying on the photolysis of the cobalt-carbon bond to generate a reactive alkyl radical.[13]

We previously outlined in Chapter 2 how the square planar cobalt complexes $[Co^{III}(ap^{Ar})_2]^-$ can act as nucleophiles but are also mild two electron reductants poised for multi-electron reactivity.[7] These complexes demonstrate the ability of redox-active amidophenolate ligands to deliver electrons for bond-forming reactions at square planar cobalt(III) centers (see Figure 2.1) with halide electrophiles.[7] However, these reactions were simply an exploration of proof-of-principle and serve little purpose to a synthetic chemist. In Chapter 3, we build upon this investigation and show how the nucleophilic properties of these complexes also facilitate the well-defined two-electron pseudo-oxidative addition of alkyl halides at the cobalt(III) metal center. This activation of alkyl halides represents one step in coupling cycles needed to form new carbon-carbon bonds from alkyl halides. Characterization of the product of the $[Co^{III}(ap^{Ar})_2]^-$ reaction with various alkyl halides and examination of the mechanism gives insight into how this cobalt complex can be used to facilitate multi-electron reactivity.

3.2. Experimental Details

3.2.1. General Considerations

Unless otherwise specified, all manipulations were performed under anaerobic conditions using standard vacuum line techniques, or in an inert atmosphere glove box under purified nitrogen. NMR spectra were acquired on a Varian Mercury 300 spectrometer (300.323 MHz for ^{1}H) at ambient temperature. Chemical shifts are reported in parts per million (ppm) relative to TMS, with the residual solvent peak serving as an internal reference. UV–visible absorption spectra were acquired using a Varian Cary 50 spectrophotometer equipped with a water-jacketed cell holder fitted to a Peltier temperature controller. Unless otherwise specified, all electronic absorption spectra were recorded at 25 °C in 1 cm quartz cells. UV–vis chemical kinetics data were fit by iterative multivariate analysis using the commercially available software Specfit/32 from Spectrum Software Associates. IR spectra were obtained by attenuated total reflection (ATR) through a diamond plate on a Bruker Optics Alpha-P FTIR spectrometer. All mass spectra were recorded in the Georgia Institute of Technology Bioanalytical Mass Spectrometry Facility. Electrospray ionization mass spectrometry (ESI–MS) was carried out with acetonitrile or tetrahydrofuran solutions using a Micromass Quattro LC spectrometer. Gas chromatography–mass spectrometry (GC–MS) analyses used an Agilent 6890 GC equipped with an autosampler and a Restek Rxi-5ms column (30 m x 0.25 mm i.d., 0.25 μm film thickness). 1 μL injections were made at a 50:1 split ratio. The GC oven program consisted of a hold at 30 °C for 1 min, followed by a 15 °C min^{-1} ramp to 300 °C, and then a hold at 300 °C for 11 minutes. The mass spectrometer used in tandem was a Micromass AutoSpec electro-ionization (EI) detector. Elemental analyses

were performed by Atlantic Microlab, Inc., Norcross, GA. All analyses were performed in duplicate, and the reported compositions are the average of the two runs.

3.2.2. Methods and Materials

Anhydrous acetonitrile (CH_3CN), tetrahydrofuran (THF), toluene, and dichloromethane (CH_2Cl_2) solvents for air- and moisture-sensitive manipulations were purchased from Sigma-Aldrich, further dried by passage through columns of activated alumina, degassed by at least three freeze-pump-thaw cycles, and stored under N_2 prior to use. CH_3CN and THF solvents used for cross-coupling reactions were further dried over CaH_2 and $Na_{(s)}$, respectively. Deuterated acetonitrile (CD_3CN) and tetrahydrofuran (THF–d_8) were purchased from Cambridge Isotope Laboratories, degassed by three freeze-pump-thaw cycles, vacuum distilled from CaH_2 or $Na_{(s)}$, respectively, and stored under a dry N_2 atmosphere prior to use. $Co^{III}(ap^{Ph})(isq^{Ph})$, $Co^{III}(ap^{iPr})(isq^{iPr})$, $Co^{III}(ap^{Cl})(isq^{Cl})$, $Na[Co^{III}(ap^{Ph})_2]$, $Na[Co^{III}(ap^{iPr})_2]$, and $Na[Co^{III}(ap^{Cl})_2]$[7,14] were prepared by previously published methods and as reported in Chapter 2. Iodobenzene, methyl triflate (CH_3OTf) and the haloalkanes, dicholoromethane–d_8 (CD_2Cl_2), methyl iodide (CH_3I), bromochloromethane (CH_2ClBr), ethyl bromide (EtBr), ethyl iodide (EtI), octyl bromide (OctBr), benzyl chloride ($PhCH_2Cl$), benzyl bromide ($PhCH_2Br$), iodobenzene (PhI) and vinyl bromide (C_2H_2Br) were purchased from Sigma-Aldrich and degassed before use. All other chemicals were purchased from Sigma-Aldrich and used as received.

3.2.3. Synthesis of $Co^{III}(CH_2Cl)(isq^{Ph})_2$

A 5 dram scintillation vial was charged with $Na[Co^{III}(ap^{Ph})_2]$ (0.070 g, 0.104 mmol) and CH_3CN (10 mL). To the resulting dark purple solution was added CH_2Cl_2 (32.5 μL, 0.508 mmol). The reaction mixture was fitted with a Teflon-lined cap, wrapped in aluminum foil, and stirred for 12 hours under N_2 during which time a color change to emerald green was observed and green solids precipitated from solution. The solids were collected by vacuum filtration and the organometallic product was extracted into toluene and filtered to remove NaCl. Removal of the solvent *in vacuo* afforded $Co^{III}(CH_2Cl)(isq^{Ph})_2$ (0.023 g, 0.033 mmol, 32%) as green powder. The solids were purified by slow cooling of a saturated 3:1 CH_3CN:CH_2Cl_2 solution to yield single crystals of $Co^{III}(CH_2Cl)(isq^{Ph})_2$ suitable for study by X-ray diffraction. UV–vis (toluene) λ_{max}, nm (ε, M^{-1} cm^{-1}): 445 (3260), 600 (2070), 845 (19800). ESI–MS (*m/z*): 698 $[M]^+$. FTIR (ATR) cm^{-1}: 3055 (w), 3038 (w), 2956 (m), 2900 (m), 2861 (m), 2156 (w), 2023 (w), 1973 (w), 1578 (w), 1535 (w), 1482 (m), 1458 (m), 1446 (m), 1434 (m), 1390 (w), 1378 (w), 1357 (m), 1303 (m), 1261 (m), 1216 (w), 1201 (w), 1183 (w), 1166 (w), 1139 (s), 1105 (m), 1025 (m), 1002 (m), 923 (m), 911 (w), 882 (w), 859 (m), 766 (w), 739 (s), 693 (s), 661 (s), 619 (w), 609 (w), 594 (w), 571 (w), 541 (w), 510 (m). ^1H NMR (300 MHz, 1:1 CD_3CN:THF–d_8, δ): 7.54 (10H), 7.18 (2H), 6.91 (2H), 4.53 (1H), 3.90 (1H), 1.14 (18H), 1.10 (18H) (all br s). Samples of $Co^{III}(CH_2Cl)(isq^{Ph})_2$ for elemental analysis were obtained from toluene solutions. The reported analysis is for $Co^{III}(CH_2Cl)(isq^{Ph})_2 \bullet 0.75C_7H_8$, and the presence of toluene in the sample was confirmed by ^1H NMR spectroscopy. Anal. Calcd for $C_{46.25}H_{58}N_2CoO_2Cl$: C, 72.30; H, 7.61; N, 3.65: Found: C, 72.42; H, 7.69; N, 3.86.

3.2.4. Synthesis of $Co^{III}(Et)(isq^{Ph})_2$

This complex was prepared by the procedure described above for preparation of $Co^{III}(CH_2Cl)(isq^{Ph})_2$, using $Na[Co^{III}(ap^{Ph})_2]$ (0.070 g, 0.104 mmol) and EtBr (0.39 μL, 0.530 mmol) in place of CH_2Cl_2, to give $Co^{III}(Et)(isq^{Ph})_2$ (0.044 g, 0.065 mmol, 62%). UV–vis (toluene) λ_{max}, nm (ε, M^{-1} cm^{-1}): 420 (2040), 690 (3570), 860 (14700). ESI–MS (*m/z*): 678 $[M]^+$. FTIR (ATR) cm^{-1}: 2951 (m), 2920 (m), 2852 (m), 1589 (w), 1537 (w), 1461 (m), 1438 (m), 1409 (w), 1380 (w), 1357 (s), 1293 (w), 1259 (s), 1227 (w), 1140 (s), 1105 (s), 1002 (m), 923 (m), 911 (m), 882 (m), 859 (m), 833 (m), 785 (w), 776 (m), 739 (s), 722 (m), 692 (s), 660 (s), 647 (m), 510 (m). ^1H NMR (300 MHz, 1:1 CD_3CN:THF–d_8, δ): 7.53 (10H), 7.13 (2H), 6.94 (2H), 1.15 (36H), 0.11 (3H), -0.44 (2H) (all br s). Samples of $Co^{III}(Et)(isq^{Ph})_2$ for elemental analysis were obtained from toluene solutions. The reported analysis is for $Co^{III}(CH_2Cl)(isq^{Ph})_2 \bullet 0.6C_7H_8$, and the presence of toluene in the sample was confirmed by ^1H NMR spectroscopy. Anal. Calcd for $C_{46.2}H_{59.8}N_2CoO_2$: C, 75.59; H, 8.21; N, 3.82; Found: C, 75.08; H, 8.74; N, 3.78.

3.2.5. Synthesis of $Co^{III}(Me)(isq^{Ph})_2$

This complex was prepared by the procedure described above for preparation of $Co^{III}(CH_2Cl)(isq^{Ph})_2$, using $Na[Co^{III}(ap^{Ph})_2]$ (0.069 g, 0.103 mmol) and CH_3I (0.33 μL, 0.530 mmol) in place of CH_2Cl_2, to give $Co^{III}(Me)(isq^{Ph})_2$ (0.033 g, 0.050 mmol, 49%). UV–vis (toluene) λ_{max}, nm (ε, M^{-1} cm^{-1}): 690 (3480), 860 (13300). ESI–MS (*m/z*): 664 $[M]^+$. FTIR (ATR) cm^{-1}: 3058 (w), 2951 (m), 2903 (m), 2867 (m), 2159 (w), 2030 (w), 1977 (w), 1592 (m), 1478 (m), 1463 (m), 1439 (m), 1360 (s), 1397 (m), 1260 (m), 1229 (m), 1200 (m), 1175 (m), 1164 (m), 1140 (m), 1025 (m), 1000 (w), 909 (w), 859 (m), 832

(m), 759 (s), 742 (s), 693 (s), 667 (w), 646 (w), 605 (w), 540 (m), 526 (m), 508(m). Anal. Calcd for $C_{41}H_{53}N_2CoO_2$: C, 74.07; H, 8.04; N, 4.21; Found: C, 73.35; H, 8.00; N, 4.13.

3.2.6. X-ray crystallography

Single crystals of $Co^{III}(CH_2Cl)(isq^{Ph})$ and $Co^{III}(Et)(isq^{Ph})$ suitable for X-ray diffraction analysis were coated with Paratone N, suspended in a small fiber loop and placed in a cooled nitrogen gas stream at 173 K on a Bruker D8 APEX II CCD sealed tube diffractometer. All data collection procedures, data processing and programs were the same for both samples. Data were measured using a series of combinations of phi and omega scans with 10 seconds frame exposures and 0.5° frame widths. Data collection, indexing and initial cell refinements were all carried out using apex II software.[15] Frame integration and final cell refinements were done using saint software.[16] The final cell parameters were determined from least-squares refinement on 6134 reflections for $Co^{III}(CH_2Cl)(isq^{Ph})$ and 9366 reflections for $Co^{III}(Et)(isq^{Ph})$. The structures were solved using direct methods and difference Fourier techniques using the shelxtl program package.[17] Hydrogen atoms were placed in their expected chemical positions using the HFIX command and were included in the final cycles of least-squares with isotropic U_{ij}'s related to the atoms ridden upon. All non-hydrogen atoms were refined anisotropically. Details of data collection and structure refinement are provided in Table 3.1.

Table 3.1. Crystallographic data and structure parameters for $Co^{III}(CH_2Cl)(isq^{Ph})_2$ and $Co^{III}(CH_3CH_2)(isq^{Ph})_2$.

Complex	$Co^{III}(CH_2Cl)(isq^{Ph})_2$	$Co^{III}(CH_3CH_2)(isq^{Ph})_2$
Empirical formula	$C_{41}H_{52}ClCoN_2O_{2.5}$	$C_{42}H_{55}CoN_2O_2$
Formula weight	707.23	678.81
T (K)	173(2)	173(2)
Crystal system	monoclinic	triclinic
Space group	Pc	P-1
Unit Cell dimensions		
a (Å)	9.2497(2)	13.3036(14)
b (Å)	12.6393(3)	13.449(14)
c (Å)	16.3642(4)	13.553(14)
α (°)	90	67.671(15)
β (°)	100.550(1)	85.679(16)
γ (°)	90	64.310(15)
V ($Å^3$)	1880.77(8)	1969(4)
Z	2	2
D_{calc} (g/cm^3)	1.249	1.145
Absorption coefficient (mm^{-1})	0.565	0.470
Crystal Size (mm)	0.43 x 0.43 x 0.19	0.32 x 0.17 x 0.15
θ range for data collection (°)	2.05 to 26.33	1.82 to 27.88
Index ranges	-11 ≤ h ≤ 9	-17 ≤ h ≤ 17
	-12 ≤ k ≤ 15	-17 ≤ k ≤ 17
	-19 ≤ l ≤ 18	-17 ≤ l ≤ 17
Reflections collected	13833	33238
Reflections unique	6134	9366
Goodness of fit on F^2	1.019	1.004
R [I>2σ(I)]	0.0612	0.0558
wR^2 (all data)	0.1785	0.1266

3.3. Results

3.3.1. Synthesis and characterization of $Co^{III}(CH_2Cl)(isq^{Ph})_2$

Our previous proof-of-principle study of the two electron bond-forming reaction of $[Co^{III}(ap)_2]^-$ with a source of a "Cl^+" fragment led us to investigate other, more interesting, reaction substrates. Addition of excess CH_2Cl_2 to purple CH_3CN solutions containing the

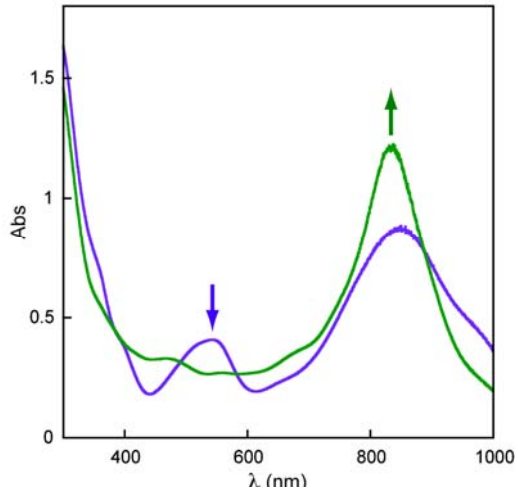

Figure 3.1. Selected UV-vis absorption data for reaction of 7.9 x 10^{-5} M $Na[Co^{III}(ap^{Ph})_2]$ (purple line) with 0.24 M CH_2Cl_2 in CH_3CN at 25°C under N_2 to generate green material at t = 240 minutes (green line), corresponding to the maximum yield observed while scanning over the entire spectral window (300-1000 nm).

$[Co^{III}(ap^{Ph})_2]^-$ (see Figure 2.1) anion gave quantitative conversion to a light sensitive bright green material over hours at 25°C (Figure 3.1). Electrospray ionization mass spectrometry (ESI-MS) of THF solutions containing the green product showed a molecular ion peak at 698 *m/z,* 49 mass units larger than the 649 *m/z* molecular ion peak corresponding to the $Co(L)_2$ core. This peak was shifted to 700 *m/z* when the reaction was performed with CD_2Cl_2 in place of CH_2Cl_2. These peaks correspond to the molecular weights of the $[Co^{III}(ap^{Ph})_2]^-$ reactant and a $[CH_2Cl]$ or $[CD_2Cl]$ fragments, respectively (Scheme 3.1).

Green crystals of the protio material were obtained from a concentrated $CH_3CN-CH_2Cl_2$ solution stored at –20°C for days. The X-ray structure contains a square pyramidal chloromethyl complex (Figure 3.2a). The figure is the superposition of two

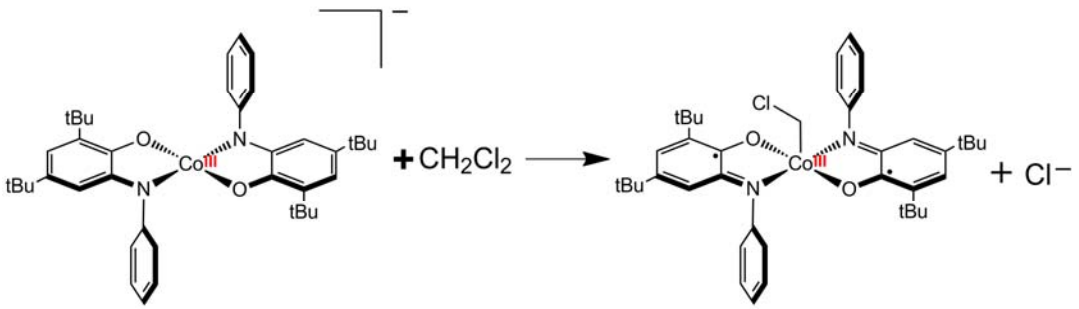

Scheme 3.1.

five-coordinate structural isomers resulting from crystallographic disorder of the chloromethyl group. The structure was solved with 75% occupancy of the C41-Cl1 fragment, drawn as solid ellipsoids, and 25% occupancy of the C41B-Cl1B fragment, drawn as faded ellipsoids. The C−O bonds, with an average length of 1.310 Å, and C−N bonds, with an average of 1.370 Å, both show contraction as compared to those observed in the fully reduced $[Co^{III}(ap)_2]^-$ complex. The quinoid-like pattern of four long and two short C−C bond distances, having average lengths as 1.427 Å and 1.373 Å, respectively, about the aminophenol ring (Figure 3.2b) match those typical for $[isq^{Ph}]^{\bullet-}$ ($[isq^{Ph}]^{\bullet-}$ = 2,4-di-*tert*-butyl-6-(phenylimino)semiquinonate).[18,19] The sum of these structural metrics suggests that the product is best described as $Co^{III}(CH_2Cl)(isq^{Ph})_2$. As compared to $[Co^{III}(ap^{Ph})_2]^-$ (Figure 2.4), the aminophenol ligand metrical data exhibit systematic geometrical changes that are characteristic of a change in ligand oxidation state.

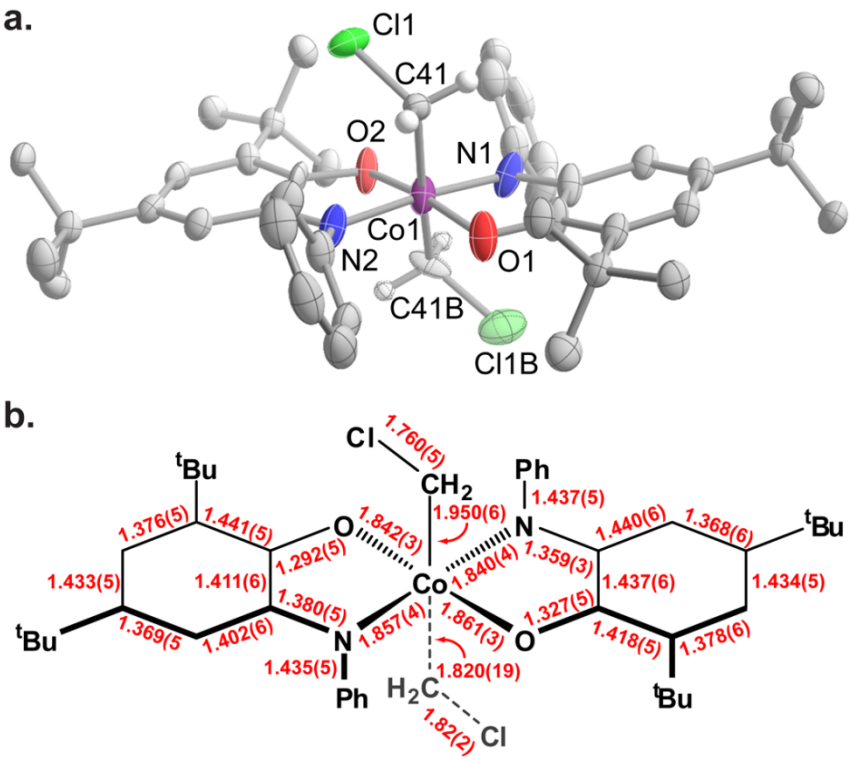

Figure 3.2. (a) Solid-state structure of $Co^{III}(CH_2Cl)(isq^{Phen})_2$ drawn with 50% probability ellipsoids. The $[isq^{Ph}]^{\bullet-}$ ligand hydrogen atoms are omitted for clarity. The figure is a superposition of two five-coordintate structural isomers resulting from crystallographic disorder of the chloromethyl group. The structure was solved with 75% occupancy of the C41-Cl1 fragment, drawn as solid ellipsoids, and 25% occupancy of the C41B-Cl1B fragment, drawn as faded ellipsoids. **(b)** Schematic of selected bond lengths (Å) in $Co^{III}(CH_2Cl)(isq^{Phen})_2$ drawn to correspond to Figure 3.2a.

3.3.2. Synthesis and characterization of $Co^{III}(Et)(isq^{Ph})_2$

Addition of 1 equivalent of EtBr to $Na[Co^{III}(ap^{Ph})_2]$ in CH_3CN yields a similar green, light-sensitive material and we obtained crystals suitable for analysis by X-ray diffraction from a concentrated solution of CH_3CN and THF stored at –20°C (Figure 3.3.a). As in the reaction with CH_2Cl_2 described above, the C−O and C−N bond lengths are contracted in comparison to the $[Co^{III}(ap^{Ph})_2]^-$ with average values of 1.322 Å and

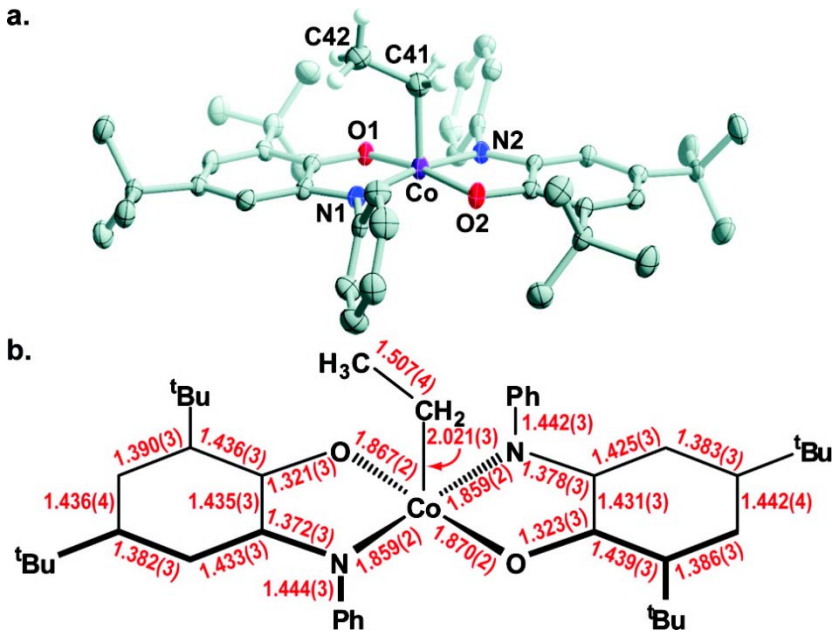

Figure 3.3. (a) Solid-state structure of $Co^{III}(CH_3CH_2)(isq^{Phen})_2$ drawn with 50% probability ellipsoids. The $[isq^{Ph}]^{\bullet-}$ ligand hydrogen atoms are omitted for clarity. **(b)** Schematic of selected bond lengths (Å) drawn to correspond to Figure 3.5a.

1.376 Å, respectively. The C−C bond distances show the characteristic pattern of two short (average length of 1.385 Å) and four long (average length of 1.423 Å) (Figure 3.3.b) indicating that the ligands each contain an organic radical and the product is best formulated as $Co^{III}(Et)(isq^{Ph})_2$.

3.3.3. Reaction scope and relative rates with $[Co^{III}(ap^{Ph})_2]^-$

Experiments were performed with a range of alkyl halides to explore the relative rates of oxidative addition to $[Co^{III}(ap^{Ph})_2]^-$. Rates of the reactions are reported under identical conditions using 5 equivalents of the organic halide and a 0.01 M $[Co^{III}(ap^{Ph})_2]^-$ solution in CH_3CN at room temperature and under nitrogen (Table 3.2). For instance, addition of CH_3I affords quantitative conversion to $Co^{III}(CH_3)(isq^{Ph})_2$ in seconds, whereas

complete reaction with CH_2Cl_2 takes 12 hours under the same conditions. The analogous reaction with CH_2ClBr requires 30 minutes. Reaction with this mixed halide species also gives exclusively the $Co^{III}(CH_2Cl)(isq^{Ph})_2$ product, as determined by ESI-MS, indicating only the carbon-bromide bond is activated. $[Co^{III}(ap^{Ph})_2]^-$ reacts with CH_3OTf (OTf^- = trifluoromethanesulfonate) to afford $Co^{III}(CH_3)(isq^{Ph})_2$ at a rate comparable to that of the fast reaction with CH_3I. Reactions with EtI or EtBr form $Co^{III}(Et)(isq^{Ph})_2$ in <1 minute and 1 hour, respectively, and reaction of $[Co^{III}(ap^{Ph})_2]^-$ with isopropyl iodide requires 3 hours. $PhCH_2Br$ reacts with $[Co^{III}(ap^{Ph})_2]^-$ to give $Co^{III}(CH_2Ph)(isq^{Ph})_2$ in 1 days, and >2 days are required for complete reaction with $PhCH_2Cl$. $[Co^{III}(ap^{Ph})_2]^-$ is inert to iodobenzene and vinyl bromide over weeks at 25 °C.

Table 3.2. Relative rates of organohalide addition to $[Co^{III}(ap^{Ph})_2]^-$.[a]

Entry	Organohalide	Reaction Time
1	CH_3I	< 30 seconds
2	CH_3OTf	< 30 seconds
3	CH_2ClBr	30 minutes
4	CH_2Cl_2	12 hours
5	EtI	< 1 minute
6	EtBr	1 hour
7	$PhCH_2Cl$	24 hours
8	$PhCH_2Br$	> 2 days
9	PhI	No Reaction
10	C_2H_3Br	No Reaction

[a] All reactions are performed under N_2 using 0.010 M $Na[Co^{III}(ap^{Phen})_2]$ and 0.050 M organohalide in CH_3CN at 25°C. Observations were monitored by visual color change.

A comparison of the relative rates of organohalide addition to $[Co^{III}(ap^{Ph})_2]^-$ revealed several pertinent trends: (1) Primary alkyl halides react with $[Co^{III}(ap^{Ph})_2]^-$ to afford the corresponding alkylcobalt(III) complexes, and the relative rates of the reactions parallel the lability of the halide. (2) All of the addition reactions are slower with more sterically demanding carbon centers. (3) No addition reaction occurs at sp^2-hybridized carbon centers. (4) The addition reactions are highly sensitive to steric bulk at the cobalt center.

3.3.4. Stability of the organometallic products

THF solutions of $Co^{III}(CH_2Cl)(isq^{Ph})_2$ are stable for days in the dark at 25°C but degrade in light to cleanly afford $Co^{III}(ap^{Ph})(isq^{Ph})$, the product of Co−$CH_2Cl$ homolysis (Scheme 3.2). Solid $Co^{III}(Et)(isq^{Ph})_2$ is stable for >2 days in the dark at 25 °C, and the UV−vis spectrum of a THF solution is unchanged over 4 hours at 25 °C. The stability of the organometallic complex to temperature decreases with the increased steric demands of the alkyl chain. The product of the reaction with isopropyl idodide, a secondary alkyl halide, is much less stable than that of primary alkyl halides of similar chain length.

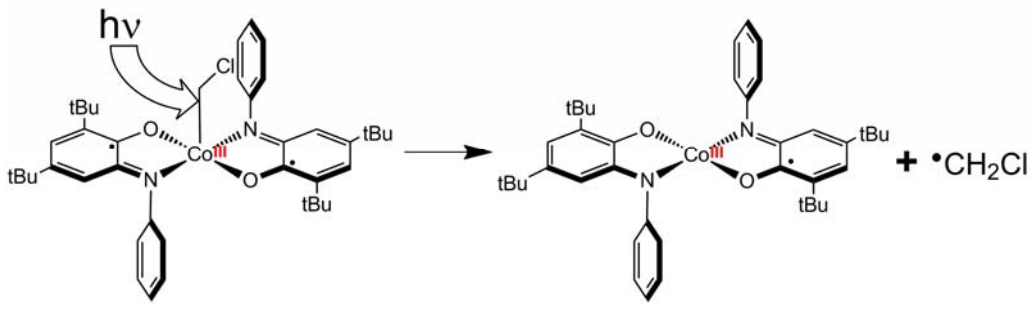

Scheme 3.2.

Similarly, the use of $[Co^{III}(ap^{iPr})_2]^-$ as opposed to $[Co^{III}(ap^{Ph})_2]^-$ produces an organometallic complex much more sensitive to temperature induced homolysis of the cobalt-carbon bond. However, even with longer alkyl halides such as octyl bromide, the product of the reaction is stable over hours when kept cool and in the absence of light.

3.3.5. Kinetic study of the reaction with CH_2Cl_2

Due to the sensitivity of $Co^{III}(CH_2Cl)(isq^{Ar})_2$ to light, kinetic studies of its formation were complicated by a competing degradation process caused by the spectrophotometer. However, when monitored at lower energy wavelengths (>700 nm), the product is stable and degradation is not a competing factor. Thus, a UV-vis kinetic study of the reaction of 7.9 x 10^{-5} M $Na[Co^{III}(ap^{Ph})_2]$ with 0.24 M CH_2Cl_2 in CH_3CN at 25°C under N_2 to generate $Co^{III}(CH_2Cl)(isq^{Ph})$ monitored from 700-950 nm exhibits clean kinetics with an isosbestic point at 911 nm (Figure 3.4). The isosbestic point indicates that the reaction proceeds directly from $[Co^{III}(ap^{Ph})_2]^-$ to $Co^{III}(CH_2Cl)(isq^{Ph})$ without observation of an intermediate. The fit to the data was obtained by iterative analysis of the full spectral window using a single exponential A→B integrated rate law model. This indicates that the reaction is first order with respect to the cobalt complex and a k_{obs} = (1.38 ± 0.02) x 10^{-4} s^{-1} can be determined.

The dependence of the reaction rate was also examined using the $[Co^{III}(ap^{iPr})_2]^-$ congener which alters the steric encumbrance around the metal center making it less accessible for the substrate (Figure 2.10). In fact, all alkyl halide additions to $[Co^{III}(ap^{iPr})_2]^-$ are significantly slowed relative to $[Co^{III}(ap^{Ph})_2]^-$. The reaction only reaches a 45% yield in 450 minutes as monitored by UV-vis spectroscopy. The rate of the

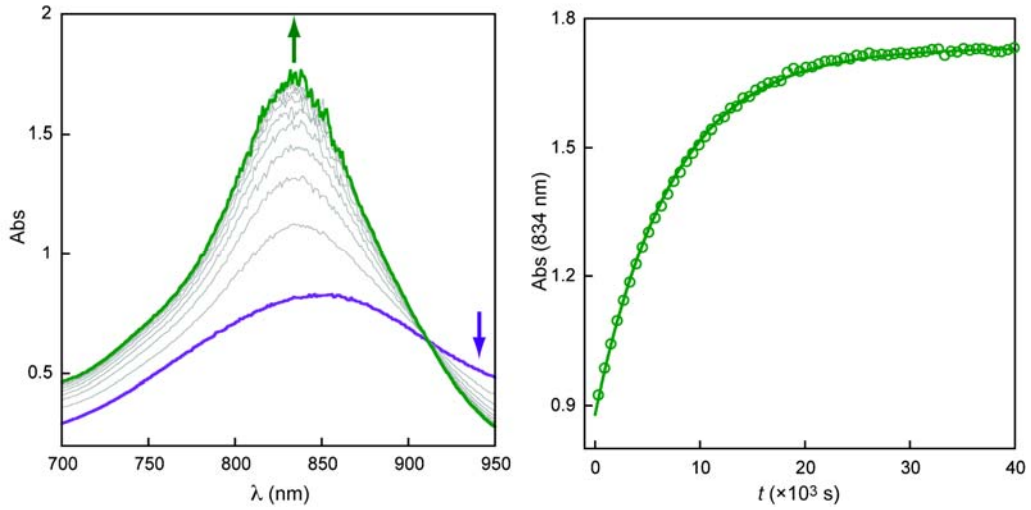

Figure 3.4. UV-vis kinetic study of reaction of $Na[Co^{III}(ap^{Ph})_2]$ with CH_2Cl_2 in CH_3CN to generate $Co^{III}(CH_2Cl)(isq^{Phen})_2$. **(a)** Spectra at t = 0 minutes (purple line), immediately prior to addition of CH2Cl2, and at 45.0 minute interevals to t = 450 minutes (green line) from acquisition of only the low energy visible photons (700-950 nm). **(b)** Selected time-resolved data showing the formation of $Co^{III}(CH_2Cl)(isq^{Phen})_2$ with λ_{max} = 834 nm (green o) derived from the data in Figure 3.4.a.

degradation of the $Co^{III}(CH_2Cl)(isq^{iPr})_2$ product is similar to that of the rate of formation and therefore valid k_{obs} values cannot be extracted. Reaction of $[Co^{III}(ap^{iPr})_2]^-$ with secondary alkyl halides shows no reactivity at 25°C over days. Use of the $[Co^{III}(ap^{Cl})_2]^-$ congener alters the reduction potential of the complex by 260 mV less negative from that of the $[Co^{III}(ap^{Ph})_2]^-$ analog. This loss of reducing power slows the rate, such that, at room temperature, the homolysis degradation pathway rate exceeds that of product formation, even when excluded from light, and the reaction never reaches complete conversion.

3.3.6. Reaction with alkyl halide radical clock

The pseudo-oxidative addition reaction of (bromomethyl)cyclopropane was studied in an attempt to gain evidence for the reaction mechanism. (Bromomethyl)cyclopropane has been used extensively as a radical clock to determine if a radical intermediate exists within a reaction (Scheme 3.3, Reaction 1).[20] The reaction was also probed with 6-bromo-1-hexene, another known radical clock (Scheme 3.3, Reaction 2).[21] These establish the presence of a radical transition state by formation of one of two products. Formation of 1b or 2b are positive indicators of a radical process. $[Co^{III}(ap^{Ph})_2]^-$ was reacted with the (bromomethyl)cyclopropane and with 4-bromo-1-butene in side-by-side reactions. Oxidative addition of 4-bromo-1-butene results in formation of the product 1b allowing for independent characterization of at least one of the possible products. ^{1}H NMR spectra of the two products were markedly different. However, assignment of the peaks was not possible due the paramagnetism of several species in the solution. The same peak broadening was apparent with reaction using 6-bromo-1-hexene as well. In variable temperature NMR experiments, colder temperatures

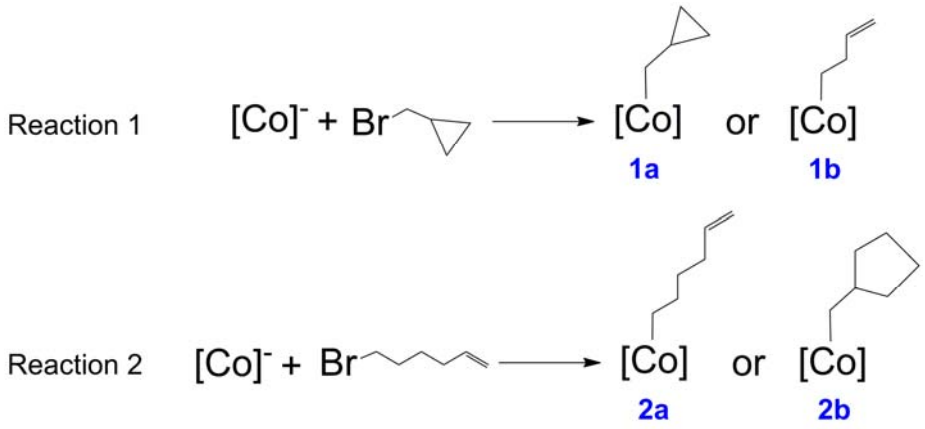

Scheme 3.3.

make the spectra less decipherable and the $Co^{III}(R)(isq^{Ph})_2$ material was not able to be stabilized enough to avoid formation of paramagnetic degradation products such as those produced by the thermal homolysis of the cobalt-carbon bond and allow assignment of the configuration of the organic fragment.

3.3.7. Lack of reactivity of $Co^{III}(Et)(isq^{Ph})_2$ with CO

Exposure of a stirred solution of $Co^{III}(Et)(isq^{Ph})_2$ in THF to an atmosphere of dry CO at room temperature while protected from light over hours yielded no observable color change. Comparison of the infrared (IR) spectra of the material before and after exposure also showed no changes and no evidence of the carbonyl peak expected with successful insertion of the CO molecule into the cobalt-alkyl bond.

3.4. Discussion

3.4.1. Pseudo-oxidative addition product

The crystallographic data for $Co^{III}(CH_2Cl)(isq^{Ph})_2$ and $Co^{III}(Et)(isq^{Ph})_2$ suggest that both are best formulated as cobalt(III) complexes with bis-iminosemiquinate ligands. This formulation that the reaction occurs with a net two electron oxidation of the $[Co^{III}(ap^{Ph})_2]^-$ fragment, but the oxidation state of the cobalt center is unchanged because each ligand supplies one electron. The oxidative addition reaction with alkyl halides is not fast. However, the stability of the product against degradation is promising for facilitation of further reactivity. Bond homolysis can be avoided by exclusion of light and temperature control. Degradation through β-hydride elimination is not rapid as the $Co^{III}(Et)(isq^{Ph})_2$ complex is stable in solution and solid state when protected from the

homolysis degradation pathway. However, the stability against both β-hydride elimination and CO insertion as observed may imply that a site *cis* to the alkyl ligand cannot be accessed. This could potentially create a barrier to successful facilitation of coupling reactions, as discussed in the following chapter.

3.4.2. Mechanistic implications of pseudo-oxidative addition

Four mechanisms that are consistent with the UV−vis kinetics indicating that the reaction was first order in metal and a simple A→B conversion were considered for generation of $Co^{III}(R)(isq^{Ar})_2$ and X^- from $[Co^{III}(ap^{Ar})_2]^-$ and R−X (Scheme 3.4). Two invoke six-coordinate oxidative addition $[Co^{III}X(R)(isq^{Ph})_2]$ products as unobserved intermediates followed by rapid loss of X^-. However, the sum of the relative reaction rates suggest that both of these pathways involving Co−X bond formation can likely be ruled out. In particular, the rapid reaction of $[Co^{III}(ap^{Ph})_2]^-$ with CH_3OTf suggests that a radical mechanism (*iv*) of initial X• transfer is unlikely. Substrates such as CH_3I and CH_3OTf do not typically react by a concerted addition mechanism (*iii*)[8] excluding that from our consideration as well.

The two remaining mechanisms both invoke conversion of $[Co^{III}(ap^{Ar})_2]^-$ directly to the five-coordinate $Co^{III}(R)(isq^{Ar})_2$ product without Co−X bond formation. These represent limits of the potential one electron versus two electron redox pathways. The observed increase in reaction rate with leaving group lability, $I^- > Br^- > Cl^-$, does not distinguish between mechanism (*i*) versus (*ii*). Previously reported reactions of $Co^{III}(ap^{Ar})(isq^{Ar})$ with sources of net [Cl•] to generate $Co^{III}Cl(isq^{Ar})_2$ demonstrate the ability of $Co^{III}(ap^{Ar})(isq^{Ar})$ to function as a radical trap.

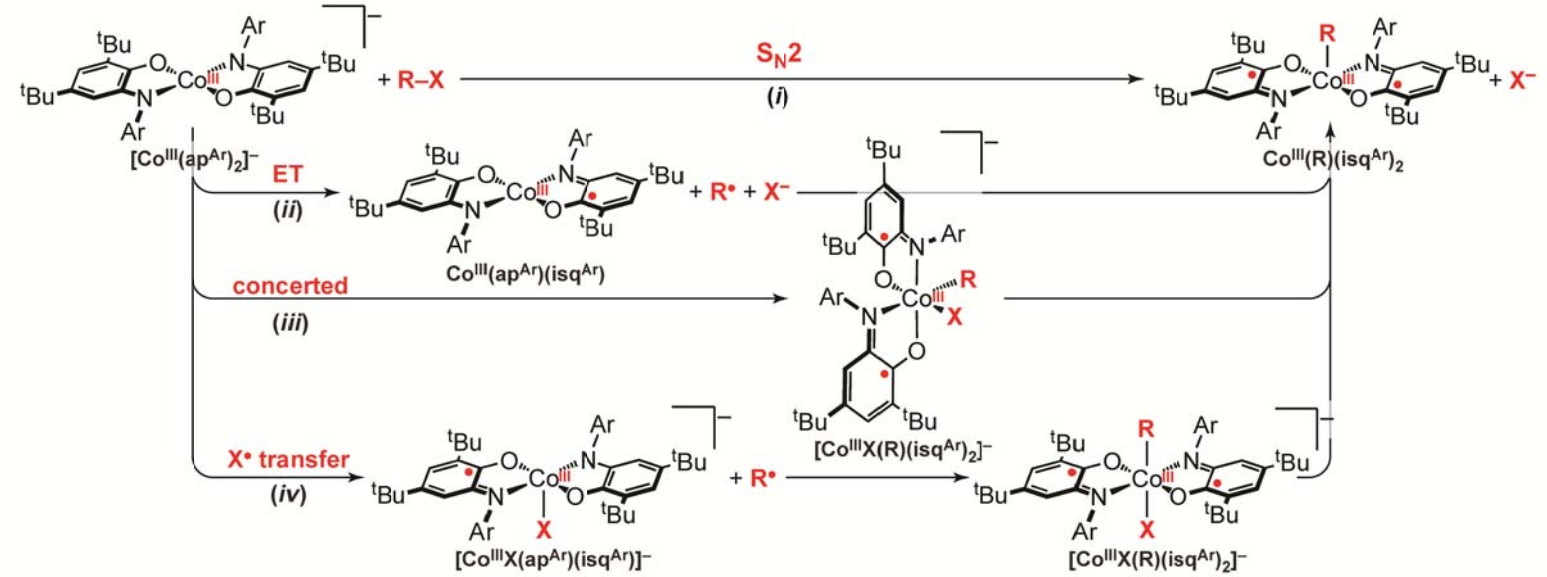
+ R–X
S$_N$2
(i)
+ X$^-$
[Co^{III}(ap^{Ar})$_2$]$^-$
Co^{III}(R)(isq^{Ar})$_2$
ET
(ii)
+ R$^•$ + X$^-$
Co^{III}(ap^{Ar})(isq^{Ar})
concerted
(iii)
[Co^{III}X(R)(isq^{Ar})$_2$]$^-$
X$^•$ transfer
(iv)
+ R$^•$
[Co^{III}X(ap^{Ar})(isq^{Ar})]$^-$
[Co^{III}X(R)(isq^{Ar})$_2$]$^-$

Scheme 3.4

However, the sum of the other experimental observations does not support an electron transfer (ET) mechanism (*ii*). For example, the $[Co^{III}(ap^{iPr})_2]^-$ anion is a better one electron reductant than $[Co^{III}(ap^{Ph})_2]^-$, but it reacts with alkyl halides at a significantly decreased rate. Additionally, its slow reactions with secondary alkyl halides as compared to primary haloalkanes are inconsistent with a mechanism of initial outer-sphere ET (*ii*).

Instead, this sensitivity to steric hindrance at carbon, as well as to steric encapsulation of the cobalt(III) center by the $[ap^{iPr}]^{2-}$ ligands, is most consistent with the S_N2-type mechanism (*i*) wherein Co−R bond formation requires direct attack of the nucleophilic cobalt center on the alkyl halide electrophile. The slow reaction with benzyl halides further highlights the steric constraints of the system. These data support the mechanistic conclusions presented indicating a S_N2-type reaction to form the 5-coordinate cobalt(III) complex.

3.5. Conclusions

The ability of redox-active ligands to facilitate two electron pseudo-oxidative addition reaction at mononuclear square planar cobalt(III) complexes is predicated on two properties: (1) The $[Co^{III}(ap^{Ar})_2]^-$ species are very strong nucleophiles, reminiscent of "supernucleophilic" cobaloxime(I) complexes and square planar iridium(I) compounds that undergo S_N2-type oxidative addition of R−X.[22,23] However, these cobalt(III) anions are unusual nucleophiles. They have diradical S = 1 ground states, and their reactions with haloalkanes occur without a change in oxidation state at the cobalt(III) centers because the redox-active aminophenol-derived ligands in $[Co^{III}(ap^{Ar})_2]^-$ supply both of the necessary redox equivalents for the net two electron transformation. (2) The

$[Co^{III}(ap^{Ar})_2]^-$ complexes are 200−400 mV less reducing than most cobaloxime(I) species. Notably, the surprising proclivity for two electron reactions over one electron redox forms a basis for probably development of new well-defined first-row metal catalysts for selective coupling cycles, as discussed in Chapter 4.

3.6. References

1. Brown, D. G., Chemistry of vitamin B12 and related inorganic model systems. *Progr. Inorg. Chem.* **1973,** *18*, 177-286.

2. Schrauzer, G. N.; Deutsch, E., Reactions of cobalt(I) supernucleophiles. The alkylation of vitamin B12s, cobaloximes(I), and related compounds. *J. Am. Chem. Soc.* **1969,** *91*, 3341-50.

3. Jensen, F. R.; Madan, V.; Buchanan, D. H., Stereochemistry of the alkylation of cobalt(I). *J. Am. Chem. Soc.* **1970,** *95* (5), 1414-1416.

4. Bigotto, A.; Costa, G.; Mestroni, G.; Nardin-Stefani, L.; Puxeddu, A.; Reisenhofer, E.; Tauzher, G., Extension of the models approach to the study of coordination chemistry of vitamin B12 group compounds. *Inorg. Chim. Acta, Rev.* **1970,** *4*, 41-49.

5. Hisaeda, Y.; Nishioka, T.; Inoue, Y.; Asada, K.; Hayashi, T., Electrochemical reactions mediated by vitamin B12 derivatives in organic solvents. *Coord. Chem. Rev.* **2000,** *198*, 21-37.

6. Connelly, P.; Espensen, J. H., Cobalt catalyzed evolution of molecular hydrogen. *Inorg. Chem.* **1986,** *25*, 2684-2688.

7. Smith, A. L.; Clapp, L. A.; Hardcastle, K. I.; Soper, J. D., Redox-active ligand-mediated Co-Cl bond-forming reactions at reducing square planar cobalt(III) centers. *Polyhedron* **2010,** *29*, 164-169.

8. Crabtree, R. H., *The Organometallic Chemistry of the Transition Metals, 3rd ed.* Wiley: New York, New York, 2001.

9. Terao, J.; Kambe, N., Transition metal-catalyzed C-C bond formation reactions using alkyl halides. *Bull. Chem. Soc. Jpn.* **2006,** *79*, 663-672.

10. Netherton, M. R.; Fu, G. C., Nickel-catalyzed cross-couplings of unactivated alkyl halides and pseudohalides with organometallic compounds. *Adv. Synth. Catal.* **2004,** *346*, 1525-1532.

11. Rudolph, A.; Lautens, M., Secondary alkyl halides in transition-metal-catalyzed cross-coupling reactions. *Angew. Chem., Int. Ed.* **2009,** *48*, 2656-2670.

12. Ishiyama, T.; Abe, S.; Miyaura, N.; Suzuki, A., Palladium-catalyzed alkyl-alkyl cross-coupling reaction of 9-alkyl-9-BBN derivatives with iodoalkanes possessing B-hydrogens. *Chem. Lett.* **1992**, 691-694.

13. Rangel, M.; Arcos, T.; De, C. B., Photolysis Primary Products of Alkylcobaloximes Controlled by the Cobalt-Carbon Bond Strength. *Organometallics* **1999,** *18*, 3451-3456.

14. Smith, A. L.; Soper, J. D., unpublished work detailed in Chapter 2.

15. apex II, Analytical X-Ray Systems, Brukers AXS, Inc., Madison, WI, 2005.

16. saint Version 6.45A, Analytical X-ray Systems, Brukers AXS, Inc., Madison, WI, 2003.

17. shelxtl Version 6.12, Analytical X-ray Systems, Bruker AXS, Inc., Madison, WI, 2002.

18. Bill, E.; Bothe, E.; Chaudhuri, P.; Chlopek, K.; Herebian, D.; Kokatam, S.; Ray, K.; Weyhermueller, T.; Neese, F.; Wieghardt, K., Molecular and electronic structure of four- and five-coordinate cobalt complexes containing two o-phenylenediamine- or two o-aminophenol-type ligands at various oxidation levels: An experimental, density functional, and correlated ab initio study. *Chem. Eur. J.* **2005,** *11*, 204-224.

19. Poddel'sky, A. I.; Cherkasov, V. K.; Abakumov, G. A., Transition metal complexes with bulky 4,6-di-tert-butyl-N-aryl(alkyl)-o-iminobenzoquinonato ligands: Structure, EPR and magnetism. *Coord. Chem. Rev.* **2009,** *253*, 291-324.

20. Guerinot, A.; Reymond, S.; Cossy, J., Iron-catalyzed cross-coupling of alkyl halides with alkenyl Grignard reagents. *Angew. Chem., Int. Ed.* **2007,** *46*, 6521-6524.

21. Wakaabayashi, K.; Yorimitsu, H.; Oshima, K., Cobalt-catalyzed tandem radical cyclization and cross-coupling reaction: Its application to benzyl-substitued heterocycles. *J. Am. Chem. Soc.* **2001,** *123*, 5374-5375.

22. Schrauzer, G. N.; Sibert, J. W.; Windgassen, R. J., Photochemical and thermal cobalt-carbon bond cleavage in alkylcobalamins and related organometallic compounds. Comparative study. *J. Am. Chem. Soc.* **1968,** *90*, 6681-6688.

23. Labinger, J. A.; Osborn, J. A., Mechanistic studies of oxidative addition to low-valent metal complexes. Stereochemistry at carbon in addition of alkyl halides to iridium(I). *Inorg. Chem.* **1980,** *19*, 3230-3236.

Homogeneous carbon-carbon coupling facilitated by cobalt(III) metal centers

4.1. Introduction

Even after a century of study, development of homogeneous catalysts to facilitate coupling of carbon molecules remains a topic of much research and interest.[1,2] One function of transition metal catalysts for coupling is to mediate electron movement to break and make bonds, forming the desired product. This coupling of two carbon fragments into one molecule can occur through a radical of an outer-sphere electron transfer reaction in which organic radicals are generated and then spontaneously form the product. This radical pathway leads to disorganized product formation, however, as the radical fragments are free to react with any potential site they encounter in the reaction pot. To control the formation of products and avoid unwanted side-reactions, coupling often must be occur in concerted, two-electron steps. Selective product formation eliminated the need for costly and extensive purification.

Second and third row transition metals, particularly palladium, are used as catalysts to facilitate carbon-carbon bond-forming reactions because these metals have a proclivity for two electron oxidation state changes.[3-5] Some palladium catalytic systems have been extensively developed and optimized as a result of elegant and insightful mechanistic studies.[6,7] This research has led to an understanding of the reactions, their controlling factors, and successful optimization.[5,8,9] Some of the most well established reaction types catalyzed by palladium are the cross-coupling of unactivated organic halides with organometallic nucleophiles[1,2,6,8-13] and the oxidative homocoupling of

organometallic nucleophiles (Scheme 4.1).[7,14] Palladium lends itself to successful coupling of sp- and sp^2-hybridized carbon atoms.[4,5] However, these reactions are often not able to catalyze aliphatic carbon bonds.[12] The oxidative addition reactions of alkyl halides to form the alkyl-palladium intermediates are slow and the product is prone to β-hydride elimination. This was believed to limit the reaction to use of reagents without β-hydrogen atoms or requires elaborate ligand design to stabilize the intermediate and allow successful carbon-carbon bond formation. Recent work has been done with nickel and palladium to design catalysts to better facilitate these reactions.[15,16]

First row transition metals have gained recent popularity in the search for new coupling catalysts.[11,17-23] However, these metals are prone to oxidation state changes that vary by one electron. This causes them to most often facilitate coupling reactions through radical pathways.[23,24] Often these metals are used as catalysts in the form of metal salts with various reagents, which can act as ligands, added to the reaction mixture. [11,20,22,25-27] Most often, the success of particular of metal-ligand combinations generated *in situ* is not well understood.[18]

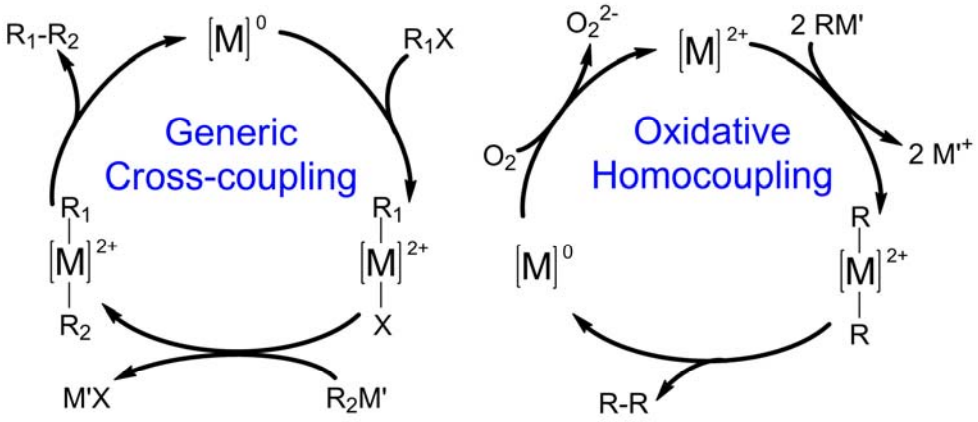

Scheme 4.1

The reaction of organic halides with organometallic nucleophile sources has been successfully catalyzed using first row transition metals.[10,28-33] In particular, Negishi-type couplings make use of organozinc reagents as the carbon nucleophile source, allowing conditions more tolerant of various solvents and functional groups.[34-36] However, mechanistic studies on first row metals facilitating this type of reactivity are often conflicting and rely on large assumptions applied from previously studied systems. This is due to the difficulty of identifying the active catalytic species and isolating intermediates of the reactions.[14,23,30,37,38] There has been little progress in the development of a general understanding of how they work.[25,31,39] In fact, some proposed mechanisms are simply based on comparison to well studied palladium and nickel systems and believed to be concerted[29] while others are believed to be radical based.[40] Oxidative coupling of organometallic nucleophiles has also received extensive attention at first row transition metals.[7,30,36,41] Similar to the cross-coupling systems, these involve use of added reagents which may act as ligands. The proposed mechanisms for this homocoupling are most often inconsistent and based on generalizations to other systems as well.[30]

In our previous work (Chapter 3), we demonstrated that $[Co^{III}(ap)_2]^-$ reacts as a nucleophile to activate alkyl halides and form a stable cobalt-carbon bond.[42,43] This reactivity is reminiscent of alkylcobalamins which have been isolated and studied.[44,45] The alkylcobalamins have been shown to undergo homolytic cleavage of the cobalt-carbon bond and create an alkyl radical able to react.[44,46] The radical reactivity of these complexes is not ideal for controlled, selective coupling in a laboratory setting. However, the cobalt bis-amidophenolate complexes are reduced by two electrons at much less

negative redox potentials than those demonstrated by the two, single electron steps to reduced cobalt(III) to cobalt(I) in the cobalamin system.[44-47] The more modest reduction potentials of our system are favorable for facilitation of both the oxidative addition and reductive elimination of coupled organic product and suggest our complex may not rely on a similar, radical pathway.

In this study we examined the possibility of using the isolated $Co^{III}(R)(isq^{Ar})_2$ to selectively form new carbon-carbon bonds through the multi-electron proclivity the system has already been demonstrated to possess. Herein, we report the successful use of the isolated complex in step-wise Negishi type cross coupling of alkyl halides. We have also isolated and characterized the cationic $[Co^{III}(CH_3CN)(isq^{Ar})_2]^+$ complex and shown that it facilitates oxidative carbon-carbon homocoupling. Examination of these two coupling reactions shows that they are mechanistically the same with regard to reaction of the second organic fragment and elimination of the coupled product. However, both of these reactions exhibit a low yield. Detailed studies of the mechanism indicate that carbon-carbon bond-formation is facilitated through concerted, inner-sphere steps. The study also reveals challenges to the reactions as steric crowding around the metal center limits the coupling yields.

4.2. Experimental Details

4.2.1. General considerations

Unless otherwise noted, all manipulations were performed under anaerobic conditions using standard vacuum line techniques, or in an inert atmosphere glove box under purified nitrogen. All NMR spectra were acquired on a Varian Mercury 300 spectrometer (300.323 MHz for ^{1}H) at ambient temperature. Chemical shifts are reported in parts per million (ppm) relative to TMS, with the residual solvent peak serving as an internal reference. Solution state magnetic moments were determined by Evans' NMR method.[48] UV–visible absorption spectra were acquired using a Varian Cary 50 spectrophotometer. Unless otherwise specified, all electronic absorption spectra were recorded at ambient temperatures in 1 cm quartz cells. IR spectra were obtained using attenuated total reflection (ATR) with a diamond plate on a Thermo Scientific Nicolet 4700 Fourier-transform infrared spectrophotometer. All mass spectra were recorded in the Georgia Institute of Technology Bioanalytical Mass Spectrometry Facility. Electrospray ionization mass spectrometry (ESI-MS) was carried out with acetonitrile (CH_3CN) or tetrahydrofuran (THF) solutions using as Micromass Quattro LC spectrometer. (GC–MS) analyses used an Agilent 6890 GC equipped with an autosampler and a Restek Rxi-5ms column (30 m x 0.25 mm i.d., 0.25 μm film thickness). 1 μL injections were made at a 50:1 split ratio. The GC oven program consisted of a hold at 30 °C for 1 min, followed by a 15 °C min^{-1} ramp to 300 °C, and then a hold at 300 °C for 11 minutes. The mass spectrometer used in tandem was a Micromass AutoSpec electro-ionization (EI) detector.

4.2.2. Methods and materials

Anhydrous acetonitrile (CH_3CN), tetrahydrofuran (THF), toluene, dichloromethane (CH_2Cl_2), and pentane solvents for air- and moisture-sensitive manipulations were purchased from Sigma–Aldrich, further dried by passage through columns of activated alumina, degassed by at least three freeze–pump–thaw cycles, and stored under N_2 prior to use. Methanol (MeOH) (anhydrous, 99.0%) was purchased from Honeywell Burdick & Jackson, and used as received. Deuterated acetonitrile (CD_3CN) was purchased from Cambridge Isotope Laboratories, degassed by three freeze–pump–thaw cycles, vacuum distilled from CaH_2, and stored under a dry N_2 atmosphere prior to use. $Co^{III}(ap^{Ph})(isq^{Ph})$, $Co^{III}(ap^{iPr})(isq^{iPr})$, $Co^{III}(ap^{Cl})(isq^{Cl})$, $Na[Co^{III}(ap^{Ph})_2]$, $Na[Co^{III}(ap^{iPr})_2]$, $Na[Co^{III}(ap^{Cl})_2]$ and all $Co^{III}(R)(isq^{Ar})_2$ were prepared by previously published methods[47] and as reported in Chapters 2 and 3. $Co(ClO_4)_2{\cdot}6H_2O$ and $Co_2(CO)_8$ were purchased from Strem Chemical, Inc. All other chemicals were purchased from Sigma–Aldrich and used as received. Prior to use, the concentrations of all organometallic reagents were determined by iodometric titrations,[49] and the concentrations of the corresponding protio impurities were quantified by GC–MS analyses of the THF solutions and comparison to calibration curves derived from the pure materials.

4.2.3. Preparation of $[Co^{III}(CH_3CN)(isq^{Ph})_2][BF_4]$

A 5 dram scintillation vial was charged with $Co^{III}(isq^{Ph})(ap^{Ph})$ (0.219 g, 0.337 mmol) and 1 equivalent of $AgBF_4$ (0.067 g, 0.338 mmol). 10 mL of CH_3CN was added and the solution was stirred under nitrogen at room temperature for 1 hour. The solution was filtered through celite and the volume was reduced to 3 mL in vacuo. It was then

chilled to –20°C for 4 hours until a blue-green precipitate formed. The precipitate was isolated by filtration (0.208 g, 0.267 mmol, 79.5%) and stored under nitrogen. UV–vis (CH_3CN) nm (ε, M^{-1} cm^{-1}): 625 (8840) and 900 (10460). ESI-MS (*m*/*z*): 649.2 and 690.4 $[M]^+$. ^1H NMR (CD_3CN): 8.84 (s, 2 H), 7.69 (m, 6 H), 7.44(m, H), 1.09 (s, 18 H) and 1.03 (s, 18 H) ppm. FTIR (ATR): 2955 (m), 2869 (m), 1660 (w) 1585 (w), 1524 (w), 1483 (w), 1362 (m), 1304 (m), 1266 (w), 1230 (w), 1202 (w), 1179 (w), 1092 (s), 1052 (s), 1024 (s), 996 (s), 923 (w), 871 (w), 785 (w), 767 (w), 741 (m), 692 (m), 652 (w), 623 (w), 605 (w), 540 (w), 504 (m), and 416(w) cm^{-1}.

4.2.4. Preparation of $[Co^{III}(CH_3CN)(isq^{iPr})_2][BF_4]$

In a procedure analogus to that above for the $[Co^{III}(CH_3CN)(isq^{Ph})_2][BF_4]$, $Co^{III}(isq^{iPr})(ap^{iPr})$ (0.242 g, 0.296 mmol) was reacted with 1 equivalent of $AgBF_4$ (0.059 g, 0.297 mmol) yielding (0.206 g, 0.218 mmol, 73.5 %). Crystals suitable for X-ray diffraction were isolated from concentrated CH_3CN solutions containing $NaPh_4B$ and stored at –20°C for days. UV–vis (CH_3CN) nm (ε, M^{-1} cm^{-1}): 625 (9240) and 900 (11470). ESI-MS (*m*/*z*): 817.4 and 858.5 $[M]^+$. ^1H NMR (CD_3CN): 8.63 (s, 2H) 7.56(t, 2H), 7.42 (d, 2H), 7.05(m, 4H), 1.30(d, 3H), 1.22(d, 3H), 1.09 (s, 18H), 1.07 (s, 18H), 0.75 (d, 3H), and 0.23 (d, 3H) ppm. FTIR (ATR): 2958 (m), 2868 (m), 1524 (w), 1508 (m), 1462 (m), 1359 (s), 1300 (m), 1263 (m), 1254 (m), 1240 (m), 1203 (w), 1167 (m), 1053 (s), 1024 (s), 996(s), 910 (w), 861 (w), 799 (w), 742 (m), 658 (m), 648 (m), 581 (w), 539 (w) 517 (m), 466 (w), and 409(w) cm^{-1}.

4.2.5. Cross-coupling reactions and quantitation of organic products

Unless otherwise noted, all coupling reactions were performed under nitrogen. In a representative procedure, a 5 dram scintillation vial was charged with freshly-prepared $Co^{III}(Et)(isq^{Ph})_2$ (0.057 g, 0.084 mmol) and a $^{-}$20°C solution of 1:1 CH_3CN:THF (8.5 mL) was added to afford a clear green solution. Between all subsequent manipulations, the solution was stored at $^{-}$20°C under N_2 to slow thermolytic degradation that homolyzes the Co–C bond. An aliquot of the 0.010 M $Co^{III}(Et)(isq^{Ph})_2$ stock solution (1 mL, 0.010 mmol) was transferred to a 2 mL GC autosampler vial and 0.5 M PhZnBr in THF (40 μL, 0.020 mmol) was added via syringe. An immediate color change was observed. The vial was fitted with a Teflon-lined septum cap, shaken vigorously, and the reaction mixture was allowed to warm to ambient temperature under N_2. For analysis of the organic products, the reaction was quenched after 60 min (unless otherwise specified) by addition of trifluoroacetic acid (CF_3CO_2H, TFA) (0.8 μL, 0.020 mmol) and *n*-decane (1 μL) was added to serve as an internal standard. The solution was stored at –20 °C prior to GC–MS analysis, as described above. The organic products were quantitated by comparison of the EI–MS detector response against calibration curves derived from the pure materials and injection variation was controlled with an *n*-decane internal standard of comparable concentration to the analytes.

4.2.6. Homocoupling reactions and quantitation of organic products

Unless otherwise noted, all coupling reactions were performed under nitrogen. In a representative procedure similar to that used for cross-coupling, a 5 dram scintillation vial was charged with freshly-prepared $[Co^{III}(CH_3CN)(isq^{Ph})_2][BF_4]$ (0.058 g, 0.085 mmol)

solution of 1:1 CH_3CN:THF (8.5 mL) was added to afford a clear blue-green solution. An aliquot of the 0.010 M $[Co^{III}(CH_3CN)(isq^{Ph})_2][BF_4]$ stock solution (1 mL, 0.010 mmol) was transferred to a 2 mL GC autosampler vial and 0.5 M HxZnBr in THF (40 μL, 0.020 mmol) was added via syringe and an immediate color change was observed. The vial fitted with a Teflon-lined septum cap, shaken vigorously, and the reaction mixture was allowed to warm to ambient temperature under N_2. For analysis of the organic products, the reaction was quenched after 60 min (unless otherwise specified) by addition of trifluoroacetic acid (CF_3CO_2H, TFA) (0.8 μL, 0.020 mmol) and *n*-decane (1 μL) was added to serve as an internal standard. The organic products were quantitated by comparison of the EI–MS detector response against calibration curves derived from the pure materials and injection variation was controlled with the *n*-decane internal standard.

4.2.7. Quantitation of metal containing species after coupling reactions

In a representative procedure for analysis of species present in dilute solutions before and after coupling reactions, a 10 μL aliquot of the 0.010 M cobalt solution was diluted to 2.10 mL with a 1:1 CH_3CN:THF. The final 0.05 mM solution was analyzed in 1 cm pathlength cuvettes. Unless otherwise specified, the absorbance was measured within 10 minutes of the dilution.

In a representative procedure for analysis of species present in concentrated solutions before and after coupling reactions, solutions were prepared to be 1.0 mM cobalt complex. The coupling reactions were performed at this concentration and the absorbace of the solutions were measured without any further dilution following the reactions. These solutions were analyzed in 0.5 mm pathlength cuvettes.

4.2.8. Preparation and characterization of $Co^{III}(nPr)(isq^{iPr})_2$

$Co^{III}(nPr)(isq^{iPr})_2$ was prepared by the procedure described previously for preparation of $Co^{III}(CH_2Cl)(isq^{Ph})_2$ (Chapter 3),[42] using $Na[Co^{III}(ap^{Ph})_2]$ (0.062 g, 0.092 mmol) and propylBr (0.1 mL, 1.10 mmol) to give $Co^{III}(nPr)(isq^{Ph})_2$ (0.023 g, 0.033 mmol, 36%). UV–vis (1:1 CH_3CN:THF) λ_{max}, nm (ε, M^{-1} cm^{-1}): 860 (34000).

In an alternate procedure, a 5 dram scintillation vial was charged with $[Co^{III}(CH_3CN)(isq^{Ph})_2][BF_4]$ (0.057 g, 0.060 mmol) dissolved in 6.0 mL of a 1:1 CH_3CN:THF mixture. An 1.0 mL aliquot of this solution was mixed with 13 µL of 0.590 M solution of nPrZnBr in THF (13 µL, 0.0076 mmol) was added and mixed well. The material was characterized as the organometallic product with comparison of the UV-vis with similar products. The solution was allowed to sit at –20°C under nitrogen and excluded from light for 5 days. Green crystals were isolated from the solution and analyzed by X-ray crystallographic analysis.

4.2.9. X-ray crystallography

Single crystals of $[Co^{III}(CH_3CN)(isq^{Ph})_2][Ph_4B]\bullet 2CH_3CN$ and $Co^{III}(nPr)(isq^{Ph})_2$ suitable for X-ray diffraction analysis were coated with Paratone N, suspended in a small fiber loop and placed in a cooled nitrogen gas stream at 173 K on a Bruker D8 APEX II CCD sealed tube diffractometer. Diffraction data for $[Co^{III}(CH_3CN)(isq^{Ph})_2][Ph_4B]\bullet 2CH_3CN$ and $Co^{III}(nPr)(isq^{Ph})_2$ was collected using graphite monochromated Cu Kα (λ = 1.54178 Å) radiation. Data were measured using a series of combinations of phi and omega scans with 10 second frame exposures and 0.5° frame widths. Data collection, indexing and initial cell refinements were all carried out using

apex II software.[50] Frame integration and final cell refinements were done using saint software. [51]The final cell parameters were determined from least-squares refinement on 21,821 and 11,496 reflections for $[Co^{III}(CH_3CN)(isq^{Ph})_2][Ph_4B]\bullet 2CH_3CN$ and $Co^{III}(nPr)(isq^{Ph})_2$ respectively. The structures were solved using direct methods and difference Fourier techniques using the shelxtl program package.[52] Hydrogen atoms were placed in their expected chemical positions using the HFIX command and were included in the final cycles of least-squares with isotropic U_{ij}'s related to the atoms ridden upon. All non-hydrogen atoms were refined anisotropically. Details of data collection and structure refinement are provided in Table 4.1.

Table 4.1. Crystallographic data and structure parameters for $[Co^{III}(CH_3CN)(isq^{iPr})_2][Ph_4B]\bullet 2CH_3CN$ and $Co^{III}(nPr)(isq^{iPr})_2$.

Complex	**$[Co^{III}(CH_3CN)(isq^{iPr})_2][Ph_4B]\bullet 2CH_3CN$**	**$Co^{III}(nPr)(isq^{iPr})_2$**
Empirical formula	$C_{82}H_{103}BCoN_5O_2$	$C_{55}H_{81}CoN_2O_2$
Formula weight	1260.43	861.15
T (K)	173 (2)	173 (2)
Crystal system	monoclinic	triclinic
Space group	P2(1)/c	P-1
Unit Cell dimensions		
a (Å)	12.0245 (15)	11.976 (3)
b (Å)	16.511 (2)	12.342 (3)
c (Å)	39.028 (5)	18.919 (5)
α (°)	90	89.732 (4)
β (°)	90.636 (2)	78.016 (4)
γ (°)	90	73.124 (4)
V (Å^3)	7747.9 (17)	2613.0 (11)
Z	4	2
D_{calc} (g/cm^3)	1.081	1.095
Absorption coefficient (mm^{-1})	0.268	0.367
Crystal Size (mm)	0.55x0.24x0.06	0.50x0.216x0.088
θ range for data collection (°)	1.04 to 30.30	1.10 to 27.10
Index ranges	-16≤h≤16	-15≤h≤15
	-23≤k≤22	-15≤k≤15
	-53≤l≤53	-24≤l≤24
Reflections collected	141 027	41 654
Reflections unique	21 821	11 496
Goodness of fit on F^2	1.039	1.007
R [I>2σ(I)]	0.0744	0.0663
wR^2 (all data)	0.2429	0.1854

4.3. Results

4.3.1. Step-wise cross-coupling facilitated by $[Co^{III}(ap^{Ar})_2]^-$

The accessibility of the alkyl-cobalt(III) complexes (Chapter 3) prompted us to pursue reductive carbon-carbon bond-forming reactions with organozinc compounds. Treating $Co^{III}(Et)(isq^{Ph})_2$ (Et=ethyl) with RZnBr (R=aryl or alkyl) in a 1:1 CH_3CN:THF solution results in an immediate color change from kelly green to light brown. When diluted, this light brown solution appears green again but with much less intensity. Reaction of 10 mM $Co^{III}(Et)(isq^{Ph})_2$ solution with various amounts of PhZnBr (Ph=phenyl) can be monitored by UV-vis absorption spectroscopy by diluting aliquots of the sample to 0.05 mM for analysis. Reaction with 1 equivalent of PhZnBr with $Co^{III}(Et)(isq^{Ph})_2$ decreases the amount of $Co^{III}(Et)(isq^{Ph})_2$ observed in the dilute sample to approximately

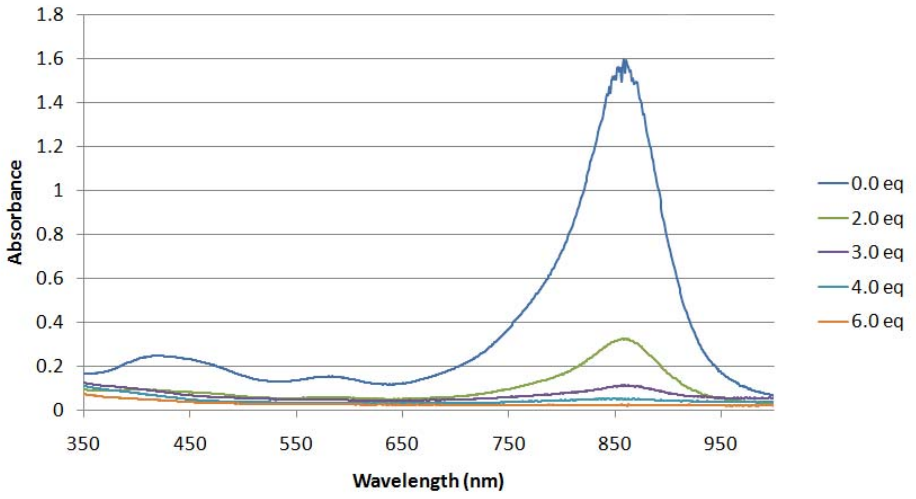

Figure 4.1. Reaction of $Co^{III}(Et)(isq^{Ph})_2$ with equivlalents of 0.4 M PhZnBr in 50:50 CH_3CN:THF at room temperature under nitrogen. Reaction is performed with 10 mM solutions and diluted to 0.05 mM for analysis.

50%. Subsequent additions progressively decrease the amount of the detectable organometallic (Figure 4.1). Complete consumption of $Co^{III}(Et)(isq^{Ph})_2$ requires >6 equivalent of PhZnBr. When the brown solution formed as a result of the addition of 6 equivalents of PhZnBr with a 10 mM solution of $Co^{III}(Et)(isq^{Ph})_2$ is oxidized with air exposure, 60% of the cobalt species used in the reaction is observed by UV-vis in the form of $Co^{III}(Br)(isq^{Ph})_2$. This indicates that the brown color is not a result of degradation of $Co(L)_2$ and demonstrates that the core complex is intact in some new form.

When monitored in 1 mM $Co^{III}(Et)(isq^{Ph})_2$ solutions and analyzed without further dilution, addition of 1 equivalent of PhZnBr again results in a decrease of the absorbance to 56% of the original intensity (Figure 4.2). However, addition of 2, 4, and 6 equivalents all results in formation of light brown solutions with identical absorbtion

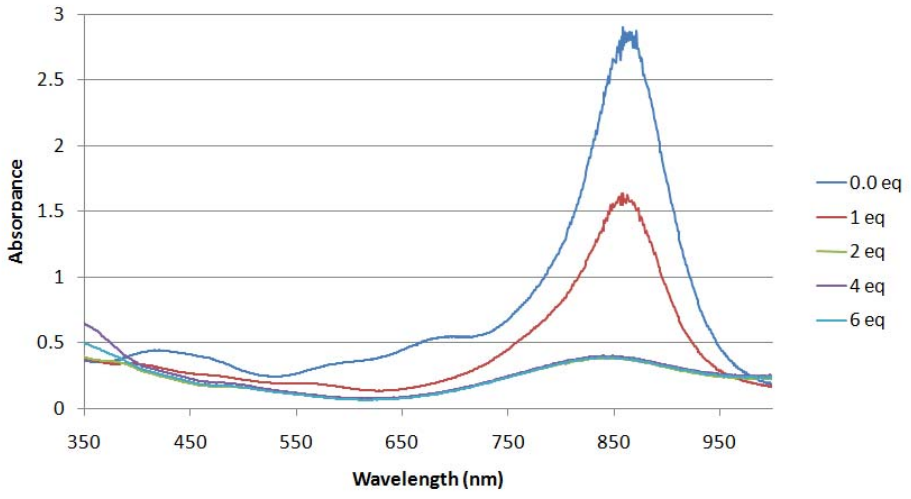

Figure 4.2. (a) Reaction of $Co^{III}(Et)(isq^{Ph})_2$ with equivlalents of 0.4 M PhZnBr in 50:50 CH_3CN:THF at room temperature under nitrogen. Reaction is performed and analyzed as 1 mM solutions.

spectra at this higher concentration (Figure 4.2). When the brown solutions containing >2 equivalents of PhZnBr are allowed to sit overnight under nitrogen and exposed to light, the solutions turn purple and have a UV-vis absorption identical to that of independently prepared $[Co^{III}(ap)_2]^-$. However, when kept at –20°C in the dark, the material remains brown over days. When the 1 mM light brown solution containing 2 equivalents of PhZnBr is exposed to air, stepwise oxidation of the cobalt material can be observed (Figure 4.3). Immediately upon exposure to air, the brown solution becomes purple with UV-vis features indicative of $[Co^{III}(ap^{Ph})_2]^-$. This is followed by formation of a royal blue solution with features indicative of $Co^{III}(isq^{Ph})(ap^{Ph})$. Finally, the solution transforms to navy blue with a UV-vis spectrum identical to that of $Co^{III}(Br)(isq^{Ph})_2$.

In an attempt to identify the light brown material, we speculated that its formation

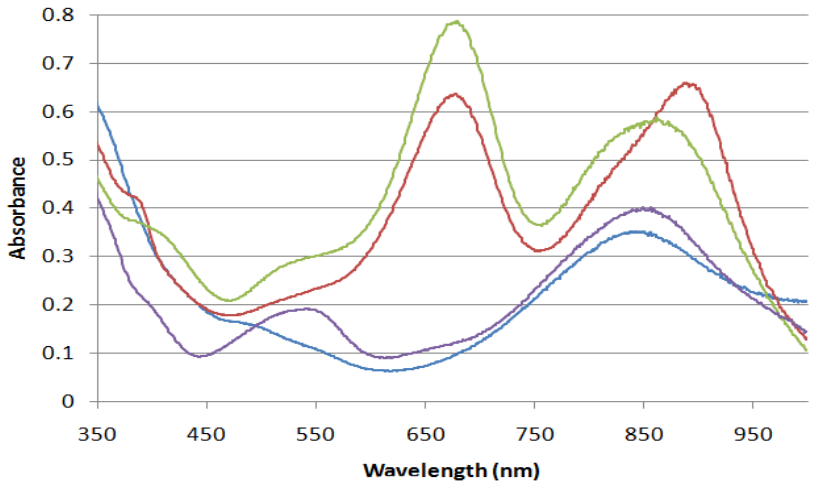

Figure 4.3. Brown solution formed (blue line) by reaction of $Co^{III}(Et)(isq^{Ph})_2$ with 2 equivalents of PhZnBr monitored at 1 mM with exposure to air. After air exposure observed to transition to first the spectrum indicated as the purple line and similar to that of $[Co^{III}(ap^{Ph})_2]^-$, followed by the red spectrum which is similar to that of $Co^{III}(isq^{Ph})(ap^{Ph})$, and finally persisting as the green spectrum similar to that of $Co^{III}(Br)(isq^{Ph})_2$.

may be a result of an interaction between the $ZnBr^+$ produced in the coupling reaction and some form of the $Co(L)_2$ core. Each metal species was independently examined in 1:1 CH_3CN:THF in the presence of 10 equivalents of $ZnBr_2$, a potential source of Zn^{2+} and Br^-, under an atmosphere of nitrogen at room temperature. Addition of $ZnBr_2$ to either green $Co^{III}(Et)(isq^{Ph})_2$ or royal blue $Co^{III}(isq^{Ph})(ap^{Ph})$ produced no color change. Reaction of purple $[Co^{III}(ap^{Ph})_2]^-$ with $ZnBr_2$ produced an immediate color change to royal blue and a UV-vis spectrum similar to that of $Co^{III}(isq^{Ph})(ap^{Ph})$. $ZnBr_2$ should not oxidize $[Co^{III}(ap^{Ph})_2]^-$ given the known oxidation potential.[47] However, as described in Chapter 2, $[Co^{III}(ap^{Ph})_2]^-$ in THF has a similar blue color and UV-vis absorption to that observed with $ZnBr_2$. This color change may be the result of its interaction with the complex and dispersion of an aggregate similar to that observed with THF. However, this interaction does not lead to the observed brown material. $[Co^{III}(isq^{Ph})_2]^+$ reacts with $ZnBr_2$ to form a mixture of the cation and neutral species showing partial reduction of the material. Reaction of $ZnBr_2$ with any of the known cobalt containing species, however, did not result in the formation of the observed brown material.

Due to broadening created by paramagnetic species in the solution, ^1H NMR spectra of the coupling reactions cannot be obtained and neither the cobalt containing species nor organic products can be identified. Gas chromatography-mass spectrometry (GC-MS) can be used to analyze the brown solutions which result from the reaction of $Co^{III}(Et)(isq^{Ph})_2$ with PhZnBr to examine the organic products of the cross-coupling reaction (Table 4.2).[53] Addition of 2 equivalents of PhZnBr has been shown by UV-vis to consume the majority of the $Co^{III}(Et)(isq^{Ph})_2$ in solution. However, analysis of the organic product indicates only an 11% yield of cross-coupled ethylbenzene. The analogous

reaction with HxZnBr (Hx=hexyl) similarly affords *n*-octane in a 5% yield. The cross-coupling product of both reactions increases to 15% yield with added excess of RZnBr reaching a maximum yield with 6-10 equivalents. Both reactions give small quantities of the corresponding homocoupling byproducts, biphenyl (<2%) and dodecane (<7%) even with large excess of RZnBr. Notably, the yield of homocoupled product does not proportionally correlate with the addition of greater excesses of RZnBr or the observed increase in cross-coupling yield. The nonstatistical distribution between the yields of the two products suggests that the products are not formed by exchange of the carbon fragments followed by radical cobalt-carbon bond homolysis and random coupling of the organic radical.

Table 4.2. Cross-coupling yields from reaction of $Co^{III}(Et)(isq^{Ph})_2$ with equivalents of PhZnBr or HxZnBr.[a]

PhZnBr	Et-Ph[b]	Ph-Ph[b]
2 equiv	11%	1.6%
4 equiv	15%	2.4%
6 equiv	15%	1.7%
10 equiv	15%	1.8%

HxZnBr	Octane[b]	Dodecane[b]
2 equiv	5%	2%
4 equiv	10%	7%
6 equiv	15%	8%

[a.] All reactions performed using 10 mM $Co^{III}(Et)(isq^{Ph})_2$ with RZnBr in 1:1 CH_3CN:THF under nitrogen.
[b.] Reported yields are the average of ≥2 trials performed using separate batches of $Co^{III}(Et)(isq^{Ph})_2$. Values quantitated based on $Co^{III}(Et)(isq^{Ph})_2$ as the limiting reagent.

Quenching the reaction solutions prior to GC-MS analysis of the organic products is done to control consistent reaction time and to ensure possible air exposure during analysis does not compromise the results. It was verified that quenching the reaction

with stoichiometric amounts of trifluroacetic acid (TFAA) did not increase or decrease the amount of coupled product detected. It was also verified that the amount of time that sealed, quenched samples sat before analysis did not alter the observed results. Solutions of $Co^{III}(Et)(isq^{Ph})_2$ with PhZnBr quenched at various times following the mixing of the reagents show no increase in coupling yield occurs after 1 hour. All solutions were therefore quenched with small amounts of TFAA at 1 hour following reaction, unless otherwise noted.

Both CH_3CN and THF are suitable solvents known in the literature for use with the coupling of organozinc reagents.[34] $Co^{III}(Et)(isq^{Ar})_2$ is insoluble in CH_3CN preventing its use alone for coupling. However, the stability of $[Co^{III}(ap^{Ar})_2]^-$ in THF is unclear due to color changes previously examined with inconclusive results (Chapter 2). $Co^{III}(Et)(isq^{Ar})_2$ can be fully dissolved in a 1:1 mix of CH_3CN:THF and no color change is observed at concentrations ≥1 mM. Also, the reaction of $Co^{III}(Et)(isq^{Ph})_2$ with PhZnBr in pure THF yields slightly less of the desired product than the same reaction performed in a 1:1

Table 4.3. Cross-coupling yields of $Co^{III}(Et)(isq^{Ph})_2$ and PhZnBr in THF and 1:1 THF:CH_3CN solvent.[c]

Cross-Coupling		
Solvent	**Et-Br**[d]	**Ph-Ph**[d]
1:1 CH_3CN:THF	13%	7.4%
THF	7.7%	8.1%

[c.] All reactions performed using 10 mM $Co^{III}(Et)(isq^{Ph})_2$ with PhZnBr in 1:1 CH_3CN:THF under nitrogen.

[d.] Reported yields are based on a side-by-side examination using the same batch of $Co^{III}(Et)(isq^{Ph})_2$. Values quantitated based on $Co^{III}(Et)(isq^{Ph})_2$ as the limiting reagent.

solvent mix of CH_3CN and THF (Table 4.3). A 1:1 mix of CH_3CN:THF allows all materials to remain homogeneous in solution and are was chosen for all coupling reactions.

Reaction with more nucleophilic organometallic reagents was also investigated. Use of PhLi, PhMgBr, or PhZnBr with $Co^{III}(Et)(isq^{Ph})_2$ each afford a color change to brown and detection of the desired cross-coupled product, ethylbenzene (Table 4.4). The lithium reagent (PhLi) and organozinc reagent give similar yields of the cross-coupling product but the homocoupling side product of the lithium reagent is found at seven times greater concentration. While the Grignard reagent (PhMgX) gives two fold better cross-coupling yields in comparison to the organozinc reagent, biphenyl is formed in twice the amount of the desired ethylbenzene. Reactions with the organozinc reagents give a more favorable ratio of cross-coupled to homocoupled product.

Table 4.4. Cross-coupling yields of $Co^{III}(Et)(isq^{Ph})_2$ with RLi, RMgX and RZnX.[e]

	PhLi [f]		**PhMgBr** [f]		**PhZnBr** [g]	
	Et-Ph [h]	**Ph-Ph** [h]	**Et-Ph** [h]	**Ph-Ph** [h]	**Et-Ph** [h]	**Ph-Ph** [h]
2 equiv	6.4%	61%	23%	38%	5.9%	3.1%
6 equiv	7.1%	47%	26%	63%	10%	7.0%
10 equiv	7.9%	52%	24%	69%	11%	10%

e. Reported yields are based on a side-by-side examination using the same batch of $Co^{III}(Et)(isq^{Ph})_2$.
f. Reaction performed using 10 mM $Co^{III}(Et)(isq^{Ph})_2$ in THF.
g. Reaction performed using 10 mM $Co^{III}(Et)(isq^{Ph})_2$ in 1:1 mixture of CH_3CN:THF.
h. Values quantitated based on $Co^{III}(Et)(isq^{Ph})_2$ as the limiting reagent.

Reaction of $Co^{III}(Et)(isq^{Ph})_2$ with PhZnBr and PhZnI yield similar amounts of cross-coupled product indicating that the halide of the organometallic reagent does not affect the yield. It has been suggested in literature that the method used in the preparation of RZnX may play a role in the reactivity of the reagent.[54] However, similar yields for the cross-coupling reaction of $Co^{III}(Et)(isq^{Ph})_2$ with PhZnBr prepared from phenyl lithium, PhMgBr, or as purchased from Sigma-Aldrich are observed. Preparation of the organozinc also appears to play no part in the limited yield.

To examine the effect of the length of the alkyl chain on the coupling yield, $Co^{III}(nPr)(isq^{Ph})_2$ (nPr=nPropyl) was reacted with PnZnBr (Pn=pentyl) and the cross-coupling product octane was observed in a maximum of 14% yield (Table 4.5). However, when $Co^{III}(Pn)(isq^{Ph})_2$ was reacted with nPrZnBr under identical conditions, the yield was decreased (4.2%).

Table 4.5. Cross-coupling yield of reaction of $Co^{III}(nPr)(isq^{Ph})_2$ with PnZnBr and $Co^{III}(Pn)(isq^{Ph})_2$ and nPrZnBr.[i]

	$Co^{III}(Pn)L_2$ + nPrZnBr [j]	**$Co^{III}(nPr)L_2$ + PnZnBr** [j]
2 equiv	1.6%	3.0%
6 equiv	3.9%	11%
10 equiv	4.2%	14%

[i] All reactions performed using 10 mM $Co^{III}(R_1)(isq^{Ph})_2$ with R_2ZnBr in 1:1 CH_3CN:THF under nitrogen.

[j] Reported yields are based on a side-by-side examination. Values quantitated based on $Co^{III}(R_1)(isq^{Ph})_2$ as the limiting reagent.

Treatment of $Co^{III}(Hx)(isq^{Ph})_2$ with nPrZnBr yields the cross-coupling product nonane. Reaction using $Co^{III}(^{4Me}Pn)(isq^{Ph})_2$ (^{4Me}Pn=4-methylpentyl) under identical conditions instead yields the branched 2-methyloctane at 30% of the former reaction with the straight chain alkyl fragment (Table 4.6). This branching in the alkyl chain, even away from its attachment site at the metal center, may disfavor the cross-coupling product formation.

Table 4.6. Cross-coupling yield of reaction of $Co^{III}(Hx)(isq^{Ph})_2$ and $Co^{III}(^{4Me}Pn)(isq^{Ph})_2$ with nPrZnBr.[k]

	Straight Chain [m]	**Branched Chain**[m]
2 equiv	9.7%	7.4%
6 equiv	13%	10%

k. All reactions performed using 10 mM $Co^{III}(R)(isq^{Ph})_2$ with nPrZnBr in 1:1 CH_3CN:THF under nitrogen.
m. Reported yields are based on a side-by-side examination. Values quantitated based on $Co^{III}(R)(isq^{Ph})_2$ as the limiting reagent.

The reactions reported thus far were limited in that any free ethyl-fragment, derived from the $Co^{III}(Et)(isq^{Ph})_2$ starting material, or the homocoupling product of the ethyl fragments, butane, cannot be quantitated due to their volatility and limitations of analysis by GC-MS. Reaction of $Co^{III}(Oc)(isq^{Ph})_2$ with HxZnBr allows possible detection of each alkyl fragment (Scheme 4.2, Table 4.7). In the solutions quenched after 1 hour,

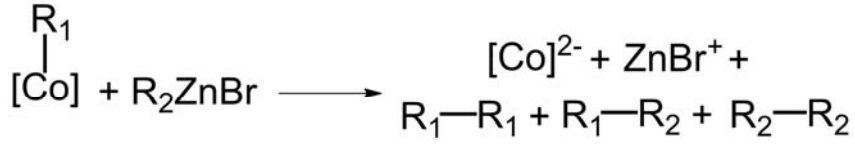

Scheme 4.2

the cross-coupled product, tetradecane (R_1-R_2, $C_{14}H_{30}$), is detected at a maximum of 9% yield. The homocoupling product of the organozinc reagent, dodecane (R_2-R_2, $C_{12}H_{26}$) is also found in 6% yield. Notably, there is no evidence of formation of the homocoupling product of the octyl fragment originally installed on the cobalt complex, hexadecane (R_1-R_1, $C_{16}H_{34}$). If coupling was a radical process or if the alkyl-fragments could exchange and scramble through a dialkyl-cobalt complex, a mix of products would be observed including R_1-R_1. However, the absence of hexadecane suggests that coupling is not a result of organic radical formation through Co-R_1 homolysis followed by radical coupling as this would lead to a statistical probability that two R_1 radicals would interact. It also suggests that alkyl exchange facilitated by an equilibrium between $Co^{III}(R_1)(isq^{Ar})_2$ and $[Co^{III}(R_1)(R_2)(isq^{Ar})_2]^-$ does not exist.

Detection and quantitation of all the alkyl fragments in solutions that were allowed to sit for 1 hour as opposed to 4 days after the reaction is also revealing. When the light brown solutions are quenched and analyzed after 1 hour, an average of 100% of the C_6 fragments from HxZnBr is found and 13% of those found are in the form of hexene. However, when the solutions are allowed to sit overnight under N_2 in light, 102% of the C_6 fragment are found and 30% of them are in the form of the unsaturated hexene. At one hour, only 36% of the C_8 fragments are found with 8% of those originally added in the form of unsaturated octene and 21% of those added in the form of octane. After 4 days, the amount of the C_8 fragment found increases to an average of 47% with 11% of those added are found in the form of octene and 30% in the form of octane. The ratio of octene to octane in the two samples remains the same. However, the ratio of hexene to hexane shows significant change, from 1:4 to 1:1. The increase in C_6 and C_8

fragments detected with time implies that the undetected fragments are likely, at least in part, bound to the metal. When $Co^{III}(Hx)(isq^{Ph})_2$ or $Co^{III}(Oc)(isq^{Ph})_2$ are independently prepared and analyzed similarly, none of the alkyl-fragments are detected. However, there is no increase in the yields of either the cross-coupling or homocoupling side reaction observed with the added time after the reaction. This suggests that the

Table 4.7. Cross-coupling yields from reaction of $Co^{III}(Oc)(isq^{Ph})_2$ with equivalents of HxZnBr.[n]

Quenched after 1 hour

	C_6H_{14} [p]	C_6H_{12} [p]	C_8H_{18} [q]	C_8H_{16} [q]	$C_{12}H_{26}$ [q]	$C_{14}H_{30}$ [q]	$C_{16}H_{34}$ [q]
2 equiv	44%	9.6%	16%	4.0%	4.4%	3.8%	0%
4 equiv	59%	14%	23%	7.4%	6.6%	5.3%	0%
6 equiv	51%	11%	20%	8.9%	5.2%	6.5%	0%
10 equiv	78%	16%	26%	13%	5.1%	8.6%	0%

Quenched after 4 days

	C_6H_{14} [p]	C_6H_{12} [p]	C_8H_{18} [q]	C_8H_{16} [q]	$C_{12}H_{26}$ [q]	$C_{14}H_{30}$ [q]	$C_{16}H_{34}$ [q]
2 equiv	46%	32%	26%	11%	5.0%	4.2%	0%
4 equiv	48%	29%	32%	8.2%	6.6%	4.5%	0%
6 equiv	61%	26%	30%	7.1%	6.3%	6.3%	0%
10 equiv	66%	32%	31%	16%	4.8%	7.8%	0%

[n.] All reactions performed using 10 mM $Co^{III}(Oc)(isq^{Ph})_2$ with HxZnBr in 1:1 CH_3CN:THF under nitrogen.

[p.] Values quantitated based on amount of HxZnBr added.

[q.] Reported yields are based on a side-by-side examination using the same batch of $Co^{III}(Oc)(isq^{Ph})_2$. Values quantitated based on $Co^{III}(Oc)(isq^{Ph})_2$ as the limiting reagent.

alkyl chains on the metal are trapped in such a way that coupling and elimination of the product is not possible.

We have synthesized $Co^{III}(Et)(isq^{Ar})_2$ with ligand substitutions in which Ar=iPr or Cl as well (see Figure 2.2). The isopropyl substituents (Ar=iPr) on the N-aryl add steric bulk around the metal center where as the added chrlorides (Ar=Cl) increase the oxidation potential by approximately 260 mV (Chapter 2). Reaction of $Co^{III}(Et)(isq^{iPr})_2$ with excess PhZnBr exhibits a decrease in both the cross-coupling yield (1.3%) and the observed homocoupling side product (1.5%) in comparison to reaction with $Co^{III}(Et)(isq^{Ph})_2$ (Table 4.8). It is also noted that, unlike $Co^{III}(Et)(isq^{Ph})_2$, there is little increase in the yield with the addition of an excess of PhZnBr. Reaction of $Co^{III}(Et)(isq^{Cl})_2$ with PhZnBr results in a higher yield of both the cross-coupling product (22%) and the homocoupling product (5%). There is no difference observed between addition of 2 equivalents and 6 equivalents for this complex. The combination of these data suggests that increased steric encumbrance surrounding the metal center disfavors successful coupling. It is also indicates that even with altered redox potential making elimination of the product more

Table 4.8. Cross-coupling yield of reaction of $Co^{III}(Et)(isq^{Ar})_2$ with PhZnBr where Ar=Ph, iPr, and Cl.[r]

	2 equiv		6 equiv	
	Et-Ph [s]	**Ph-Ph** [s]	**Et-Ph** [s]	**Ph-Ph** [s]
Ar=Phen	14%	1.3%	19%	2.0%
Ar=iPr	1.2%	0.3%	1.3%	1.5%
Ar=Cl	21%	4.7%	23%	4.7%

[r.] All reactions performed using 10 mM $Co^{III}(Et)(isq^{Ar})_2$ with PhZnBr in 1:1 CH_3CN:THF under nitrogen.
[s.] Reported yields are based on a side-by-side examination. Values quantitated based on $Co^{III}(Et)(isq^{Ar})_2$ as the limiting reagent.

favorable, coupling is still diminished by the basic structure of the complex and high yields cannot be achieved.

From examination of the two reactions which make up this step-wise Negishi-like coupling, we have found that the oxidative addition step is much slower than the transmetallation and elimination of the product. However, the product of the oxidative addition is stable to β-hydride elimination suggesting that there is the potential to facilitate the coupling catalytically in a one-pot reaction. $Na[Co^{III}(ap^{Ph})_2]$ in 1:1 CH_3CN:THF was reacted with 10 equivalents of PhZnBr and 100 equivalents of EtBr under various conditions to examine the potential for this catalytic Negishi-type cross-coupling (Table 4.9). When the reaction is performed at room temperature for 3 days, the cross-coupling product ethylbenzene is found in a yield of 23% (Table 4.9). The homocoupling side product, biphenyl, was found in 28% yield. When the same reaction was held at 0°C over 6 days, the cross-coupling product yield is similar at 24% yield and the homocoupling product observed is 17%. Heating the reaction to 60°C for 24 hours

decreases the cross-coupling yield to 14% while the homocoupling product is found in 26% yield, similar to that observed for the room temperature reaction. The mixture of PhZnBr with excess EtBr results in no detection of the desired cross coupling product in the absence of metal catalyst. At room temperature and chilled, the yield of the cross-coupling reaction was 1.5 times that of the stoichiometric reaction (Table 4.2) indicating that turnover is minimal at best. The reactions also demonstrate much higher yields of the homocoupled side-product.

Table 4.9. Cross-coupling yields from reaction of $[Co^{III}(ap^{Ph})_2]^-$ with EtBr and PhZnBr.[t]

Conditions	Et-Ph [u]	Ph-Ph [u]
RT, 3 days	23%	28%
0°C, 6 days	24%	17%
60°C, 24 hours	14%	26%

[t.] All reactions performed using 10 mM $Na[Co^{III}(ap^{Ph})_2]$ in 1:1 CH_3CN:THF under nitrogen with 10 equivalents of PhZnBr and 100 equivalents of EtBr.
[u.] Reported yields are based on a side-by-side examination. Quantitated based on $[Co^{III}(ap^{Ph})_2]^-$ as the limiting reagent.

4.3.2. Identification of source of homocoupling side-product

In an attempt to identify the source of the undesired homocoupling side-product formed during the cross-coupling reaction, PhZnBr was reacted with $[Co^{III}(ap^{Ph})_2]^-$, $Co^{III}(isq^{Ph})(ap^{Ph})$ and $[Co^{III}(CH_3CN)(isq^{Ph})_2]^+$. Examination of each reaction by UV-vis indicates that addition of excess PhZnBr to all three results in the the same brown solution observed in the cross-coupling reaction. Each solution was then analyzed for the homocoupled product, biphenyl (Table 4.10). Both the $Co^{III}(isq^{Ph})(ap^{Ph})$ and $[Co^{III}(ap^{Ph})_2]^-$ species show only a slight increase in biphenyl detected when compared to

the control solution containing no metal catalyst. However, the $[Co^{III}(CH_3CN)(isq^{Ph})_2]^+$ species formed biphenyl with the large excess of PhZnBr in 13% yield suggesting it may be responsible for the observed side product.

Table 4.10. Yield of homocoupling of PhZnBr by $[Co^{III}(ap^{Ph})_2]^-$, $Co^{III}(isq^{Ph})(ap^{Ph})$ and $[Co^{III}(CH_3CN)(isq^{Ph})_2]^+$.[v]

	$[Co^{III}(ap^{Ph})_2]^-$ [w]	$Co^{III}(ap^{Ph})(isq^{Ph})$ [w]	$[Co^{III}(isq^{Ph})_2]^+$ [w]
2 equiv	1.9%	1.0%	11%
6 equiv	5.9%	1.3%	13%

[v.] All reactions performed using 10 mM $[Co^{III}(L)_2]$ and PhZnBr in 1:1 CH_3CN:THF under nitrogen.

[w.] Reported yields are for the biphenyl homocoupling product and are based on a side-by-side examination. Values quantitated based on $[Co^{III}(L)_2]$ as the limiting reagent.

4.3.3. Preparation and characterization of $[Co^{III}(CH_3CN)(isq)_2]^+$

To examine the potential of the $[Co^{III}(isq^{Ph})_2]^+$ complex to homocouple organozinc reagents, we first synthesized and characterized the previously unisolated complex. Oxidation of $Co^{III}(ap^{Ar})(isq^{Ar})$ with one equivalent of $AgBF_4$ in CH_3CN, under nitrogen and at room temperature affords a color change from blue to blue-green within an hour (Figure 4.4). Solutions of the blue-green product in CH_3CN or 1:1 CH_3CN:THF are stable over weeks at room temperature. However, in pure THF, the ESI-MS of the material shows significant decomposition and formation of coordinatively saturated $Co^{III}(isq)_3$. $Co^{III}(isq)_3$ is observed in only small amounts in 1:1 CH_3CN:THF solutions.

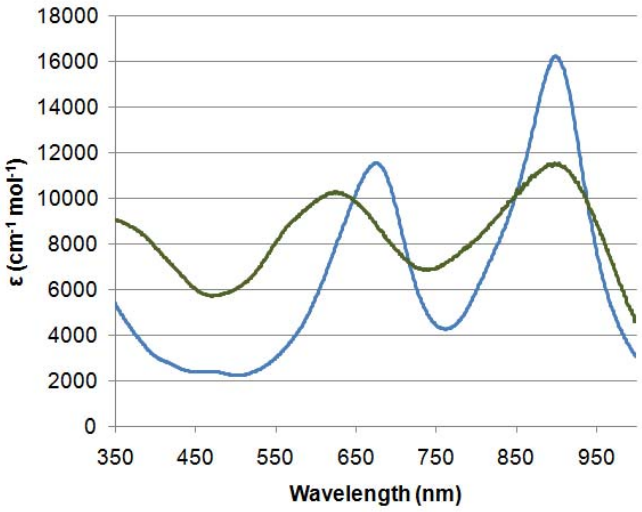

Figure 4.4. UV-vis absorption spectra of $Co^{III}(isq^{Ph})(ap^{Ph})$ (blue line) and the one electron oxidized product $[Co^{III}(isq^{Ph})_2]^+$ (green line).

Salt metathesis with $NaPh_4B$ results in no change in the UV-vis absorption but affords the $[Ph_4B]^-$ salt. A single crystal X-ray structure of $[Co^{III}(CH_3CN)(isq^{iPr})_2](Ph_4B)\bullet 2CH_3CN$ is provided in Figure 4.5.a. The complex contains

two coplanar amidophenol-derived ligands bound to the cobalt center with a single CH_3CN solvent molecule coordinated in an axial position making the complex square pyramidal and monocationic. The crystal contains two other CH_3CN molecules which to do not interact with the complex. The C–O average bond length of 1.294 Å and C–N average bond length of 1.343 Å (Figure 4.5.b.) both are significantly contracted in comparison to those previously reported for the $[Co^{III}(ap^{Ar})_2]^-$ and $Co^{III}(isq^{Ar})(ap^{Ar})$ structures (Chapter 2).[47] The C–C bond distances of both ligands exhibit a significant quinoid distortion with two short and four long bonds. The sum of this data indicates that both ligands should be assigned as iminosemiquinonate[55] and suggests that the complex is best formulated as $[Co^{III}(CH_3CN)(isq^{Ph})_2]^+$ (isq^{Ph} = 2,4-di-tert-butyl-6-(phenylimino)semiquinonate). The complex has sharp signals as detected by ^1H NMR in CD_3CN and Evan's method analysis confirms that the complex is S=0. The diamagnetism of the complex indicates that the metal and ligand radicals are antiferromagnetically coupled.[47,55] Mixing solutions of blue-green $[Co^{III}(CH_3CN)(isq^{Ph})_2]^+$ with purple $[Co^{III}(ap^{Ph})_2]^-$ lead to formation of a royal blue solution and UV-vis absorption spectrum indicative of formation of $Co^{III}(isq^{Ph})(ap^{Ph})$ implying that the complexes spontaneously comproportionate.

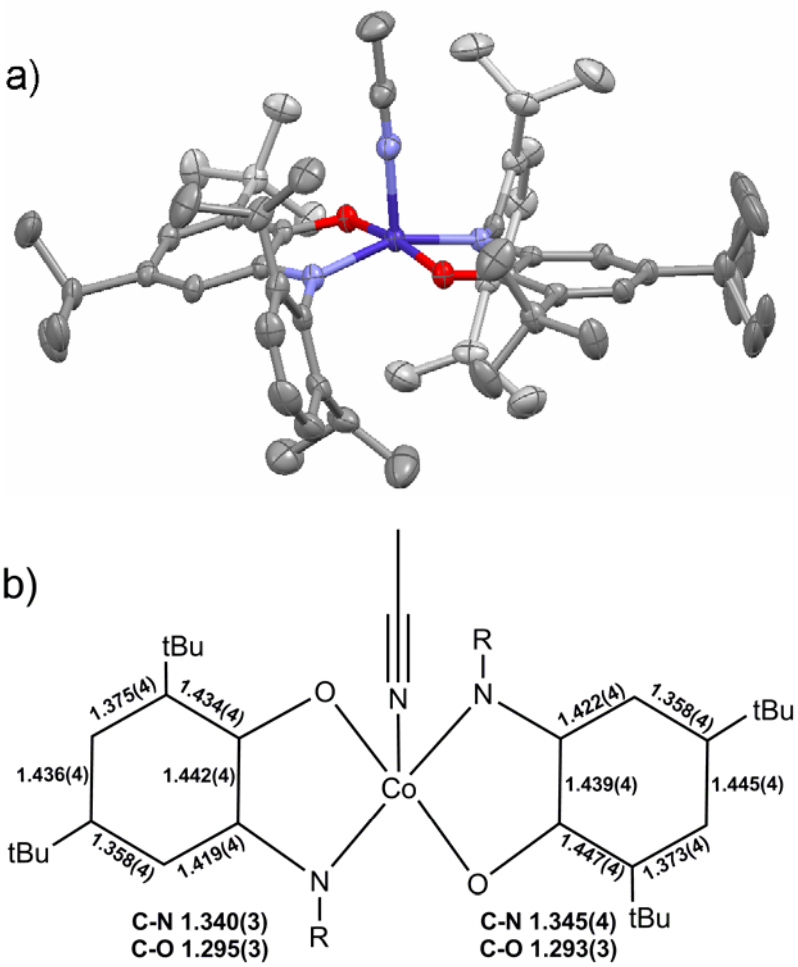

Figure 4.5. (a) Solid-state structure of $[Co^{III}(CH_3CN)(isq^{iPr})][Ph_4B]\bullet 2CH_3CN$ drawn with 50% probability ellipsoids. Hydrogen atoms, counter ion and solvent molecules omitted for clarity. **(b)** Schematic of selected bond lengths (Å) in $[Co^{III}(CH_3CN)(isq^{iPr})][Ph_4B]\bullet 2CH_3CN$.

4.3.4. Homocoupling facilitated by $[Co^{III}(CH_3CN)(isq^{Ph})_2]^+$

Reaction of $[Co^{III}(CH_3CN)(isq^{Ph})_2]^+$ with excess PhZnBr in a 1:1 CH_3CN:THF solution results in color change from blue-green to the same light brown solution observed in the cross-coupling reactions. Addition of 2 equivalents of PhZnBr gives a

5.3% yield (Table 4.11). However, with excess PhZnBr, the reaction proceeds to higher yields. Analogous reaction with 2 equivalents of HxZnBr yields just 1.8% of the the sp^3-sp^3 homocoupling product dodecane. With 20 equivalents the dodecane is observed in 30% yield.

Table 4.11. Homocoupling yields from reaction of $[Co^{III}(CH_3CN)(isq^{Ph})_2]^+$ with equivalents of PhZnBr or HxZnBr under nitrogen.[y]

PhZnBr	Ph-Ph[z]
2 equiv	5.3%
6 equiv	12%
10 equiv	15%
20 equiv	20%

HexZnBr	Dodecane[z]
2 equiv	1.8%
6 equiv	23%
10 equiv	28%
20 equiv	32%

[y.] All reactions performed using 10 mM $[Co^{III}(CH_3CN)(isq^{Ph})_2](BF_4)$ with RZnBr in 1:1 CH_3CN:THF under nitrogen.
[z.] Reported yields are the average of 2 trials performed using separate batches of $[Co^{III}(CH_3CN)(isq^{Ph})_2](BF_4)$. Values quantitated based on $[Co^{III}(CH_3CN)(isq^{Ph})_2]^+$ as the limiting reagent.

Oxidative homocoupling requires the use of a sacrificial oxidant to complete the catalytic cycle. Exposure of the reaction solutions of $[Co^{III}(CH_3CN)(isq^{Ph})_2]^+$ in the presence of RZnBr to air uses ambient O_2 as an oxidant. In a side-by-side study, reaction with PhZnBr under air increases the yield of the homocoupling product 3.4 times to 48%. Use of HxZnBr demonstrates an increase of 1.5 times to 42%. This represents a very small amount of catalytic turnover. Exposure of independently prepared $[Co^{III}(ap^{Ar})_2]^-$ to air results in partial degradation of the core and a mix of

$Co^{III}(isq^{Ar})(ap^{Ar})$ and $[Co^{III}(CH_3CN)(isq^{Ar})_2]^+$ implying that use of ambient air as an oxidant for the system may not be ideal.

Table 4.12. Homocoupling yields from reaction of $[Co^{III}(CH_3CN)(isq^{Ph})_2]^+$ with equivalents of PhZnBr or HxZnBr with and without air.[aa]

PhZnBr	Ph-Ph[bb]
2 equiv	3.4%
2 equiv + air	10%
10 equiv	14%
10 equiv + air	48%

HexZnBr	Dodecane[bb]
2 equiv	1.3%
2 equiv + air	1.1%
10 equiv	28%
10 equiv + air	42%

aa. Reactions performed using 10 mM $[Co^{III}(CH_3CN)(isq^{Ph})_2](BF_4)$ with PhZnBr in 1:1 CH_3CN:THF.

bb. Reported yields are based on a side-by-side examination using the same batch of $[Co^{III}(CH_3CN)(isq^{Ph})_2](BF_4)$. Values quantitated based on $[Co^{III}(CH_3CN)(isq^{Ph})_2]^+$ as the limiting reagent.

Characterization of $[Co^{III}(CH_3CN)(isq^{Ph})_2]^+$ demonstrates that the complex requires a weakly coordinating solvent to maintain stability both in the solid state and in solution. It has been shown in similar systems within our group that addition of a weakly coordinating ligand such as a halide increases the yield of similar homocoupling reactions.[56] There are indications in literature to suggest that pyridine or SCN^- can stabilize $[Co^{III}(CH_3CN)(isq^{Ph})_2]^+$ and may be labile in solution.[57] Addition of 10 equivalents of either pyridine or $SCN^-$to the solution of metal complex prior to the introduction of the organozinc reagent. There was no color change observed with these additions. However, the yield of the reaction of $[Co^{III}(CH_3CN)(isq^{Ph})_2]^+$ with PhZnBr in the presence of these reagents does not increase when run under N_2 or catalytically using air as an oxidant.

Reaction of $[Co^{III}(CH_3CN)(isq^{Ar})_2]^+$ in 1:1 CH_3CN:THF with substoichiometric amounts of nPrZnBr under nitrogen causes an immediate color change from blue-green to kelly green. The kelly green material has an UV-vis spectrum identical to that of the previously isolated and characterized organometallic $Co^{III}(R)(isq^{Ar})_2$ (Chapter 3) and indicates formation of $Co^{III}(nPr)(isq^{Ar})_2$. Addition of excess equivalents of the organozinc reagent results in an immediate color change of the solution from the kelly green intermediate to the light brown material as previously observed.

Titrating $[Co^{III}(CH_3CN)(isq^{Ph})_2]^+$ with substoichiometric amounts of nPrZnBr gives a maximum yield of $Co^{III}(nPr)(isq^{Ph})_2$ with addition of 0.75 equivalents as monitored at 860 nm (λ_{max} for $Co^{III}(nPr)(isq^{Ar})_2$) (Figure 4.6.a). The maximum amount of $Co^{III}(nPr)(isq^{Ph})_2$ observed equates to 42% conversion of $[Co^{III}(CH_3CN)(isq^{Ph})_2]^+$. Subsequent additions result in a decrease of the UV-vis intensity and formation of the brown material. Solutions monitored by UV-vis containing 0.50, 0.75, and 1.0 equivalents of nPrZnBr over 4 hours all show a gradual decrease in the absorbance at 860 nm with time. This indicates that the formation of $Co^{III}(nPr)(isq^{Ar})_2$ is rapid and the material is then degraded by homolysis due to light exposure.

When the same titration is performed using the bulky substituted $[Co^{III}(CH_3CN)(isq^{iPr})_2]^+$ with substiochiometric nPrZnBr, the maximum amount of $Co^{III}(nPr)(isq^{iPr})_2$ is not observed until 2.5 equivalents are added. The absorbance corresponds to 98% conversion of $[Co^{III}(CH_3CN)(isq^{iPr})_2]^+$ to $Co^{III}(nPr)(isq^{iPr})_2$ (Figure 4.6.b). Addition of 0.75 equivalents to $[Co^{III}(CH_3CN)(isq^{iPr})_2]^+$ displays 40% yield of $Co^{III}(nPr)(isq^{iPr})_2$, similar to that observed with $[Co^{III}(CH_3CN)(isq^{Ph})_2]^+$. These two observations indicate that while steric bulk surrounding the metal center does not have

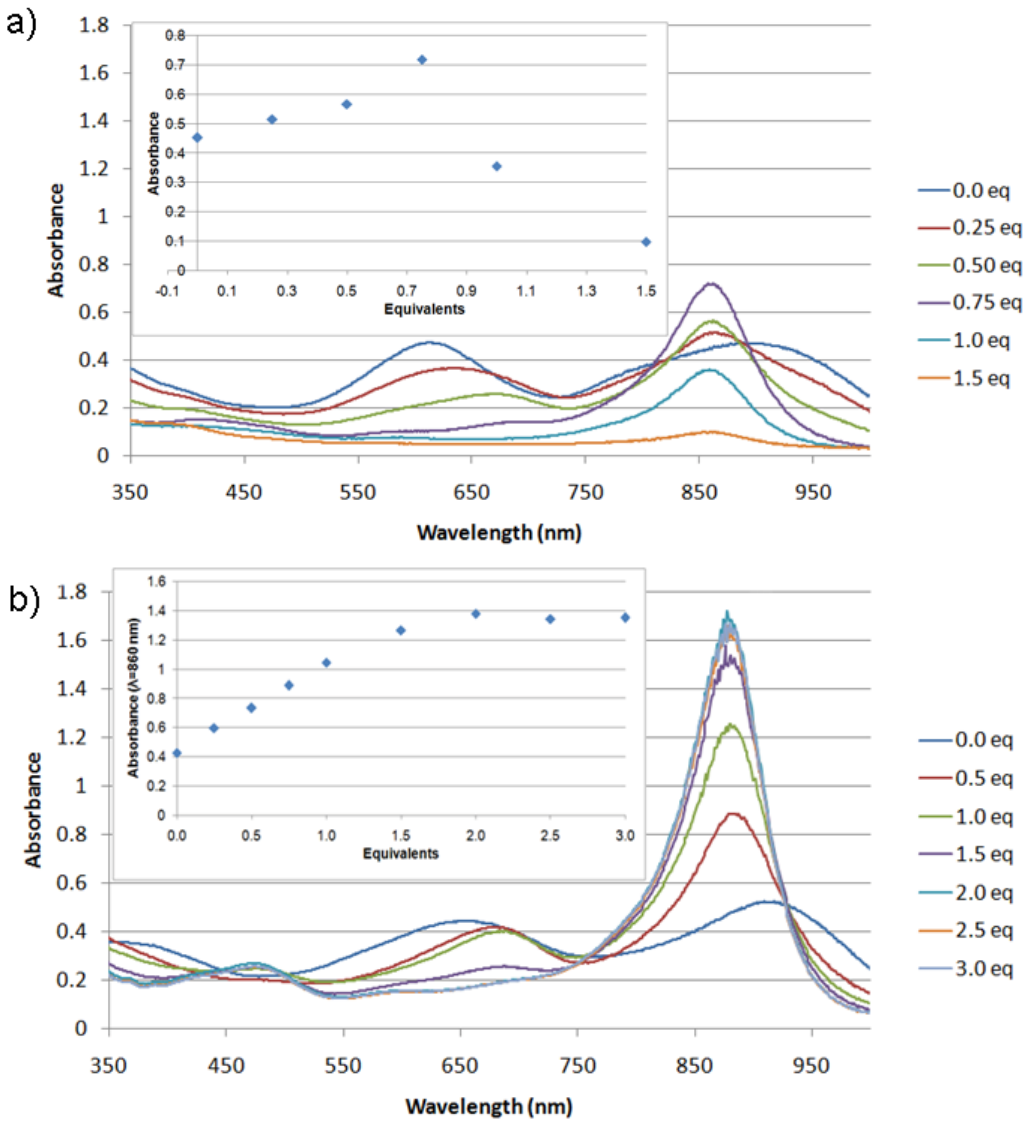

Figure 4.6. (a) Reaction of $[Co^{III}(CH_3CN)(isq^{Ph})_2]^+$ with equivalents nPrZnBr resulting in a maximum amount of $Co^{III}(nPr)(isq^{Ph})_2$ formation corresponding to a 42% yield. **(b)** Reaction of $[Co^{III}(CH_3CN)(isq^{iPr})_2]^+$ with equivalents of nPrZnBr resulting in a maximum amount of $Co^{III}(nPr)(isq^{iPr})_2$ formation corresponding to a 98% yield. Yields of the reactions are quantified based on product formation measured at 860 nm.

an effect on the installation of the first alkyl fragment and formation of $Co^{III}(nPr)(isq^{Ar})_2$, the added bulk inhibits reaction with the second fragment and formation of the brown material. Combined with the GC-MS yields for the comparable cross-coupling reactions (Table 4.8), this inhibition of the reaction with the second alkyl fragment is believed to also prevent formation of the coupling product.

From a reaction of $[Co^{III}(CH_3CN)(isq^{iPr})_2]^+$ with 0.75 equivalents of nPrZnBr chilled at –20°C over days, crystals of the product suitable for X-ray diffraction analysis were isolated (Figure 4.7.a). The crystal structure shows that the kelly green material is $Co^{III}(nPr)(isq^{iPr})_2$. The square pyramidal coordination of the ligands is similar to the previously reported $Co^{III}(Et)(isq^{Ph})_2$ structure (detailed in Chapter 3). The average of the C–O bond lengths is 1.298 Å and the C–N is 1.362 Å (Figure 4.7.b). The bond lengths of the ligands display the characteristic four long (average length is 1.418 Å) and two short (average length is 1.361 Å) indicative that both are iminosemiquinonate[55] and the complex is assigned as $Co^{III}(nPr)(isq^{iPr})_2$, the same as all previously reported $Co^{III}(R)(isq^{Ph})_2$ analogs.

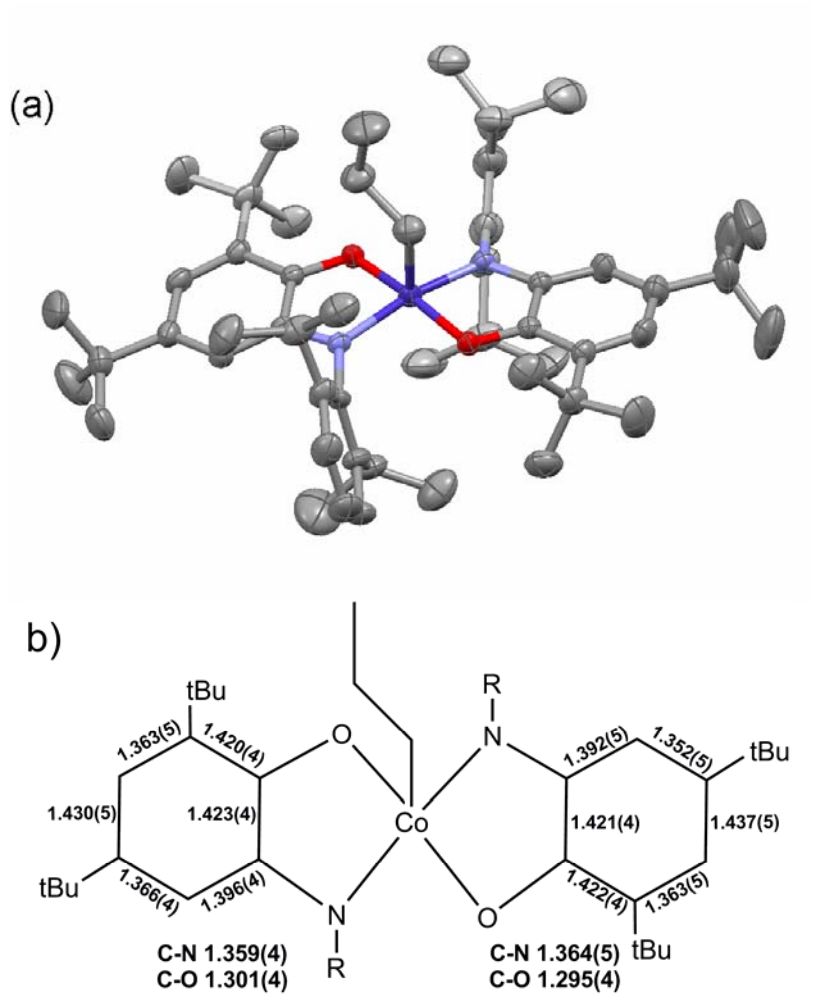

Figure 4.7. (a) Solid-state structure of $Co^{III}(nPr)(isq^{iPr})_2$ drawn with 50% probability ellipsoids. Hydrogen atoms omitted for clarity. **(b)** Schematic of selected bond lengths (Å) in $Co^{III}(nPr)(isq^{iPr})_2$.

4.4. Discussion

4.4.1. Characterization of $[Co^{III}(CH_3CN)(isq^{Ar})_2]^+$ and implication of its electronic structure

In a previous report (Chapter 2),[47] we detailed the synthesis, isolation and characterization of $Na[Co^{III}(ap^{Ar})_2]$ and the one electron oxidized material $Co^{III}(isq^{Ar})(ap^{Ar})$. Isolation of the cationic $[Co^{III}(CH_3CN)(isq^{Ar})_2]^+$ represents an important step in our understanding of the electronic series of these complexes. This form of the fully oxidized material has never before been isolated without coordination of a stabilizing anionic ligand.[58,59] The structural and electronic characterization of $[Co^{III}(CH_3CN)(isq^{Ar})_2]^+$ shows that the two electron oxidation of $[Co^{III}(ap^{Ar})_2]^-$ occurs with both electrons derived from the ligand set. This supports our previous belief from characterization of reaction products (Chapter 2 and 3) that the two highest energy electrons accessed both electronically and during reactivity are in molecular orbitals that are largely ligand derived. As a result of oxidation, no other structural changes are evident.

4.4.2. Similarities between the two coupling reactions

Reaction of $Co^{III}(R_1)(isq^{Ar})_2$ with R_2ZnBr leads to formation of a new carbon-carbon bond in a step-wise Negishi-type coupling reaction (Scheme 4.3) similar to those previously reported at palladium and nickel. The reaction is successful with both sp^2 and sp^3-hybridized organozinc reagents in similarly low yields. We also observe a side reaction, homocoupling of the organometallic nucleophiles, in both stoichiometric, step-wise reactions and the catalytic reactions using $[Co^{III}(ap^{Ar})_2]^-$.

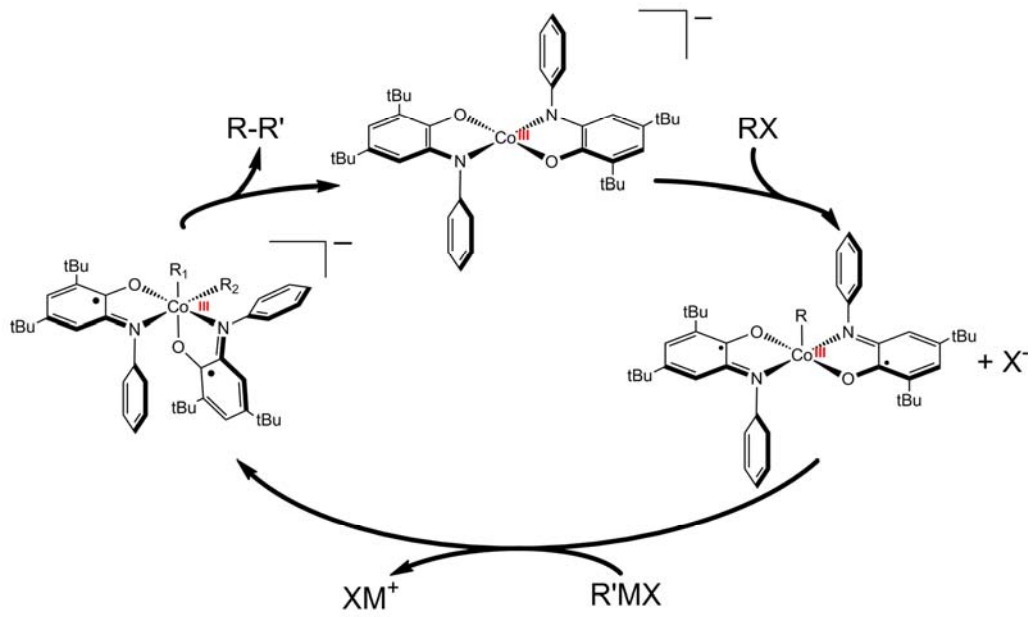

Scheme 4.3

Investigation of the source of this side reaction found that the fully oxidized form of the complex, $[Co^{III}(CH_3CN)(isq^{Ar})_2]^+$, successfully couples organozinc reagents forming a new carbon-carbon bond as well. This reaction performed under nitrogen is part of an oxidative homocoupling cycle which can be made catalytic with use of a sacrificial

oxidant (Scheme 4.4).[30] Exposure of the solutions to air however only demonstrates small amounts of turnover. Examination of the reaction of $[Co^{III}(CH_3CN)(isq^{Ph})_2]^+$ with substoichiometric amounts of nPrZnBr, indicate that the homocoupling and cross-coupling have $Co^{III}(R)(isq^{Ph})_2$ as a common intermediate. Both reactions are believed to be the same mechanistically with regards to the reaction with the second organometallic nucleophile and the elimination of the new organic product.

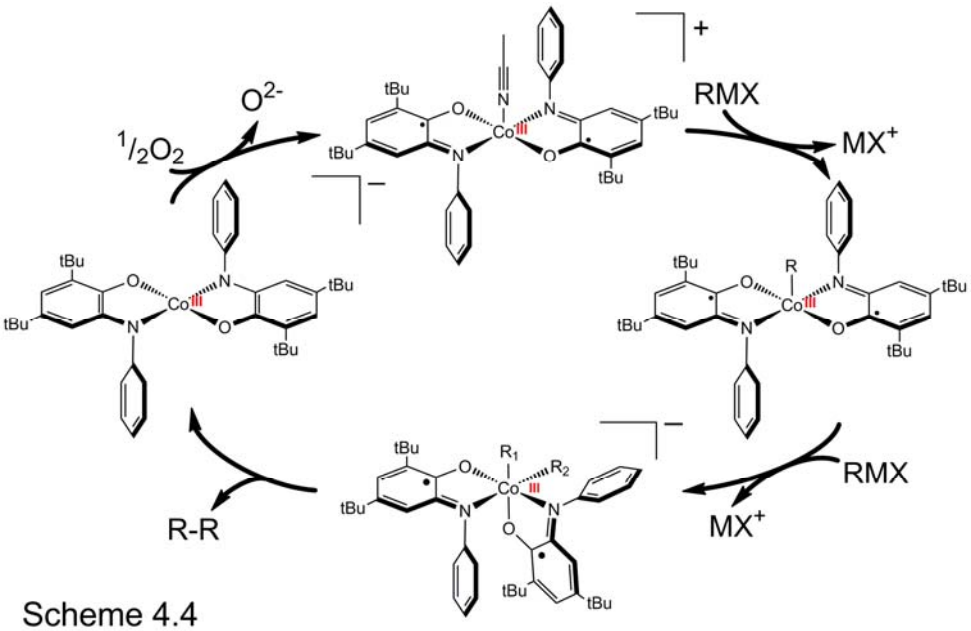

Scheme 4.4

4.4.3. Limitations of catalytic turnover

When the cross-coupling reaction is performed in a single, one pot reaction as opposed to the stepwise study previously outlined, only 1.5 turnovers is observed, based on the step-wise coupling yields. The reagents were not charged equally based on the

relative rates of the slow reaction to oxidatively add the alkyl halide to the cobalt complex as opposed to the rapid reaction with RZnX to form the coupled product. An excess of alkyl halide was used in comparison to the organozinc reagent to kinetically push the reaction to favor cross-coupling. However, there is very little turnover observed. The homocoupling side reaction may be controlled with temperature without impairing the cross-coupling yield. However, heating the reaction greatly decreases the cross-coupling yield. This is possibly due to thermal instability of the $Co^{III}(R)(isq^{Ar})_2$ intermediate.

Completion of the catalytic oxidative homocoupling cycle requires use of a two electron oxidant to transform the metal species from $[Co^{III}(ap^{Ar})_2]^-$ to $[Co^{III}(CH_3CN)(isq^{Ar})_2]^+$. The use of benign and readily available oxygen from the air has many benefits and has been shown to be used successfully to couple organometallic sources of carbon nucleophiles.[41,60] When the homocoupling solutions are exposed to ambient air for 1 hour, coupling yields do increase. However, there is only evidence of 2-3 turnovers, even when a large excess of reagent is available. The independent oxidation of $[Co^{III}(ap^{Ar})_2]^-$ to $[Co^{III}(CH_3CN)(isq^{Ar})_2]^+$ using ambient air exposure is known to produce a mix of neutral and cationic species along with significant degradation of the core complex. This indicates that facile turnover is unlikely using air as the oxidant for the system. However, the stoichiometric yields were so low that further exploration for a suitable oxidant did not appear of value.

4.4.4. Mechanistic implications of coupling reactions

Given the limited yield of the coupling reactions and the inability to overcome this low yield, we turned to understand the mechanism of the reactions and explain the limited yield. Mechanistic studies of the pseudo-oxidative addition of $[Co^{III}(ap^{Ar})_2]^-$ with alkyl halides to form $Co^{III}(R)(isq^{Ar})_2$ (Scheme 4.5, Reaction 1a) have been previously reported (Chapter 3) and is believed to proceed in a S_N2-like reaction. In studies of reactivity starting with the isolated $Co^{III}(R)(isq^{Ar})_2$, the pathway to form the organometallic plays no role and the reaction with the second alkyl and product formation can be examined separately. Formation of $Co^{III}(R)(isq^{Ar})_2$ from $[Co^{III}(CH_3CN)(isq^{Ar})_2]^+$ (Scheme 4.5, Reaction 1b) is a simple acid-base reaction which occurs rapidly.

The sum of the data presented indicates that the coupling reaction is facilitated through inner-sphere, concerted reactions. The sensitivity of the coupling reaction to the

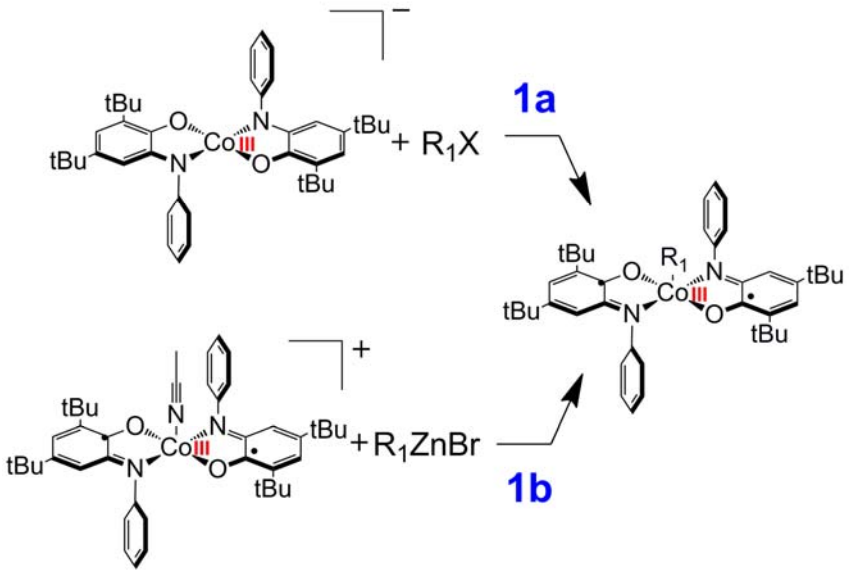

Scheme 4.5

steric bulk of both the ligands surrounding the metal center as well as the size of the organic fragments to be coupled implies that the coupling is facilitated directly at the metal center. Also, with increased amounts of organozinc reagent, the yield of the step-wise cross-coupling reaction increases while the homocoupled product formation does not increase proportionally. This suggests that the homocoupling reaction is a side-reaction and not indicative of radical coupling which allows uncontrolled product formation. A possible reaction pathway involving inner-sphere, concerted reactivity for the transmetallation and reductive elimination of the reaction is proposed in Scheme 4.6.

Treatment of $Co^{III}(R_1)(isq^{Ar})_2$ with R_2ZnBr results in immediate color changes and the concentration of the coupling products observed does not increase over time. This implies that the low yield, which can be increased with excess RZnBr, is not a result of a kinetic barrier. It also suggests that Reaction 3 is rapid and that elimination of the organic product from the metal is irreversible. As there is no formation of hexadecane

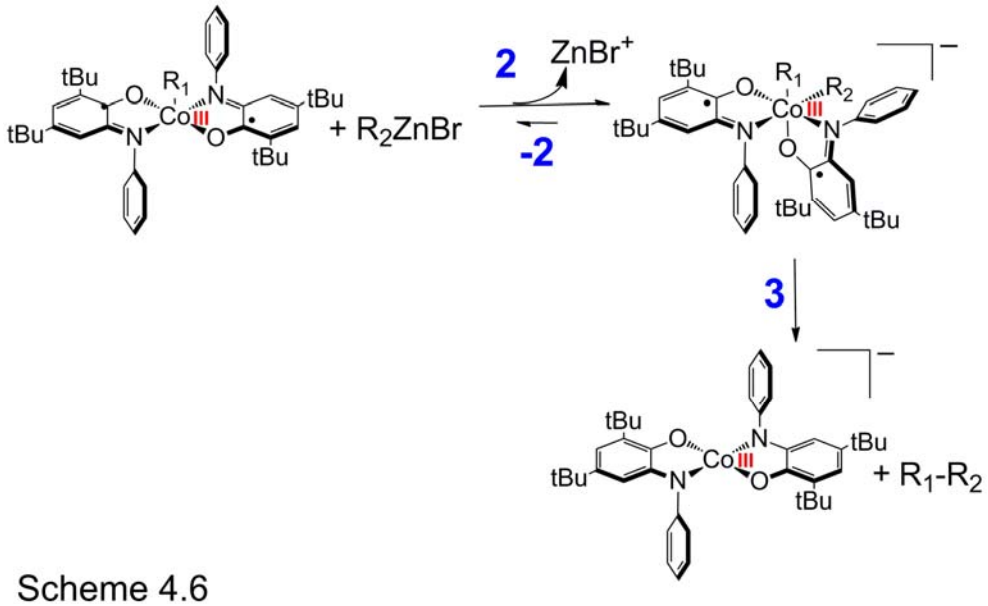

Scheme 4.6

(Scheme 4.4, R_1-R_1) observed in the reaction of $Co^{III}(Oc)(isq^{Ph})_2$ with HxZnBr, there is no evidence that an equilibrium exist between the monoalkyl and dialkyl complexes. If Reaction –2 is a competitive pathway in the cross-coupling, there is a statistical probability of formation of both homocoupled products R_1-R_1 and R_2-R_2 as the alkyl-fragments could exchange (Scheme 4.2). This conclusion also agrees with the previous observation that the homocoupling product is formed as a side-reaction and is not a result of scrambling of the alky fragments in the reaction.

4.4.5. Challenges to coupling using $[Co^{III}(ap^{Ar})_2]^-$ and $[Co^{III}(isq^{Ar})_2]^+$

The limited success of this system at carbon-carbon coupling reactions illustrates the role that sterics of the catalytic species plays in its reactivity. We have presented cases in which the cross-coupling yield is sensitive to both the length of the alkyl chains coupled and the steric encumbrance the ligands create surrounding the metal center. Cross-coupling reactions using the $Co^{III}(Et)(isq^{iPr})_2$ containing added bulk at the ligands show a 13 fold decrease and almost complete inhibition of the reaction in comparison to the yield of the unsubstituted $Co^{III}(Et)(isq^{Ph})_2$. As previously discussed (Chapter 2), the isopropyl groups are situated such that they crowd around the metal center.

UV-vis titrations of the $[Co^{III}(CH_3CN)(isq^{Ph})_2]^+$ in comparison to $[Co^{III}(CH_3CN)(isq^{iPr})_2]^+$ are revealing as well. Reaction with substoichiometric amounts of nPrZnBr up to 0.75 equivalents produce $Co^{III}(nPr)(isq^{Ar})_2$ in equal amounts for both Ar=Ph and iPr. It is the addition of the second organic fragment that is suppressed by the steric congestion. This is evidenced by quantitative formation of $Co^{III}(R)(isq^{iPr})_2$ as opposed to the maximum yield of 42% $Co^{III}(R)(isq^{Ph})_2$ which then proceeds on to brown

material and organic product. The stability of $Co^{III}(Et)(isq^{iPr})_2$ with 2 to 3 equivalents of nPrZnBr, illustrates the inability to access the six-coordinate dialkyl complex. These observations indicate that steric bulk does not greatly affect the binding of the first organic fragment to the metal but disfavors binding of the second organic fragment.

When the cross-coupling reaction is performed with $Co^{III}(Et)(isq^{Cl})_2$ in comparison to the $Co^{III}(Et)(isq^{Ph})_2$ complex only a slight increase in the yield is observed. Electronically, $Co^{III}(R)(isq^{Cl})_2$ should be much more electrophilic than $Co^{III}(R)(isq^{Ph})_2$ and reactive with the organozinc reagent. However, it is evident from the marginal increase in the product formation that the steric constraints of the ligand are more significant than can be overcome by the 260 mV adjustment of the redox potential.

Examination of the organic molecules in the coupling solutions cannot account for the sum of all R_1 and R_2 added to the reaction. The reaction of $Co^{III}(Oc)(isq^{Ph})_2$ with HxZnBr indicates that the brown material may contain the unreacted R_1 molecules as the amount found increases over time. While characterization of the brown material formed from the coupling reactions was not conclusive, we have demonstrated that it contains at least the majority of the $Co(L)_2$ core and is not a product of degradation. From these observations, we believe that the brown material is a form of the organometallic cobalt complex, trapped by the R_2ZnBr in such a way that it cannot facilitate coupling and produce new carbon-carbon bonds.

The sum of all the data concerning the sensitivity of the reactions to both the sterics of the organic fragments and of the complex supports the conclusion that the coupling occurs through an inner-sphere reaction. The added information that the steric constraint greatly affects reaction with the second alkyl fragment demonstrates that the

coupling cycle requires installation of this organic fragment at the cobalt center. We previously reported that $Co(Et)(isq^{Ph})_2$ is not prone to β-hydride elimination and shows no evidence of CO insertion into the cobalt-carbon bond (Chapter 3). Both of these facts may indicate that the five-coordinate complex is not able to isomerize to allow access to a site *cis* to the alkyl ligand. While similar complexes containing the same amidopheonol-derived ligand on rhenium[61] or a modified amidophenol-derived ligand on zirconium[62] have been reported to exist with labile ligands in *cis* sites, calculations are required to determine if this is accessible with the cobalt(III) species. If this isomerization is disfavored, the two alkyl fragments cannot arrange *cis* to one another to combine and eliminate from the metal center. This may be the root of the limited coupling yields.

4.5. Conclusions

We previously demonstrated the ability of the nucleophilic $[Co^{III}(ap^{Ar})_2]^-$ to pseudo-oxidatively add alkyl halides forming a stable cobalt-carbon bond. In this study, we have demonstrated that the isolated organometallic $Co^{III}(R)(isq^{Ar})_2$ can be used to facilitate Negishi-type cross-coupling in a step-wise fashion with both sp^2 and sp^3 organozinc reagents. Synthesis and characterization of the oxidized $[Co^{III}(CH_3CN)(isq^{Ar})_2]^+$ indicates that the two electron difference between the anion and cation are both formally derived from the ligand set. We believe this species may be responsible for the homocoupling side reaction observed from the cross-coupling solutions. This cation can be shown independently to oxidatively homocouple organozinc reagents. Observation of the intermediate $Co^{III}(R)(isq^{Ar})_2$ from reaction of $[Co^{III}(CH_3CN)(isq^{Ar})_2]^+$ with RZnBr implies that these two coupling reactions are

mechanistically the same with regard to the reaction of the cobalt complex with the second organic-fragment, formation of the new carbon-carbon bond, and elimination of the coupled product.

The yield of both coupling reactions however is low. Examination of the metal species following the coupling reactions indicated that the cobalt material is not degraded by the reaction. However, the material does react with something in the solution quenching its characteristic charge transfer bands and making its quantitation and identification difficult. It is believed to exist in a reduced state and contain alkyl fragments.

Mechanistic investigation of the reactions shows that the bond-forming reaction is inner-sphere and occurs the metal center. Furthermore, this is apparently no equilibrium between the monoalkyl- and dialkyl-intermediates. The coupling reaction occurs with immediate addition of the organozinc reagent. We believe that elimination of the coupled product is rapid and irreversible. However, formation of the dialkyl complex in an isomeric form able to eliminate the coupled organic product is disfavored.

The coupling yield is greatly affected by sterics. Increased steric bulk around the metal center makes installation of the second organic fragment disfavored and thereby inhibits the coupling reaction. We believe that the low yield of all coupling reactions with all analogs of the complex are due to this steric hinderance concerning installation of the second organic-fragment at the metal center. However, we have demonstrated successful facilitation of an inner-sphere coupling reaction at a first row transition metal, typically prone to radical reactivity, with the use of redox-active ligands.

4.6. References

1. Suzuki, A., Cross-Coupling Reactions Of Organoboranes: An Easy Way To Construct C-C Bonds *Nobel Lecture* **2010**.

2. Negishi, E.-i., Magical Power of Transition Metals: Past, Present, and Future. *Nobel Lecture* **2010**.

3. Davies, P. W., Organometallics. Transition metals in organic synthesis. *Annu. Rep. Prog. Chem., Sect. B: Org. Chem.* **2008,** *104*, 68-87.

4. Molnar, A., Efficient, Selective, and Recyclable Palladium Catalysts in Carbon-Carbon Coupling Reactions. *Chem. Rev.* **2011,** *111*, 2251-2320.

5. Diederich, F.; Stang, P. J.; Editors, *Metal-catalyzed Cross-coupling Reactions*. Wiley-VCH: 1998; p 517.

6. Brennfuehrer, A.; Neumann, H.; Beller, M., Palladium-Catalyzed Carbonylation Reactions of Aryl Halides and Related Compounds. *Angew. Chem., Int. Ed.* **2009,** *48*, 4114-4133.

7. Zhao, Y.; Wang, H.; Hou, X.; Hu, Y.; Lei, A.; Zhang, H.; Zhu, L., Oxidative Cross-Coupling through Double Transmetallation: Surprisingly High Selectivity for Palladium-Catalyzed Cross-Coupling of Alkylzinc and Alkynylstannanes. *J. Am. Chem. Soc.* **2006,** *128*, 15048-15049.

8. Suzuki, A., Carbon-carbon bonding made easy. *Chem. Commun.* **2005**, 4759-4763.

9. Negishi, E.-i.; Hu, Q.; Huang, Z.; Wang, G.; Yin, N. In *Palladium- or nickel-catalyzed cross-coupling reactions with organozincs and related organometals*, John Wiley & Sons Ltd.: 2006; p 457-553.

10. Terao, J.; Kambe, N., Transition metal-catalyzed C-C bond formation reactions using alkyl halides. *Bull. Chem. Soc. Jpn.* **2006,** *79*, 663-672.

11. Terao, J.; Kambe, N., Cross-Coupling Reaction of Alkyl Halides with Grignard Reagents Catalyzed by Ni, Pd, or Cu Complexes with π-Carbon Ligand(s). *Acc. Chem. Res.* **2008,** *41*, 1545-1554.

12. Milne, J. E.; Buchwald, S. L., An Extremely Active Catalyst for the Negishi Cross-Coupling Reaction. *J. Am. Chem. Soc.* **2004,** *126*, 13028-13032.

13. Han, C.; Buchwald, S. L., Negishi Coupling of Secondary Alkylzinc Halides with Aryl Bromides and Chlorides. *J. Am. Chem. Soc.* **2009,** *131*, 7532-7533.

14. Fu, G. C., The Development of Versatile Methods for Palladium-Catalyzed Coupling Reactions of Aryl Electrophiles through the Use of P(t-Bu)3 and PCy3 as Ligands. *Acc. Chem. Res.* **2008,** *41*, 1555-1564.

15. Netherton, M. R.; Fu, G. C., Nickel-catalyzed cross-couplings of unactivated alkyl halides and pseudohalides with organometallic compounds. *Adv. Synth. Catal.* **2004,** *346*, 1525-1532.

16. Smith, S. W.; Fu, G. C., Nickel-catalyzed Negishi cross-couplings of secondary nucleophiles with secondary propargylic electrophiles at room temperature. *Angew. Chem., Int. Ed.* **2008,** *47*, 9334-9336.

17. Rudolph, A.; Lautens, M., Secondary alkyl halides in transition-metal-catalyzed cross-coupling reactions. *Angew. Chem., Int. Ed.* **2009,** *48*, 2656-2670.

18. Hatakeyama, T.; Hashimoto, S.; Ishizuka, K.; Nakamura, M., Highly Selective Biaryl Cross-Coupling Reactions between Aryl Halides and Aryl Grignard Reagents: A New Catalyst Combination of N-Heterocyclic Carbenes and Iron, Cobalt, and Nickel Fluorides. *J. Am. Chem. Soc.* **2009,** *131*, 11949-11963.

19. Bedford, R. B.; Nakamura, M.; Gower, N. J.; Haddow, M. F.; Hall, M. A.; Huwe, M.; Hashimoto, T.; Okopie, R. A., Iron-catalysed Suzuki coupling? A cautionary tale. *Tetrahedron Lett.* **2009,** *50*, 6110-6111.

20. Czaplik, W. M.; Mayer, M.; Cvengros, J.; Jacobi, v. W. A., Coming of Age: Sustainable Iron-Catalyzed Cross-Coupling Reactions. *ChemSusChem* **2009,** *2*, 396-417.

21. Fuerstner, A.; Martin, R., Advances in iron catalyzed cross coupling reactions. *Chem. Lett.* **2005,** *34*, 624-629.

22. Sherry, B. D.; Fuerstner, A., The Promise and Challenge of Iron-Catalyzed Cross Coupling. *Acc. Chem. Res.* **2008,** *41*, 1500-1511.

23. Cahiez, G.; Moyeux, A., Cobalt-Catalyzed Cross-Coupling Reactions. *Chem. Rev.* **2010,** *110*, 1435-1462.

24. Cotton, F. A., *Advanced Inorganic Chemistry, 6th Edition*. Wiley-Interscience: 1999.

25. Nakamura, M.; Matsuo, K.; Ito, S.; Nakamura, E., Iron-catalyzed cross-coupling of primary and secondary alkyl halides with aryl Grignard reagents. *J. Am. Chem. Soc.* **2004,** *126*, 3686-3687.

26. Knochel, P.; Singer, R. D., Preparation and reactions of polyfunctional organozinc reagents in organic synthesis. *Chem. Rev.* **1993,** *93*, 2117-88.

27. Jones, G. D.; Martin, J. L.; McFarland, C.; Allen, O. R.; Hall, R. E.; Haley, A. D.; Brandon, R. J.; Kanovalova, T.; Desrochers, P. J.; Pulay, P.; Vicic, D. A., Ligand Redox Effects in the Synthesis, Electronic Structure, and Reactivity of an Alkyl-Alkyl Cross-Coupling Catalyst. *J. Am. Chem. Soc.* **2006,** *128*, 13175-13183.

28. Ohmiya, H.; Yorimitsu, H.; Oshima, K., Cobalt-catalyzed cross-coupling reaction of chloropyridines with Grignard reagents. *Chem. Lett.* **2004,** *33*, 1240-1241.

29. Gosmini, C.; Begouin, J.-M.; Moncomble, A., Cobalt-catalyzed cross-coupling reactions. *Chem. Comm.* **2008**, 3221-3233.

30. Shi, W.; Liu, C.; Lei, A., Transition-metal catalyzed oxidative cross-coupling reactions to form C-C bonds involving organometallic reagents as nucleophiles. *Chem. Soc. Rev.* **2011,** *40*, 2761-2776.

31. Martin, R.; Fuerstner, A., Cross-coupling of alkyl halides with aryl Grignard reagents catalyzed by a low-valent iron complex. *Angew. Chem., Int. Ed.* **2004,** *43*, 3955-3957.

32. Phapale, V. B.; Guisan-Ceinos, M.; Bunuel, E.; Cardenas, D. J., Nickel-Catalyzed Cross-Coupling of Alkyl Zinc Halides for the Formation of C(sp2)-C(sp3) Bonds: Scope and Mechanism. *Chem.--Eur. J.* **2009,** *15*, 12681-12688.

33. Blackmore, K. J.; Lal, N.; Ziller, J. W.; Heyduk, A. F., Catalytic Reactivity of a Zirconium(IV) Redox-Active Ligand Complex with 1,2-Diphenylhydrazine. *J. Am. Chem. Soc.* **2008,** *130*, 2728-2729.

34. Erdik, E.; Editor, *Organozinc Reagents in Organic Synthesis*. CRC: 1996; p 464

35. Phapale, V. B.; Cardenas, D. J., Nickel-catalyzed Negishi cross-coupling reactions: scope and mechanisms. *Chem. Soc. Rev.* **2009,** *38*, 1598-1607.

36. Erdik, E.; Kocoglu, M., A brief survey on the copper-catalyzed allylation of alkylzinc and Grignard reagents under Barbier conditions. *Appl. Organomet. Chem.* **2006,** *20*, 290-294.

37. Jin, L.; Zhang, H.; Li, P.; Sowa, J. R.; Lei, A., What is the Rate of the Csp2-Csp2 Reductive Elimination Step? Revealing an Unusually Fast Ni-Catalyzed Negishi-Type Oxidative Coupling Reaction. *J. Am. Chem. Soc.* **2009,** *131*, 9892-9893.

38. Jin, L.; Xin, J.; Huang, Z.; He, J.; Lei, A., Transmetalation is the Rate-Limiting Step: Quantitative Kinetic Investigation of Nickel-Catalyzed Oxidative Coupling of Arylzinc Reagents. *J. Am. Chem. Soc.* **2010,** *132*, 9607-9609.

39. Ohmiya, H.; Yorimitsu, H.; Oshima, K., Cobalt-mediated cross-coupling reactions of primary and secondary alkyl halides with 1-(trimethylsilyl)ethenyl- and 2-trimethylsilylethynylmagnesium reagents. *Org. Lett.* **2006,** *8*, 3093-3096.

40. Ohmiya, H.; Wakabayashi, K.; Yorimitsu, H.; Oshima, K., Cobalt-catalyzed cross-coupling reactions of alkyl halides with aryl Grignard reagents and their application to sequential radical cyclization/cross-coupling reactions. *Tetrahedron* **2006,** *62*, 2207-2213.

41. Liu, C.; Zhang, H.; Shi, W.; Lei, A., Bond formations between two nucleophiles: Transition metal catalyzed oxidative cross-coupling reactions. *Chem. Rev.* **2011,** *111*, 1780-1824.

42. Smith, A. L.; Hardcastle, K. I.; Soper, J. D., Redox-Active Ligand-Mediated Oxidative Addition and Reductive Elimination at Square Planar Cobalt(III): Multielectron Reactions for Cross-Coupling. *J. Am. Chem. Soc.* **2010,** *132*, 14358-14360.

43. Dzik, W. I.; van der Vlugt, J. I.; Reek, J. N. H.; de Bruin, B., Ligands that store and release electrons during catalysis. *Angew. Chem., Int. Ed.* **2011,** *50*, 3356-3358.

44. Schrauzer, G. N.; Weber, J. H.; Beckham, T. M., Cobalt-carbon bond cleavage in substituted alkylcobalamins and alkylcobaloximes. Evidence for d-orbital participation and olefinπ complexes of cobalt(I) nucleophiles. *J. Am. Chem. Soc.* **1970,** *92*, 7078-86.

45. Schrauzer, G. N.; Sibert, J. W.; Windgassen, R. J., Photochemical and thermal cobalt-carbon bond cleavage in alkylcobalamins and related organometallic compounds. Comparative study. *J. Am. Chem. Soc.* **1968,** *90*, 6681-8.

46. Kozlowski, P. M.; Kuta, J.; Galezowski, W., Reductive Cleavage Mechanism of Methylcobalamin: Elementary Steps of Co-C Bond Breaking. *J. Phys. Chem. B* **2007,** *111*, 7638-7645.

47. Smith, A. L.; Clapp, L. A.; Hardcastle, K. I.; Soper, J. D., Redox-active ligand-mediated Co-Cl bond-forming reactions at reducing square planar cobalt(III) centers. *Polyhedron* **2010,** *29*, 164-169.

48. Evans, D. F., The determination of the paramagnetic susceptibility of substances in solution by nuclear magnetic resonance. *J. Am. Chem. Soc.* **1959**, 2003-2005.

49. Krasovskiy, A.; Knochel, P., Convenient titration method for organometallic zinc, magnesium, and lanthanide reagents. *Synthesis* **2006,** *5*, 890-891.

50. apex II, Analytical X-ray Systems, Brukers AXS, Inc., Madison, WI, 2005.

51. saint Version 6.45A, Analytical X-ray Systems, Brukers AXS, Inc., Madison, WI, 2003.

52. shelxtl Version 6.12, Analytical X-ray Systems, Bruker AXS, Inc., Madison, WI, 2002.

53. Error analysis of 4 different cross-coupling reactions of 4 batches of Co(Et)(isqPh)2 with PhZnBr show the reported error to be ±30% of the reported values. This is the experimental error and not simply the error of analysis.

54. Jin, L.; Liu, C.; Liu, J.; Hu, F.; Lan, Y.; Batsanov, A. S.; Howare, J. A. K.; Marder, T. B.; Lei, A., Revelation of the difference beteween arylzinc reagents prepared from aryl Grignard and aryllithium reagents respectively: Kinetic and structral features. *J. Am. Chem. Soc.* **2009,** *131*, 16656-16657.

55. Chun, H.; Verani, C. N.; Chaudhuri, P.; Bothe, E.; Bill, E.; Weyhermueller, T.; Wieghardt, K., Molecular and Electronic Structure of Octahedral o-Aminophenolato and o-Iminobenzosemiquinonato Complexes of V(V), Cr(III), Fe(III), and Co(III). Experimental Determination of Oxidation Levels of Ligands and Metal Ions. *Inorg. Chem.* **2001,** *40*, 4157-4166.

56. Rolle, C. J.; Soper, J. D., unpublished results.

57. Bill, E.; Bothe, E.; Chaudhuri, P.; Chlopek, K.; Herebian, D.; Kokatam, S.; Ray, K.; Weyhermueller, T.; Neese, F.; Wieghardt, K., Molecular and electronic structure of four- and five-coordinate cobalt complexes containing two o-phenylenediamine- or two o-aminophenol-type ligands at various oxidation levels: An experimental, density functional, and correlated ab initio study. *Chem. Eur. J.* **2005,** *11*, 204-224.

58. Poddel'sky, A. I.; Cherkasov, V. K.; Fukin, G. K.; Bubnov, M. P.; Abakumova, L. G.; Abakumov, G. A., New four- and five-coordinated complexes of cobalt with sterically hindered o-iminobenzoquinone ligands: synthesis and structure. *Inorg. Chim. Acta* **2004,** *357*, 3632-3640.

59. Abakumov, G. A.; Cherkasov, V. K.; Bubnov, M. P.; Abakumova, L. G.; Ikorskii, V. N.; Romanenko, G. V.; Poddel'sky, A. I., Synthesis and structures of five-coordinate bis-o-iminobenzosemiquinone complexes M(ISQ-R)2X (X = Cl, Br, I, or SCN; M = CoIII, FeIII, or MnIII). *Russ. Chem. Bull.* **2006,** *55*, 44-52.

60. Cahiez, G.; Duplais, C.; Buendia, J., Manganese-Catalyzed Oxidative Cross-Coupling of Grignard Reagents with Oxygen as an Oxidant. *Angew. Chem., Int. Ed.* **2009,** *48*, 6731-6734, S6731/1-S6731/66.

61. Lippert, C. A.; Hardcastle, K. I.; Soper, J. D., Harnessing redox-active ligands for low-barrier radical addition at oxorhenium complexes. *Inorg. Chem.* **2011**, ASAP.

62. Blackmore, K. J.; Sly, M. B.; Haneline, M. R.; Ziller, J. W.; Heyduk, A. F., Group IV Imino-Semiquinone Complexes Obtained by Oxidative Addition of Halogens. *Inorg. Chem.* **2008,** *47*, 10522-10532.

Synthesis and reactivity of low-coordinate cobalt complexes containing only one redox-active ligand

5.1. Introduction

The previous studies of the bis-amidophenolate cobalt systems detailed in Chapters 2, 3, and 4 illustrated the ability of redox-active ligands to supply electrons in reactions at the cobalt metal center. These cobalt complexes contain two aminophenol-derived ligands that coordinate to the metal through a total of two-nitrogens and two-oxygens. The ligands stabilize the accessible cobalt center in square planar or square pyramidal coordination; the latter when the oxidized complex is bound to a coordinating halide, alkyl chain or solvent molecule.[1-4] The oxygen-nitrogen coordination in this arrangement also allows favorable molecular orbital overlap for the complex to react at the cobalt center with electrons from the ligands.[1] We are interested in further exploring this cooperative metal-ligand relationship and its use for reaction chemistry. Specifically, we are curious whether we can allow the metal and ligand to work in concert by installing only one redox-active ligand on the metal center. To accomplish this goal, we look to combine the correct metal, redox-active ligand, and appropriate stabilizing ligand to maintain molecular orbital overlap and allow electron delocalization using electrons from both metal and the redox-active ligand together.

Building on the success of the bis-amidophenolate system, we believed the catechol-derived, oxygen coordinating ligand 3,5-di-tert-butylcatecholate [cat^{2-}] (Figure 5.1.a) and the amidophenol-derived, nitrogen-oxygen coordination ligand 2,4-di-tert-butyl-6-(phenylamino)phenolate [ap^{2-}] (Figure 5.1.b and 5.1.c) would be suitable for

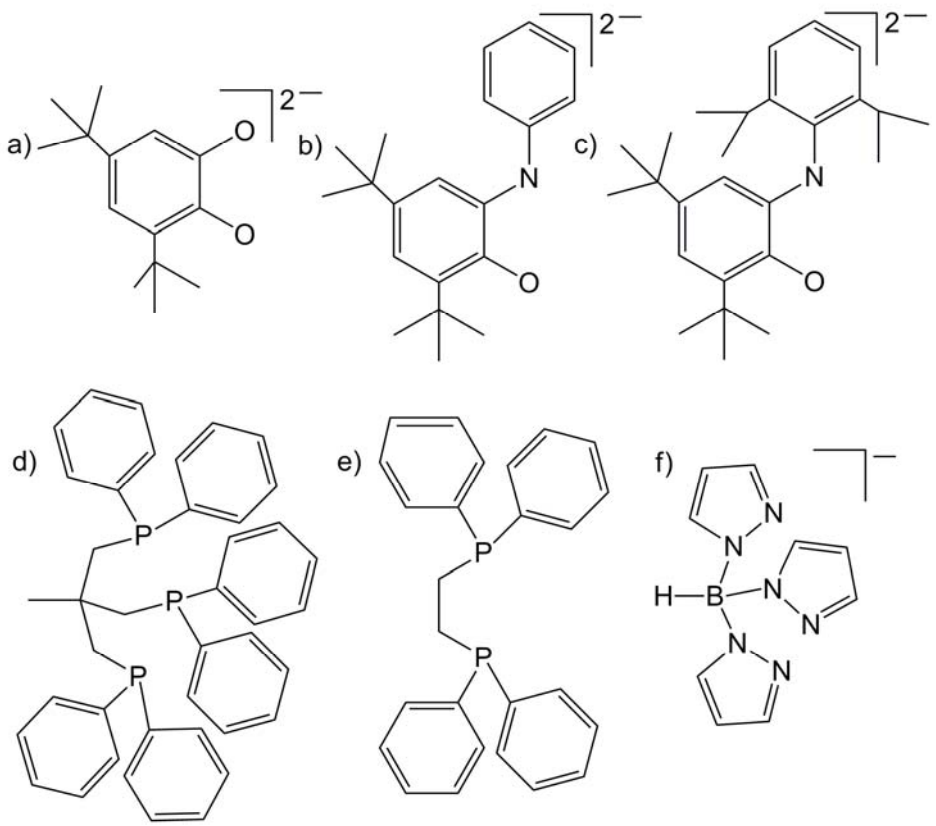

Figure 5.1. Ligands to be used. **a)** 3,5-di-tertbutylcatecholate $[(cat)^{2-}]$
b) 2,4-ditertbutyl-6-(phenylamino)phenate $[(ap^{Ph})^{2-}]$
c) 2,4-ditertbutyl-6-(2,6-diisopropylphenylimino)phenolate $[(ap^{iPr})^{2-}]$
d) 1,1,1-tris(diphenylphosphinomethyl)ethane (triphos)
e) 1,2-bis(diphenylphosphino)ethane (dppe) and **f)** trispyrazolylborate (Tp).

facilitating reactions at low-coordinate cobalt(II) and cobalt(III) centers. These redox-active ligands were chosen based on literature precedent and our group's experience using the catechol-derived ligand substituted with two tert-butyl groups in the 3 and 5 positions of the ring rather than an unsubstituted or perhalogenated versions.[5-7] The steric bulk provided by the tert-butyl groups adds stability to the low coordinate complex without hindering access to the metal center. The amidophenolate ligand without substitution on the N-phenyl $[ap^{Ph}]^{2-}$ and iminobenzoquinone with *ortho* isopropyl

substituents on the N-phenyl ring [ibq^{iPr}]$^{1-}$ can be isolated in different oxidation states. This allows different routes to metallation as cobalt salts of various oxidation states can be used as reagents (see Figure 2.2). The isopropyl subsititutions also add steric bulk in the vicinity of the metal center allowing us to modulate the steric encumbrance at the cobalt center. This approach has proven valuable for altering reactivity at the $Co(L)_2$ complexes (see Chapter 4).

Phosphine ligands were chosen as redox-inert supporting ligands because they are known to stabilize low-coordinate cobalt complexes.[8-11] Previous literature reports a cobalt complex containing a single catechol ligand that was stabilized by a tridentate phosphine ligand.[12,13] This complex used the ligand 1,1,1-tris(diphenylphosphinomethyl)ethane (triphos) (Figure 5.1.d) to maintain a single open coordination site on the 5-coordinate metal center. This complex is reported by the authors to be cationic with a formal oxidation assignment as [(triphos)Co^{III}(cat)]$^+$. However the structure data is of poor quality. The assignment of the electronic state of the complex has been questioned in various papers since the original publication.[14] The original authors also report observation of a purple, one electron reduced material.[12] They assume this to be the neutral species and report it to be unstable and not isolable, converting back to the cationic, blue material within minutes.

Cyclic voltrammetric data reported for the [(triphos)Co^{III}(cat)]$^+$ species indicates that the complex has two redox events in potential ranges suggesting it must be useful for the desired redox reactions.[12,13] The stabilizing tridentate phosphine ligand in combination with the bidentate redox-active catechol-derived ligand leaves only one open coordination site. However, triphos has been reported in other complexes to allow

reactivity through loss of cooridination of one of the phosphorous atoms of the triphos ligand.[15]

Another previous report had described a cobalt complex containing catechol-derived ligands stabilized by the bidentate bis(diphenylphospyanyl)ethane (dppe) seen in Figure 5.1.e.[16] The complex reported was a six-coordinate complex containing two catechol-derived ligands. In an elegant EPR study, the authors find strong localization of the organic radicals within the complex.[17] This bidentate ligand in combination with one bidentate redox-active ligand would produce a complex more comparable to the four-coordinate cobalt bis-amidophenolate complexes.

Besides phosphines, we speculate that chelating nitrogen-donor ligands may be suitable for stabilizing redox-active Co(L) fragments. In particular, monoanionic trispyrazolylborate (Tp) ligands (Figure 5.1.f), known as scorpionates, is known to stabilize reactive first row transition metals[18] and more particularly cobalt[19,20] in low-coordinate environments. Complexes using catechol-derived ligands have been reported and characterized as stable cobalt(II)-semiquinonate complexes.[21]

In this chapter, we detail a complementary study to the bis-amidophenolate complexes presented in the previous chapters with the synthesis of cobalt species each containing only one redox-active ligand. The complexes are stabilized in low-coordinate environments with bidentate or tridentate redox-innocent ligands. We subsequently use the (triphos)Co^{II}(cat) complex to demonstrate proof-of-principle, multi-electron reactivity at the cobalt center that uses the cooperation of the metal and ligand to each provide a single electron for the new bond formation to occur.

5.2. Experimental

5.2.1. General considerations

Unless otherwise specified, all manipulations were performed under anaerobic conditions using standard vacuum line techniques or in an inert atmosphere glove box under purified nitrogen. NMR spectra were acquired on a Varian Mercury 300 spectrometer (300.323 MHz for ^{1}H) at ambient temperature. Chemical shifts are reported in parts per million (ppm) relative to TMS, with the residual solvent peak serving as an internal reference. UV–visible absorption spectra were acquired using a Varian Cary 50 spectrophotometer equipped with a water-jacketed cell holder fitted to a Peltier temperature controller. Unless otherwise specified, all electronic absorption spectra were recorded at 25°C in 1 cm quartz cells. All mass spectra were recorded in the Georgia Institute of Technology Bioanalytical Mass Spectrometry Facility. Fast-atom bombardment mass spectrometry (FAB-MS) was performed using a VG Instruments 70-SE spectrometer. Electrospray ionization mass spectrometry (ESI–MS) was carried out with acetonitrile or tetrahydrofuran solutions using a Micromass Quattro LC spectrometer. Elemental analyses were performed by Atlantic Microlab, Inc., Norcross, GA. All analyses were performed in duplicate, and the reported compositions are the average of the two runs.

5.2.2. Materials and methods

Anhydrous acetonitrile (CH_3CN), tetrahydrofuran (THF), toluene, pentane, dichloromethane (CH_2Cl_2) solvents for air- and moisture-sensitive manipulations were purchased from Sigma-Aldrich, further dried by passage through columns of activated

alumina, degassed by at least three freeze-pump-thaw cycles, and stored under N_2 prior to use. Deuterated acetonitrile (CD_3CN) and tetrahydrofuran (THF–d_8) were purchased from Cambridge Isotope Laboratories, degassed by three freeze-pump-thaw cycles, vacuum distilled from CaH_2 or $Na_{(s)}$, respectively, and stored under a dry N_2 atmosphere prior to use. All chemicals were purchased from Sigma-Aldrich and used as received.

5.2.3. Direct synthesis of (triphos)Co^{II}(cat)

A 5 dram scintillation vial was charged with a solution of $Co_2(CO)_8$ (0.085 g, 0.248 mmol) dissolved in 7 mL of THF. A solution of 1,1,1-tris(diphenylphosphinomethyl)ethane (triphos) (0.312 g, 0.499 mmol) in THF was added dropwise while stirring. The solution was stirred for 15 min. A solution of 3,5-di-tert-butylquinone (0.146 g, .496 mmol) in THF was then added to the solution drop-wise forming a purple solution. The solution was stirred for 2 hours at room temperature and transferred to a round bottom flask. The THF was removed *in vacuo* and purple powder was collected (0.477 g, 0.487 mmol, 98.2% yield). Crystalline solids suitable for single crystal X-ray diffraction were grown from a THF solution layered with pentane and allowed to sit at room temperature for days. UV-vis (CH_3CN) nm (ε, M-1 cm-1): 512(1847); 635(sh); 810(489). ESI-MS (m/z): 903.2 $[M]^+$. Samples for elemental analysis were collected from a THF solution. Anal. Calcd for $C_{55}H_{59}CoO_2P_3$: C, 73.08; H, 6.58. Found C, 72.19; H, 7.21.

5.2.4. Synthesis of [(triphos)Co^{II}(sq)][BF$_4$]

The complex was prepared by the following new method and verified by previously reported characterization.[12] In this new method, a 5 dram scintillation vial was charged with a solution of purple (triphos)Co(cat) (0.097 g, 0.099 mmol) in CH_3CN. 1 equivalent of $AgBF_4$ (0.021 g, 0.109 mmol) was added. The solution was allowed to stir 12 hours, during which time a bright blue solution was afforded. The solution was then transferred to a round bottom flask and the CH_3CN was removed *in vacuo*. A blue powder was collected (0.076 g, .0.0713 mmol, 72.1% yield). Crystals suitable for analysis by X-ray diffraction were grown with slow diffusion of ether into THF at room temperature over days. UV-vis (CH_3CN) nm (ε, M-1 cm-1): 360(sh); 640(1860); 780 (4560).

5.2.5. Reaction of (triphos)Co^{II}(cat) with electrophilic Cl source

A 5 dram scintillation vial was charged with a purple solution of (triphos)Co(cat) (0.095 g, 0.105 mmol) in CH_3CN. A solution of 5 equivalents of 2,3,4,5,6,6-hexachloro-2,4-cyclohexadien-1-one (0.158 g, 0.525 mmol) in CH_3CN was added. A color change to bright green was observed within seconds and the solution was allowed to stir 30 minutes. The solution was then transferred to a round bottom and the CH_3CN was removed *in vacuo* and green powder was recovered.

5.2.6. Attempted synthesis of *(triphos)Co(ap^{Ar})*

A 5 dram scintillation vial was charged with a solution of $Co_2(CO)_8$ dissolved in THF. A solution of triphos in THF was added dropwise while stirring. The solution was

stirred for 15 min. A solution of 2,4-ditertbutyl-6-(2,6-diisopropylphenylimino)benzoquinone (ibq^{iPr}) in THF was then added to the solution drop-wise. After 24 hours, a purple solution formed. UV-vis (CH3CN) λ_{max}: 540 and 845 nm and FAB-MS (m/z): 649 $[M]^+$. The same procedure using sub-stoichiometric amount (0.75 equivalents) of ibq^{iPr} yielded the same material.

A 5 dram scintillation vial was charged with solutions of either $Co(ClO_4)_2 \bullet 6H_2O$ or $CoCl_2$ dissolved in THF and a solution of triphos in THF was added, an immediate precipitate formed. The solids were also produced in CH_3CN, toluene or MeOH. Subsequent reaction of the THF slurry with 2,4-ditertbutyl-6-(phenylamino)phenol (H_2ap^{Ph}) in the presence of Et_3N using either $AgBF_4$ or air as an oxidant resulted in formation of a blue-green material. The precipitate formed during the first step of the reaction was not incorporated into the solution. The mass spectrometry of the blue-green material was found to contain no significant peaks indicative of complexes containing the triphos ligand.

5.2.7. Attempted synthesis of *(dppe)Co(cat)*

A 5 dram scintillation vial was charged with a solution of $Co_2(CO)_8$ dissolved in THF. A solution of 1,2-bis(diphenylphosphino)ethane (dppe) in THF was added drop-wise while stirring. The solution was stirred for 15 min. A solution of 3,5-di-tert-butylquinone (DTBQ) in THF was then added to the solution drop-wise. After 20 minutes, an air stable purple solution formed. FAB-MS (m/z) 897.3 $[M]^+$.

Solutions of either $Co(ClO_4)_2 \bullet 6H_2O$ or $CoCl_2$ combined with a solution of dppe in a 5 dram scintillation vial formed an immediate precipitate similar to the observed with

the triphos material. Using $Co(ClO_4)_2 \bullet 6H_2O$, dppe, and 3,5-ditertbutylcatechol (DTBC) in the presence of Et_3N and air resulted in formation of a blue-green material. FAB-MS (m/z): 677 $[M]^+$ (major) and 897 $[M]^+$ (minor). Subsequent reactions showed varying amounts of the 897 m/z peak impurity which increased with longer time of mixing. No synthetic attempts were successful at eliminating the impurity or of synthesizing the desired (dppe)Co(cat) in moderate or high yield.

5.2.8. Attempted synthesis of *(dppe)Co(ap^{Ar})*

A 5 dram scintillation vial was charged with a solution of $dppeCoCl_2$ in THF and ibq^{iPr} in THF was added drop-wise forming a blue material. The material was identified as an undesired product by UV-vis and MS and isolation and further characterization was not pursued. UV-vis (THF) λ_{max}: 660 and 850 nm. ESI-MS (m/z): 649 $[M]^+$.

5.2.9. Synthesis and reactivity of (Tp)Co(ap^{Ar})

A 5 dram scintillation vial was charged with a solution of $CoCl_2$ and potassium trispyrazolylborate (KTp) in THF with air. This solution was mixed in air for 30 minutes. Then a THF solution of H_2ap^{Ph} and Et_3N were added with stirring. A navy blue precipitate formed upon mixing. The blue material was recovered by vacuum filtration and stored under N_2. UV-vis (THF) λ_{max}: 660 and 845 nm. ESI-MS (m/z): 607.1 and 679.0 $[M]^+$.

The cyclic voltammogram (CV) of the material was recorded in THF under nitrogen at room temperature. When stored in solution or exposed to air over hours, the blue (Tp)Co(ap^{Ph}) develops into a green material. Reaction of the isolated blue material with pentamethyl cobaltacene (Cp^*_2Co) in THF resulted in this same green material.

Single crystals of the green material were grown from a concentrated THF solution over days at -20^{o}C.

5.2.10. X-ray Crystallography

Single crystals of (triphos)Co(cat) and [(triphos)Co(cat)][BF_4] suitable for X-ray diffraction analysis were coated with Paratone N, suspended in a small fiber loop and placed in a cooled nitrogen gas stream and 173 K on a Bruker D8 APEX II CCD sealed tube diffractometer. Data were measured using a series of combinations of phi and omega scans with 10 s frame exposures and 0.5 degree frame widths. Data collection, indexing and initial cell refinements were all carried out using APEX II software.[22] Frame integration and final cell refinements were done using SAINT software.[23] The final cell parameters were determined from least-squares refinement on 7524 reflections for (triphos)Co(cat) and 11241 reflections for [(triphos)Co(cat)][BF_4]. The structures were solved using direct methods and difference Fourier techniques using the SHELXTL program package.[24] Hydrogen atoms were placed in their expected chemical positions using the HFIX command and were included in the final cycles of least squares with isotropic U_{ij}'s related to the atoms ridden upon. All non-hydrogen atoms were refined anisopropically. Details of data collection and structure refinement are provided in Table 5.1.

Table 5.1. Crystallographic data and structure parameters for (triphos)Co(cat) and [(triphos)Co(sq)][BF_4]•THF.

Complex	**(triphos)Co(cat)**	**[(triphos)Co(sq)][BF_4]•THF**
Empirical formula	$C_{57.15}H_{59}CoO_2P_3$	$C_{59}H_{67}BCoF_4O_3P_3$
Formula weight	929.68	1062.78
T (K)	173 (2)	173 (2)
Crystal system	orthorhombic	monoclinic
Space group	P2(1)2(1)2	P2(1)/n
Unit Cell dimensions		
a (Å)	12.9101 (6)	12.058 (4)
b (Å)	32.1153 (17)	13.990 (5)
c (Å)	11.9947 (6)	32.770 (11)
α (^{o})	90	90
β (^{o})	90	93.881 (6)
γ (^{o})	90	90
V (Å^3)	4973.1 (4)	5513 (3)
Z	4	4
D_{calc} (g/cm^3)	1.242	1.280
Absorption coefficient (mm^{-1})	3.927	0.455
Crystal Size (mm)	0.40x0.13x0.11	0.24x0.22x0.03
θ range for data collection (^{o})	2.72 to 62.46	1.76 to 30.48
Index ranges	-14≤h≤14	-6≤h≤17
	-36≤k≤32	-9≤k≤17
	-12≤l≤13	-34≤l≤45
Reflections collected	27358	17300
Reflections unique	7524	11241
Goodness of fit on F^2	1.002	0.906
R [I>2σ(I)]	0.0339	0.0885
wR^2 (all data)	0.897	0.1593

5.3. Results

5.3.1. Preparation and characterization of (triphos)Co(cat)

A stoichiometric reaction of $Co_2(CO)_8$, triphos, and quinone (triphos = 1,1,1-tris(diphenylphosphinomethyl)ethane; quinone = 3,5-di-tert-butylquinone) in THF, in a rigorously air-free environment, quickly forms a purple solution. In contrast to a previous report,[12] the purple material is stable over months in solution and can be isolated and stored in solid state indefinitely. A single crystal of the purple solids suitable for analysis

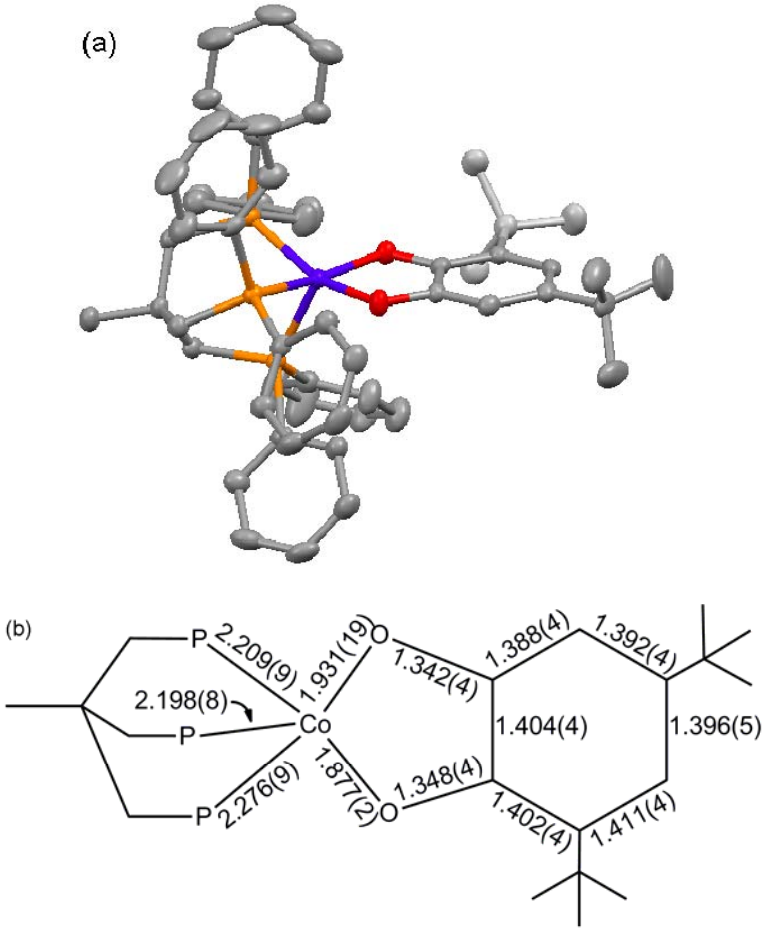

Figure 5.2. (a) X-ray crystal structure of (triphos)Co^{II}(cat) drawn with 50% probability ellipsoids. Hydrogen atoms omitted for clarity. **(b)** Schematic of selected bond lengths (Å) in (triphos)Co^{II}(cat).

by X-ray diffraction was obtained by slow diffusion of pentane into THF solutions (Figure 5.2.b). The structure (Figure 5.2.a) contains 5-coordinate cobalt bound to a tridentate triphos ligand and a bidentate, redox-active catecholate ligand. None of the three phosphorous atoms lie in a plane with the catecholate ligand. The C-O bond lengths (Figure 5.2.b) of the catecholate ligand are elongated with an average length of 1.345 Å, consistent with C-O single bonds. The C-C bond distances show all are identical within 3σ with an average length of 1.399 Å, indicating an aromatic pattern. The sum of this data suggests the ligand is a fully reduced catecholate ligand. This leads to the best assignment of the oxidation states within the complex as (triphos)Co^{II}(cat) (cat = 3,5-di-tert-butylcatecholate).

5.3.2. Alternate synthetic procedure and characterization of [(triphos)Co^{II}(sq)][BF_4]

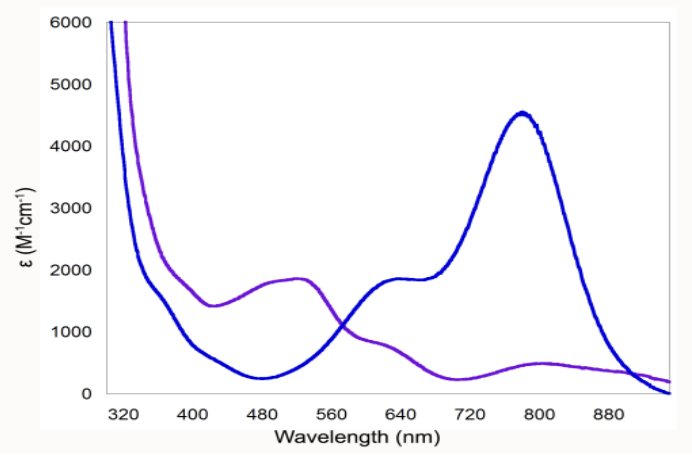

Figure 5.3. UV-vis absorption spectra for (triphos)Co^{II}(cat) (purple line) and [(triphos)Co^{II}(sq)][BF_4] (blue line) in CH_3CN at 25°C under N_2.

Synthesis of [(triphos)Co^{II}(sq)]$^+$ has been previously reported from direct synthesis.[12] However, a cleaner route to the oxidized complex came from the addition of 1 equivalent of $AgBF_4$ to the neutral (triphos)Co^{II}(cat) that afforded a color change from purple to blue with a UV-vis spectrum that matches exactly that previously reported for [(triphos)Co^{II}(sq)]$^+$ (Figure 5.3). This blue material was isolated and characterized and crystals suitable for analysis by X-ray diffraction were isolated from THF and ether

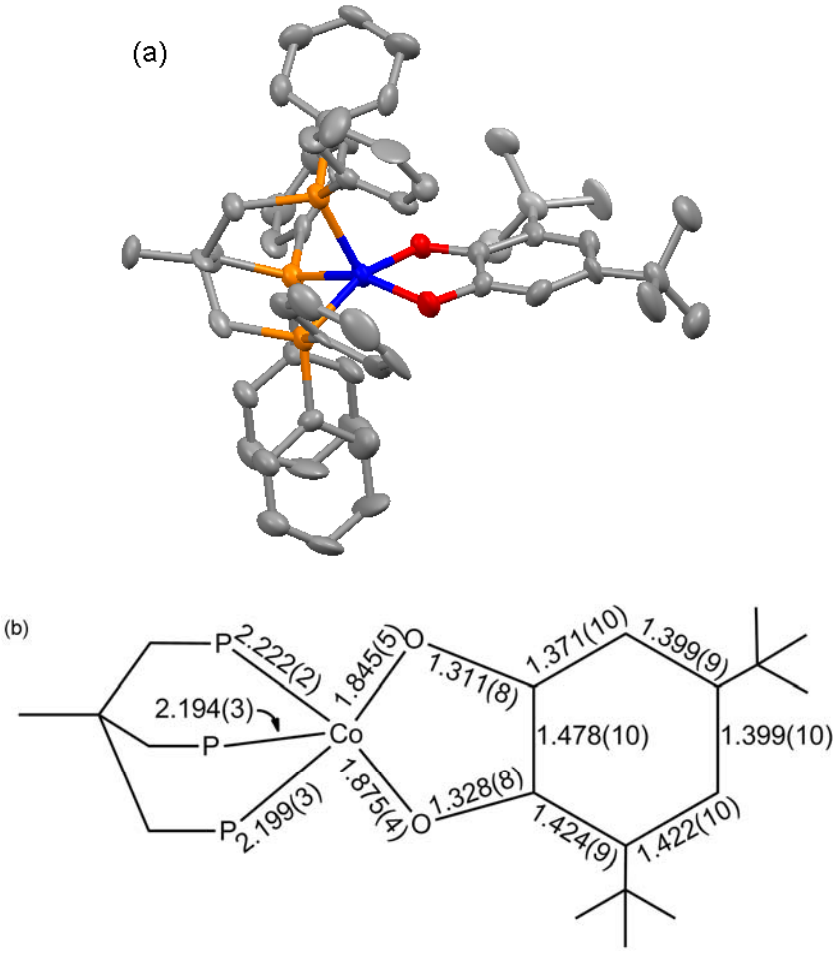

Figure 5.4. (a) X-ray crystal structure of [(triphos)Co^{II}(sq)](BF_4)•THF drawn with 50% probability ellipsoids. Hydrogen atoms, solvent and counter ion omitted for clarity. **(b)** Schematic of selected bond lengths (Å) in [(triphos)Co^{II}(sq)][BF_4]•THF.

(Figure 5.4.a). The average C-O bond lengths shorten in comparison to the neural (triphos)Co^{II}(cat) with an average length of 1.320 Å (Figure 5.4.b). The C-C bond lengths do not show the expected four long and two short pattern.[25] There is one abnormally long 1.478 Å C-C bond. However, based on the contraction of the C-O bond lengths, the complex is most appropriately assigned as [(triphos)Co^{II}(sq)]$^+$ (sq = 3,5-di-tert-butylsemiquinoate.

5.3.3. Co-Cl bond forming reactivity at (triphos)Co^{II}(cat)

Addition of 5 equivalents of yellow 2,3,4,5,6,6-hexachloro-2,4-cyclohexadien-1-one, a source of an electrophilic Cl^+ fragment, to the purple (triphos)Co^{II}(cat) in CH_3CN quickly affords a color change from purple to bright green (Figure 5.5). The green solution has a UV-vis spectrum that does not match that of [(triphos)Co^{II}(sq)]$^+$, the product of outer-sphere, one-electron oxidation. The green product is also stable in solid state if it is pre-dried *in vacuo* under nitrogen. However, all attempts to obtain crystalline

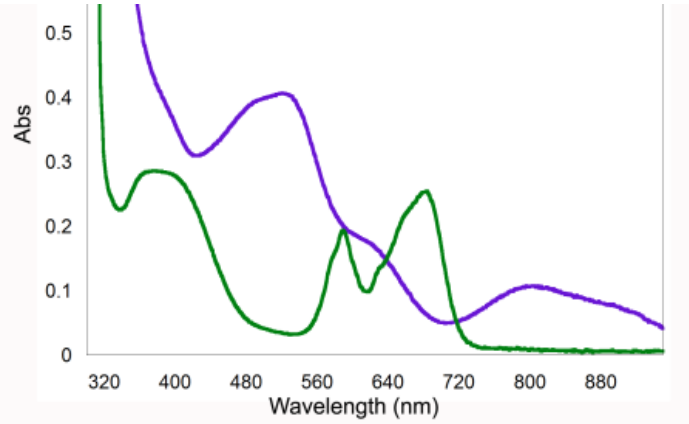

Figure 5.5. UV-vis absorption spectra following the reaction of 2.2x10^{-4} M (triphos)Co^{II}(cat) (purple line) with 5 equivalents of 2,3,4,5,6,6-hexachloro-2,4-cyclohexadien-1-one (Cl^+) in CH_3CN at 25°C under N_2 to form green material (green line) proposed to be [(triphos)Co^{III}(Cl)(sq)]$^+$.

material of suitable quality for single crystal X-ray analysis were unsuccessful. The green material has no ^{1}H NMR signal. ESI-MS of the green solution in positive mode shows a molecular peak at 938.2 m/z (Figure 5.6.a) and an isotopic envelope which matches that expected for addition of [Cl] (Figure 5.6.b). Assuming two electrons cannot be removed from the ligand, and with the previously established knowledge that the first electron is removed from the ligand, the complex is tentatively assigned as $[(triphos)Co^{III}(Cl)(sq)]^{+}$.

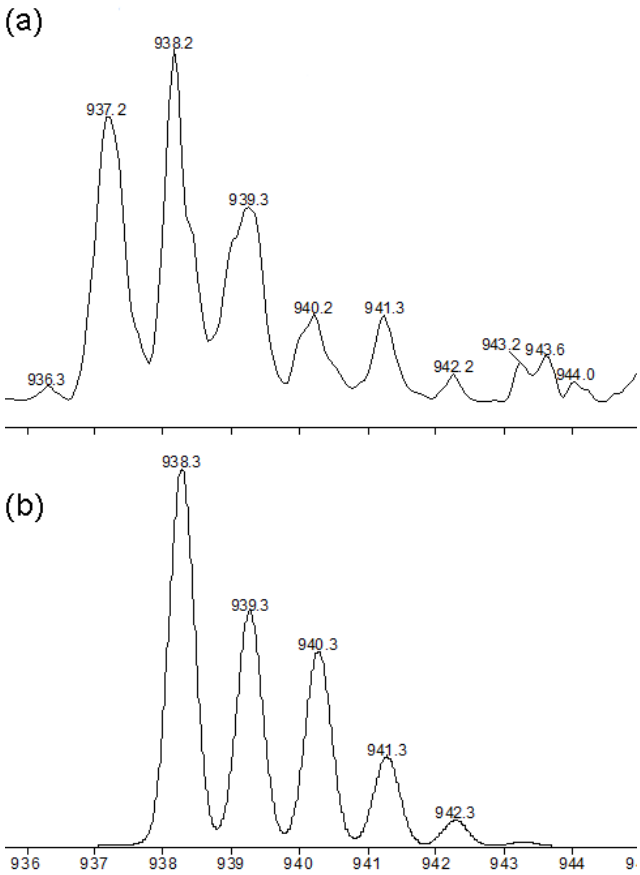

Figure 5.6. (a) Electro-spray mass spectrometery (ESI-MS) of the green product containing a peak at 938 m/z. **(b)** Calculated mass spectrum for $[(triphos)Co^{III}(Cl)(sq)]^{+}$.

5.3.4. Attempted synthesis of (triphos)Co(ap^{Ar})

Attempts to prepare the (triphos)Co(ap^{Ar}) complex analogous to the (triphos)Co(cat) species, were pursued with the same procedure used to synthesize the catecholate species. However, in contrast to the reaction with quinone (q), addition of the iminiqunione (ibq) to a solution of $Co_2(CO)_8$ under nitrogen took days to yield a color change to purple. The resulting purple material was identified as $[Co(ap^{iPr})_2]^-$ by comparison of the UV-vis and FAB-MS spectra to spectra of independently prepapred material.

To try to avoid displacing the triphos ligand installed during the first step of the synthetic route, reactions of amdophenolate (ap^{2-}) with either $Co(ClO_4)_2$ or $CoCl_2$ were examined. However, with the cobalt(II) salt, the triphos does not coordinate to the metal upon addition in THF, CH_3CN or MeOH. Thus, when the amidophenol was added, in the presence of Et_3N base, the $[Co(ap^{Ph})_2]^-$ is again readily formed, as evidenced by UV-vis and ESI-MS.

5.3.5. Attempted synthesis of (dppe)Co(cat) and (dppe)Co(ap^{Ar})

Attempts to prepare the similar complex containing the 1,2-bis(diphenylphosphino)ethane (dppe) ligand were pursued using a procedure similar to the successful synthesis of (triphos)Co^{II}(cat). This resulted in formation of a purple material that changed to green with mixing over hours. However, the green material was found to be air-stable and FAB-MS of the material contained a significant peak indicative of formation of the coordinatively saturated (dppe)Co(cat)$_2$. Repeat attempts to characterized the purple material or isolate the desired (dppe)Co(cat) resulted in

solutions contained varying amounts of (dppe)Co(cat)$_2$. The complex (dppe)Co(cat) was never found in high yield.

Reaction of Co(ClO$_4$)$_2$•6H$_2$O, 3,5-di-tert-butylcatechol, Et$_3$N and air, resulted in formation of a blue solution that persisted for minutes before progressing on to a green color. A sample of this blue material was frozen and immediately analyzed by FAB-MS. It was found that the sample contained a peak corresponding to the desired (dppe)Co(cat). However, after several attempts to reproduce the procedure, the material was unable to be isolated in the blue form again, consistently progressing on to the green which was shown by mass spectrometery to be the undesired (dppe)Co(cat)$_2$.

Synthesis with the aminophenol-derived ligands produced similarly poor results, most often producing the Co(L)$_2$ species without the dppe ligand. Pre-synthesized (dppe)Co(Cl)$_2$, available from Sigma-Aldrich, was purchased in hopes of stabilizing the dppe and cobalt and allowing easy coordination of the redox-active ligand. However, reaction with the isopropyl-subsitituted iminoquinone in air with THF or MeOH at room temperature resulted in the synthesis of Co(Cl)(isq^{iPr})$_2$, as identified by UV-vis and mass spectrometry.

5.3.6. Synthesis and characterization of (Tp)Co(ap^{Ar})

The potassium salt of the unsubstitued trispyrazolylborate (Tp) ligand was mixed with CoCl$_2$ in air. A solution of H$_2$ap^{Ph} and Et$_3$N was added with stirring immediately resulting in a navy blue precipitate. This blue precipitate has a UV-vis spectrum very similar to that of the Co(Cl)(isq)$_2$ species. However, ESI-MS reveals molecular peaks at 607 and 679 m/z, indicative of both (Tp)Co(ap^{Ph}) and a THF adduct. Similar species that

contain a bound chloride do not show evidence of the chloride by ESI-MS analysis[26] and it therefore cannot be concluded if the blue material is 5-coordinate or 6-coordinate with a chloride ligand. The blue material has a weak but unique paramagnetic ^{1}H NMR spectrum. However, the material is air sensitive over hours degrading to a brown-orange material.

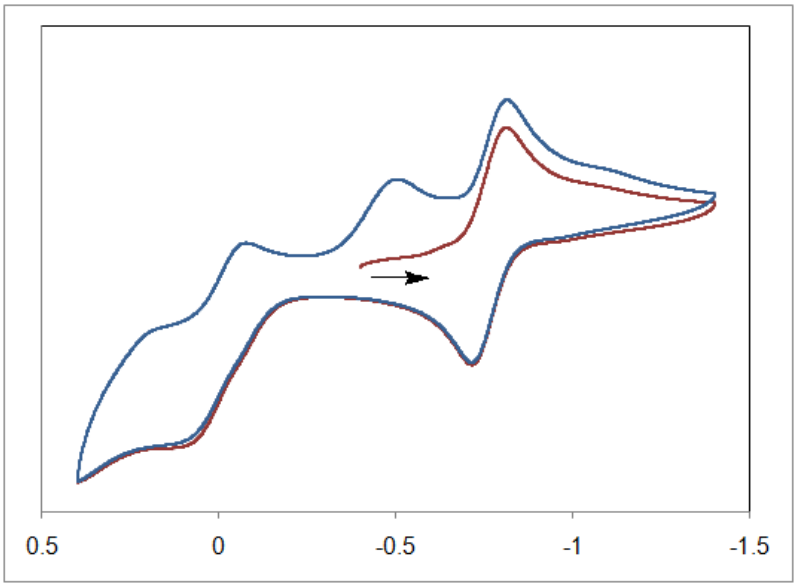

Figure 5.7. Cyclic voltammogram of blue TpCo(ap^{Ph}) material in THF containing 0.1M [$^{n}Bu_4N$][PF_6] at a 10 mm Pt electrode. Scan rate: 0.1 volts seconds^{-1}. Temperature: 25^{o}C.

The cyclic votamogram of the material in THF shows redox features at 0.0, -0.5 and -0.8 volts seen in Figure 5.7. The feature at -0.5 V is only observed with reducing current and is not observed on the first reducing sweep from the open potential. This most likely indicates that the peak is attributable to a labile ligand the oxidized form of the material gains throughout the scanning process. Reduction with Cp*$_2$Co in CH_3CN, with a potential of -1.91 V,[27] results in material which reacts and has similar UV-vis and

^{1}H NMR spectra to that of the $[Co(ap)_2]^-$ material. However, the same reduction performed in THF results in a unique green material. Single crystals of this green material were isolated from a concentrated THF solution and were shown to be $(Tp)_2Co$ (Figure 5.8.). All attempts to use the blue (Tp)Co(ap) material for reactivity with

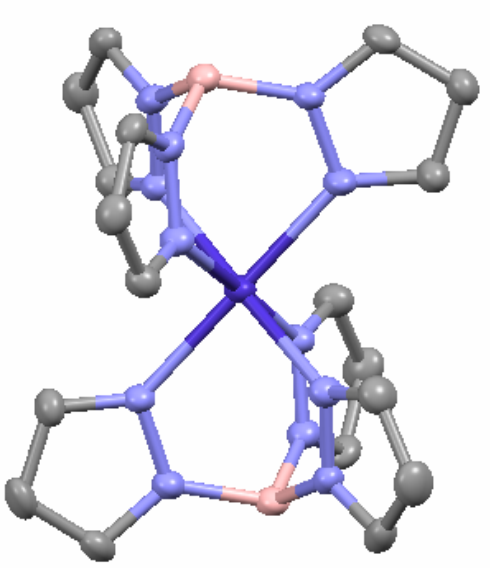

Figure 5.8. X-ray crystal structure of $(Tp)_2Co$ drawn with 50% probability ellipsoids. Hydrogen atoms omitted for clarity.

electrophilic Cl sources or with alkyl halides resulted in formation of the green $(Tp)_2Co$ material as well.

5.4. Discussion

5.4.1. Characterization of triphos-cobalt species

Based on the sum of the data, we believe assignment of the blue material as $[(triphos)Co^{II}(sq)]^+$ is a more accurate description of the electronic structure. This

disagrees with previous literature which assigned the structure as cobalt(III) with a fully reduced ligand.[12] The previously reported crystal structure was of poor quality[12] and the validity of the characterization based on it is unclear. Our X-ray crystallographic data also indicates that this assignment is better as the C-O bonds show significant double-bond character and shortening as compared to the neutral material and indicates that the oxidation occurs at the ligand. Reported Raman spectroscopic studies also seem to indicate the better oxidation state assignment is $[(triphos)Co^{II}(sq)]^{+}$.[14] Bianchini, *et al.* supported their assignment based on agreement with their magnetic data indicating the complex was diamagnetic and molecular orbital analysis.[12] However, it is now known that similar complexes show extensive anti-ferromagnetic coupling between π-based radicals in the ligand and the unpaired d-electrons of the metal.[2,28] For this reason, the diamagnetism displayed by the cationic complex cannot be taken alone as evidence that there is no organic radical localized within the complex.

It was previously reported in literature that a purple material assumed to be $(triphos)Co^{II}(cat)$ could be observed and characterized *in situ* but was unstable in solution within minutes.[12] We have now demonstrated that with careful exclusion of air and moisture the material is stable over months. The X-ray crystal structures of the neutral and cationic triphos-catecholate have nearly identical coordination but the bond lengths of the catecholate are noticeably altered. The significant difference in the bond lengths of the catechol-derived ligand between the blue cationic and purple neutral forms indicate that the oxidation of $(triphos)Co^{II}(cat)$ occurs at the ligand and not at the metal and that both species contain a cobalt(II) center. This would leave the second oxidation observed by electrochemistry to transform the cobalt(II) to cobalt(III). The oxidation

potential for these transformations occurs at -0.645 V and 0.575 V vs SCE.[12,13] In comparison to $[Co^{III}(ap^{Ph})_2]^-$, the first oxidation is very similar to -0.770 V while the second oxidation is at much more oxidizing potentials than the -0.350 V of the previously studied system (Chapter 2).

5.4.2. Multi-electron reactivity with reduced (triphos)Co^{II}(cat)

The reaction of (triphos)Co^{II}(cat) with sources of electrophilic Cl^+ in large excess affords a green material. This material has a unique UV-vis spectrum which is not observed as a product of outer-sphere oxidations of the complex. ESI-MS indicates a chloride is present. The green material is not produced when the halide is not in excess but rather the complex is simply oxidized to $[(triphos)Co^{II}(sq)]^+$ as indicated by UV-vis. This need for a large excess is likely needed due to the high potential of the second oxidation required for bond formation. There is the alternative explanation that the reaction required excess to overcome the steric hinderance to the binding of the chloride. However, the product appears stable either in solution or powder once formed so it is unlikely that this instability is a result of sterics. It is also unlikely that the cobalt exists in this product in the +4 oxidation state. From this, we therefore tentatively formulate this material as $[(triphos)Co^{III}(Cl)(sq)]^+$. Given this assignment, the two electron bond-forming reaction is facilitated by the combination of the metal and the catecholate ligand, both providing one electron for the new bond.

Reactions with more interesting electrophiles such as alkyl halides proved unsuccessful with the (triphos)Co^{II}(cat) complex. With very strong reagents, outer sphere oxidation is observed followed by degradation of the complex. The green

(triphos)Co^{III}(Cl)(sq) species could not be characterized to indicate if one or more of the coordinating phosphine arms of the triphos ligand can dissociate to allow coordination. The steric congestion of the complex and the lack of two open coordination sites likely impedes possible reactivity.

5.4.3. Instability of other complexes with a tridentate phosphine ligand

Preparation of analogs of (triphos)Co^{II}(cat) containing the amidophenol-derived ligand was attempted using the same procedure. This required use of an iminobenzoquinone ligand. It has been previously detailed in literature that the amidophenol-derived ligands without substituents in the *ortho* positions of the N-phenyl ring undergo a spontaneous, intermolecular ring closing reaction when oxidized prior to coordination to metal.[29] The 2,6-diisopropyl version was therefore chosen, as it can be isolated in the iminoquinone form, to be used in the initial synthetic attempts of the (triphos)Co(ap^{iPr}). However, the reaction appeared to take days to form isolable complex after addition of the iminobenzoquinione ligand. This resulting material was found to be $[Co^{III}(ap^{iPr})_2]^-$, even when substoichiometric amounts of the redox active ligand were added. It seems reasonable that the steric bulk of both the triphos ligand as well as the amidophenol-derived ligand with large isopropyl substituents is too sterically encumbered to bind both the $[ap^{iPr}]^{2-}$ and triphos ligands. A thermodynamic drive exists preferring to add two redox active ligands to form the 4-coordinate $[Co^{III}(ap)_2]^-$ instead of the desired 5-coordinate (triphos)Co(ap).

Attempts to use the amidophenol version of the ligand were all unsuccessful. The amidophenolate ligand did not coordinate to the metal to the pre-formed “Co(triphos)”

fragment formed from Co(0), even with the use of various oxidants or under various conditions. Reaction between cobalt(II) salts, in various solvents with the triphos resulted in precipitation of material and did not form the desired "$[Co(triphos)]^{2+}$" fragment. The steric bulk, even when unsubstituted, of the amidophenol-derived ligand in combination with the tridentate phosphine ligand containing six phenyl groups in the vicinity of the metal is prohibitive. While choosing a tridentate stabilizing ligand may be favorable to allow only one of the bidentate redox ligands to coordinate, the resulting 5-coordinate complex contains only one open coordination site which is not ideal for facilitating successful coupling reactions. Both of these factors greatly disfavor the idea that this complex will show interesting reactivity or be useful for non-radical reaction chemistry as desired. This route was eventually abandoned.

5.4.4. Instability of other complexes with a bidentate phosphine ligand

In an attempt to avoid the steric congestion and 5-coordinate complex formed with the use of the triphos ligand, the bidentate 1,2-bis(diphenylphosphino)ethane (dppe) ligand was used. We hoped to stabilize a 4-coordinate complex containing only one catechol-derived or amidophenol-derived ligand. Initial attempts using the dppe ligand with the 3,5-di-tert-butyl-quinone and Co(0) starting materials, appeared to form the coordinatively saturated $(dppe)Co(cat)_2$. This indicated that either the lack of steric bulk or the mixed coordination by the phosphine and oxygen donor atoms did not lead to the desired low-coordinate complex. Synthesis from the cobalt(II) salts initially showed promise of formation of the desired (dppe)Co(cat) when the desired complex was observed by mass spectrometery. This was only in small yield however and repeated

attempts to synthesized and isolate the material showed that this complex was not thermodynamically stable and progressed on, under a multitude of conditions, to an undesired complex quickly.

Attemped complex formation with the dppe ligand, the amidophenol-derived ligand and cobalt also yield similar, undesired results. Reaction with cobalt(II) and dppe continued to be a problematic step in the synthetic procedure. We were able to purchase dppe$CoCl_2$ as a starting material. However, a multitude of conditions and solvents all resulted in displacement of the dppe ligand and formed the previously reported $Co(Cl)(isq)_2$.

In both systems containing phosphine based stabilizing ligands, two amidophenol-derived ligands coordinate in preference over the triphos or dppe. It appears that the (dppe)Co(cat) is accessible, similar to the (triphos)Co(cat) but is un-stabilized. This seems to point to a thermodynamic instability in the complexes. One possible cause of this is the lack of steric bulk surrounding the metal to stabilize the low-coordinate environment. However, another strong possibility is that the electronic arrangement needed for the desired four-coordinate sphere may be inaccessible with the mixed phosphine, oxygen, and nitrogen donor environment. The previously described cobalt bis-iminosemiquinoate, four-coordinate complexes (Chapter 2) are believed to be stabilized not by steric encapsulation but by a favorable molecular orbital overlap allowing the square planar environment at the cobalt metal. It is possible that the phosphine atoms of the redox-innocent ligand are disrupting this electronic stability for the low-coordinate species.

5.4.5. Unstable complex with stabilizing tridentate nitrogen ligand

With the belief that the phosphine stabilizing ligands did not provide the correct electronic configuration to maintain the low-coordinate cobalt environment desired, we turned to the nitrogen donor trispyrazoleborate (Tp) ligands. It was hoped that the monoanionic ligand would also help with coordination difficulties and precipitation previously experienced with the neutral phosphine ligands.

We pursued the synthesis of a Tp complex containing an amidopenol-derived ligand in which the Tp ligand was in its fully unsubstituted form. The blue product isolated from reaction in air and identified by mass spectrometry as (Tp)Co(ap) has quasi-reversible redox features in a range that appeared useful for our reactivity study. However, the combined data from mass spectrometry and electrochemistry possibly suggest coordination of a labile chloride or THF ligand in the open coordination site. From our characterization methods, it was not possible to definitively determine if one of these was bound to the metal.

Unfortunately, we found that when left in solution over hours or with attempts to chemically reduce the complex, the material rearranged forming the $(Tp)_2Co$ complex as characterized by single crystal X-ray analysis. This spontaneous rearrangement indicates that the $(Tp)_2Co$ is thermodynamically more stable than the desired (Tp)Co(ap) containing an open coordination site. Most manipulations with the material resulted in loss of the amidophenol-derived ligand. This loss of the redox-active ligand when the material is either oxidized by air or reduced in solution is evidence of a tendency to form the more stable six-coordinate complex and suggests the material is unlikely to facilitate useful reactivity and remain intact.

5.5. Conclusion

Here, we report a series of coordinatively unsaturated cobalt species that contain only one redox-active ligand. This molecular design was pursued because we expected that it would force the cooperation between the metal and ligand in and requires each to provide a single electron for two electron reactivity with electrophiles. We have shown that oxidation of (triphos)Co^{II}(cat) gives [(triphos)Co^{II}(sq)]$^+$ and both are best assigned as cobalt(II) species. Thus the oxidation of the neutral species occurs at the redox-active ligand. We have also established that the (triphos)Co^{II}(cat) complex reacts with a source of a Cl^+ electrophile in a net two electron reaction to form a new material we tentatively assign as (triphos)Co^{III}(Cl)(sq). However, due to the steric bulk of the triphos ligand, the coordination sphere around the metal is too congested for further reactivity. While reactivity with other, more interesting electrophiles is not observed, we have established evidence for the fundamental feasibility of our strategy to incorporate only one redox-active ligand to work in concert with the cobalt metal to evoke multi-electron reactivity.

In an effort to synthesize other low coordinate complexes containing one redox-active ligand on cobalt, attempts were made at the synthesis of (triphos)Co^{II}(ap), (dppe)Co^{II}(cat), and (dppe)Co^{II}(ap). All of these proved unsuccessful. Synthesis with the tridentate nitrogen ligand Tp to form (Tp)Co(ap) resulted in formation of a new species tentatively believed to be (Tp)Co(ap). However, this complex was found to be unstable in solution and when subjected to oxidants or reductants as it consistently rearranged to form the thermodynamically more stable $(Tp)_2$Co. This study highlights the difficulty in stabilizing cobalt in low coordinate environments and allowing the metal center to be accessible for reactivity.

5.6. References

1. Smith, A. L.; Hardcastle, K. I.; Soper, J. D., Redox-Active Ligand-Mediated Oxidative Addition and Reductive Elimination at Square Planar Cobalt(III): Multielectron Reactions for Cross-Coupling. *J. Am. Chem. Soc.* **2010,** *132*, 14358-14360.

2. Smith, A. L.; Clapp, L. A.; Hardcastle, K. I.; Soper, J. D., Redox-active ligand-mediated Co-Cl bond-forming reactions at reducing square planar cobalt(III) centers. *Polyhedron* **2010,** *29*, 164-169.

3. Bill, E.; Bothe, E.; Chaudhuri, P.; Chlopek, K.; Herebian, D.; Kokatam, S.; Ray, K.; Weyhermueller, T.; Neese, F.; Wieghardt, K., Molecular and electronic structure of four- and five-coordinate cobalt complexes containing two o-phenylenediamine- or two o-aminophenol-type ligands at various oxidation levels: An experimental, density functional, and correlated ab initio study. *Chem. Eur. J.* **2005,** *11*, 204-224.

4. Poddel'sky, A. I.; Cherkasov, V. K.; Abakumov, G. A., Transition metal complexes with bulky 4,6-di-tert-butyl-N-aryl(alkyl)-o-iminobenzoquinonato ligands: Structure, EPR and magnetism. *Coord. Chem. Rev.* **2009,** *253*, 291-324.

5. Rolle, C. J.; Hardcastle, K. I.; Soper, J. D., Reactions of tetrabromocatecholatomanganese(III) complexes with dioxygen. *Inorg. Chem.* **2008,** *47*, 1892-1894.

6. Lippert, C. A.; Arnstein, S. A.; Sherrill, C. D.; Soper, J. D., Redox-Active Ligands Facilitate Bimetallic O2 Homolysis at Five-Coordinate Oxorhenium(V) Centers. *J. Am. Chem. Soc.* **2010,** *132*, 3879-3892.

7. Lippert, C. A.; Soper, J. D., Deoxygenation of Nitroxyl Radicals by Oxorhenium(V) Complexes with Redox-Active Ligands. *Inorg. Chem.* **2010,** *49*, 3682-3684.

8. Kueckmann, T. I.; Dornhaus, F.; Bolte, M.; Lerner, H.-W.; Holthausen, M. C.; Wagner, M., Broadening the scope of ancillary phosphane-type ligands: a systematic comparison of PR3, PR2BH3-, and SiR3- and their chalcogen derivatives. *Eur. J. Inorg. Chem.* **2007**, 1989-2003.

9. Rupp, R.; Huttner, G.; Kircher, P.; Soltek, R.; Buchner, M., Coordination compounds of tripodCoII and tripodCoI - selective substitution and redox behavior. *Eur. J. Inorg. Chem.* **2000**, 1745-1757.

10. Heinze, K.; Huttner, G.; Zsolnai, L.; Schober, P., Complexes of Cobalt(II) Chloride with the Tripodal Trisphosphane triphos: Solution Dynamics, Spin-Crossover, Reactivity, and Redox Activity. *Inorg. Chem.* **1997,** *36*, 5457-5469.

11. Enamullah, M.; Hasegawa, M.; Fukuda, Y.; Linert, W.; Hoshi, T., Synthesis, characterization and spin-crossover behaviors of [Co(hydroxycarboxylato)(triphos)] complexes. *Bull. Chem. Soc. Jpn.* **2002,** *75*, 2449-2453.

12. Bianchini, C.; Masi, D.; Mealli, C.; Meli, A.; Martini, G.; Laschi, F.; Zanello, P., Comprehensive experimental and interpretational study of the complex formation and transformations involving o-quinoid molecules and an L3M-type metal fragment (M = cobalt). *Inorg. Chem.* **1987,** *26*, 3683-3693.

13. Barbaro, P.; Bianchini, C.; Linn, K.; Mealli, C.; Meli, A.; Vizza, F.; Laschi, F.; Zanello, P., Dioxygen uptake and transfer by cobalt(III), rhodium(III) and iridium(III) catecholate complexes. *Inorg. Chim. Acta* **1992,** *198-200*, 31-56.

14. Hartl, F.; Barbaro, P.; Bell, I. M.; Clark, R. J. H.; Snoeck, T. L.; Vlcek, A., Jr., Valence localization in [M(triphos)(3,5-di-tert-butyl-catecholate)]+ ions (M = Co, Rh or Ir) probed by resonance Raman spectroscopy. *Inorg. Chim. Acta* **1996,** *252*, 157-166.

15. Heinze, K.; Huttner, G.; Zsolnai, L., Cobalt-catalyzed selective oxidation of the tritertiary phosphine triphos with molecular oxygen. *Chem. Ber.* **1997,** *130*, 1393-1403.

16. Kozhanov, K. A.; Bubnov, M. P.; Cherkasov, V. K.; Fukin, G. K.; Abakumov, G. A., EPR study of intramolecular dynamics in o-semiquinonic nickel complexes with PCP-pincer ligand in solution. *J. Chem. Soc., Dalton Trans.* **2004**, 2957-2962.

17. Bubnov, M. P.; Teplova, I. A.; Cherkasov, V. K.; Abakumov, G. A., EPR sstudy of o-semiquinone-catocholate cobalt complexes with bis(diphenylphsphanyl)ethane. *Eur. J. Inorg. Chem.* **2003**, 2519-2523.

18. Martin, C.; Munoz-Molina, J. M.; Locati, A.; Alvarez, E.; Maseras, F.; Belderrain, T. R.; Perez, P. J., Copper(I)-Olefin Complexes: The Effect of the Trispyrazolylborate Ancillary Ligand in Structure and Reactivity. *Organometallics* **2010,** *29*, 3481-3489.

19. Shay, D. T.; Yap, G. P. A.; Zakharov, L. N.; Rheingold, A. L.; Theopold, K. H., Intramolecular C-H activation by an open-shell cobalt(III) imido complex. *Angew. Chem., Int. Ed.* **2005,** *44*, 1508-1510.

20. Shiro, H., Akita, M. Moro-oka, Y., New aspects of the cobalt-dioygen complex chemistry opened by hydrotris(pyrazoly)borate ligands (TpR): unique properties of TpRCo-dioxygen complexes. *Coord. Chem. Rev.* **2000,** *198*, 61-87.

21. Ruf, M.; Noll, B. C.; Groner, M. D.; Yee, G. T.; Pierpont, C. G., Pocket Semiquinonate Complexes of Cobalt(II), Copper(II), and Zinc(II) Prepared with the Hydrotris(cumenylmethylpyrazolyl)borate Ligand. *Inorg. Chem.* **1997,** *36*, 4860-4865.

22. apex II, Analytical X-ray Systems, Brukers AXS, Inc., Madison, WI, 2005.

23. saint Version 6.45A, Analytical X-ray Systems, Brukers AXS, Inc., Madison, WI, 2003.

24. shelxtl Version 6.12, Analytical X-ray Systems, Bruker AXS, Inc., Madison, WI, 2002.

25. Chun, H.; Verani, C. N.; Chaudhuri, P.; Bothe, E.; Bill, E.; Weyhermueller, T.; Wieghardt, K., Molecular and Electronic Structure of Octahedral o-Aminophenolato and o-Iminobenzosemiquinonato Complexes of V(V), Cr(III), Fe(III), and Co(III). Experimental Determination of Oxidation Levels of Ligands and Metal Ions. *Inorg. Chem.* **2001,** *40*, 4157-4166.

26. Poddel'sky, A. I.; Cherkasov, V. K.; Fukin, G. K.; Bubnov, M. P.; Abakumova, L. G.; Abakumov, G. A., New four- and five-coordinated complexes of cobalt with sterically hindered o-iminobenzoquinone ligands: synthesis and structure. *Inorg. Chim. Acta* **2004,** *357*, 3632-3640.

27. Connelly, N. G.; Geiger, W. E., Chemical Redox Agents for Organometallic Chemistry. *Chem. Rev.* **1996,** *96*, 877-910.

28. Pierpont, C. G.; Lange, C. W., The chemistry of transition metal complexes containing catechol and semiquinone ligands. *Prog. Inorg. Chem.* **1994,** *41*, 331-442.

29. Abakumov, G. A.; Druzhkov, N. O.; Kurskii, Y. A.; Shavyrin, A. S., NMR study of products of thermal transformation of substituted N-aryl-o-quinoneimines. *Russ. Chem. Bull.* **2003,** *52*, 712-717.

Future directions and conclusions

6.1. Conclusions

In this study, we looked to install multi-electron redox capacity at a cobalt complex using redox-active ligands. These ligands are able to exist in various oxidation states themselves and are therefore able to support and participate in redox events. We have prepared an electronic series in three oxidation states: monoanionic $[Co^{III}(ap)_2]^-$, neutral $Co^{III}(isq)(ap)$, and cationic $[Co^{III}(CH_3CN)(isq)_2]^+$ species. Contrary to previous reports in literature, steric bulk from the ligands surrounding the metal center is not required to stabilize the cobalt center in the square planar coordination environment. Characterization of the ligands of all three of these complexes through X-ray crystal analysis show that the metal center remains cobalt(III) through the redox changes. This indicates that two electron oxidation from the monanion to the cation occurs with both electrons being extracted formally from the ligand set. Both of these electrons are accessible at modest potentials indicating that these complexes may be prone to multi-electron redox changes as desired.

In a proof-of-concept study, we demonstrated that $Co^{III}(isq)(ap)$ reacts with halide radicals to form a new cobalt-halide bond in a single electron reaction. On the contrary, $[Co^{III}(ap)_2]^-$ appears to be prone to multi-electron reactivity in reactions with "Cl^+" and not chloride radical sources. Characterization of the $Co^{III}(Cl)(isq)_2$ product indicates that the product remains cobalt(III) and therefore the electrons used to form the new bond are formally delivered from the ligand set. Mechanistic studies of the net two electron reaction with $[Co^{III}(ap)_2]^-$ show no evidence of the reaction proceeding through

sequential radical steps but instead suggest a single, two electron step is responsible for the bond-formation. This atypical multi-electron capacity at cobalt(III) is a result of the electronic overlap of the cobalt and the redox-active amidophenol-derived ligands allowing the ligands to participate in bond formation.

Given the nucleophilicity of the $[Co^{III}(ap)_2]^-$ and its noted proclivity for multi-electron reactivity, we pursued reaction with more interesting reagents. The first step in palladium catalyzed Kumada or Negishi cross-coupling reactions involves the activation of an organic halide. The classic catalysts for these systems are often limited in that oxidative addition of alkyl halides is generally slow and results in products susceptible to unwanted β-hydride elimination.[1,2] Alkyl halides are, therefore, generally believed to be difficult reagents to use to form new carbon-carbon bonds. However, $[Co^{III}(ap)_2]^-$ reacts with alkyl halides to pseudo-oxidatively add the alkyl at the cobalt center and forms a stable product. This reaction proceeds with primary and secondary alkyl halides and regardless of the leaving group. The reaction is even successful at activating carbon-chloride bonds unlike many similar catalytic systems. The product of the reaction can be isolated and was found to be best assigned as $Co^{III}(alkyl)(isq)_2$. This assignment indicates that the reaction occurs, again, with the new bond formed with two electrons formally derived from the ligand set and with no change in the oxidation state of the metal center. Mechanistic investigations of the pseudo-oxidative addition suggest the reaction is S_N2-like. This supports the previous observations that $[Co^{III}(ap)_2]^-$ is able to facilitate preferred concerted, multi-electron reactions with the aid of the redox-active ligands.

A study of stepwise Negishi-type cross-coupling was completed using the isolated $Co^{III}(alkyl)(isq)_2$ in a reaction with organozinc reagents. The cross-coupling reaction is successful with use of both sp^2- and sp^3- hybridized organozinc reagents. The yield is increased with excess organizinc reagent but the yields are still too low to make the reaction useful (maximum yields of approximately 20%). Similarly, the two electron oxidized complex $[Co^{III}(CH_3CN)(isq)_2]^+$ reacts with organozinc reagents to couple two carbanions and form a new carbon-carbon bond. This oxidative coupling reaction is successful with both sp^2-sp^2 and sp^3-sp^3 carbon-carbon bond formation but gives similar yields to the cross-coupling reaction. The use of air as an oxidant allows some amount of catalytic turnover but only two to three turns. When followed substoichiometrically and under nitrogen, the oxidative homocoupling reaction can be observed to form the five-coordinate organometallic complex isolated from the reaction of $[Co^{III}(ap)_2]^-$ with alkyl halides. This indicates that after the first alkyl or aryl is installed on the $[Co^{III}(CH_3CN)(isq)_2]^+$ through a simple acid-base reaction, the homocoupling and cross-coupling reactions proceed by the same pathway.

The yield of both coupling reactions is decreased by increased steric bulk of the organic fragments or around the metal center created by substituents on the ligand. Examination of all the organic fragments in a cross-coupling reaction indicates that there is no exchange between the first alkyl fragment added to the cobalt complex and the carbanion. Comparison of the homocoupling reaction with varying steric bulk around the metal indicates that the added steric congestion does not disfavor the addition of the first alkyl fragment. However, the addition of the second alkyl fragment is almost completely inhibited with the increase bulk around the metal center. This result more importantly

implies that the coupling of the two carbon fragments is entirely inner-sphere requiring installation of both at the metal center for coupling. The cobalt complexes facilitate these reactions selectively and avoid radical steps and intermediates more typical of cobalt systems in the absence of the redox-active ligands.[3,4]

In a complementary study, use of bidentate or tridentate stabilizing ligands in combination with one redox-active catechol-derived or amidophenol-derived ligand was investigated. By designing the complex with only one redox-active ligand, the metal and ligand are forced to work in concert with one another to facilitate multi-electron reactions. We hoped to learn if a proclivity for two electron reactions could be obtained with this approach as well. In synthesis of (triphos)Co^{II}(cat) and the one electron oxidized $[(triphos)Co^{II}(sq)]^{+}$ we found that the cation had been previously mis-assigned electronically. With the new assignment, it is evident that the oxidation occurs in the ligand and not the metal. Reaction of (triphos)Co^{II}(cat) with a Cl^{+} reagent generated a new material that we describe as (triphos)Co^{III}(Cl)(sq). Given the assumption that this is, in fact, the product formed, this implies that the two electrons used to create the new cobalt-halide bond are derived from both the ligand and the metal, one from each. We believe (triphos)Co^{II}(cat) is unreactive with other electrophiles due to the steric bulk congesting the metal center.

Synthesis with the tridentate phosphine ligand (triphos) and the amidophenol-derived ligands proved unsuccessful. We believe this was attributable to the large steric demands of both ligands. Use of a smaller bidentate phosphine (dppe) failed to stabilize either the catecholate or amiophenolate species into a four-coordinate environment. Coordination with the tridentate trispyrazolborate ligand (Tp) was believed to be

successful with the amidophenolate. However, various routes of reactivity with the complex all lead to degradation of the material and formation of undesired $(Tp)_2Co$.

Throughout the course of both of these studies, steric crowding at the metal center was a problem. These ligands congest the coordination sphere with the bulky N-phenyl slowing or inhibiting bond-forming reactions at the metal center. While the amidophenolate ligands show promise with facilitation of some reactivity, the correct stabilizing ligand to balance the electronic overlap and open environment surrounding the metal has yet to be found. However, we have shown that it is possible to use the redox-active ligands in combination with cobalt to create a proclivity for multi-electron reactions at the metal that is naturally prone to radical reactions.

6.2. Future Directions

The reactivity of the cobalt bis-amidophenolate system previously outlined by this dissertation is limited by a consistent problem with steric crowding at the metal center where all bond-forming reactions take place. This crowding disrupts the oxidative addition of alkyl halides to the fully reduced $[Co^{III}(ap)_2]^-$ and impedes the carbon-carbon coupling reaction of $Co^{III}(R)(isq)_2$ with RZnX. We demonstrate early in this study that the amidophenol-derived ligands do not need steric bulk in the vicinity of cobalt to maintain open coordination sites at the metal center. Within our research group, use of the same amiodophenol-derived ligands in combination with other metals such as manganese and iron show these complexes do not activate alkyl halides similarly to the cobalt complexes. The iron and manganese do demonstrate potential for facilitation of oxidative coupling reactions[5,6] but are still not as efficient as current palladium based systems.

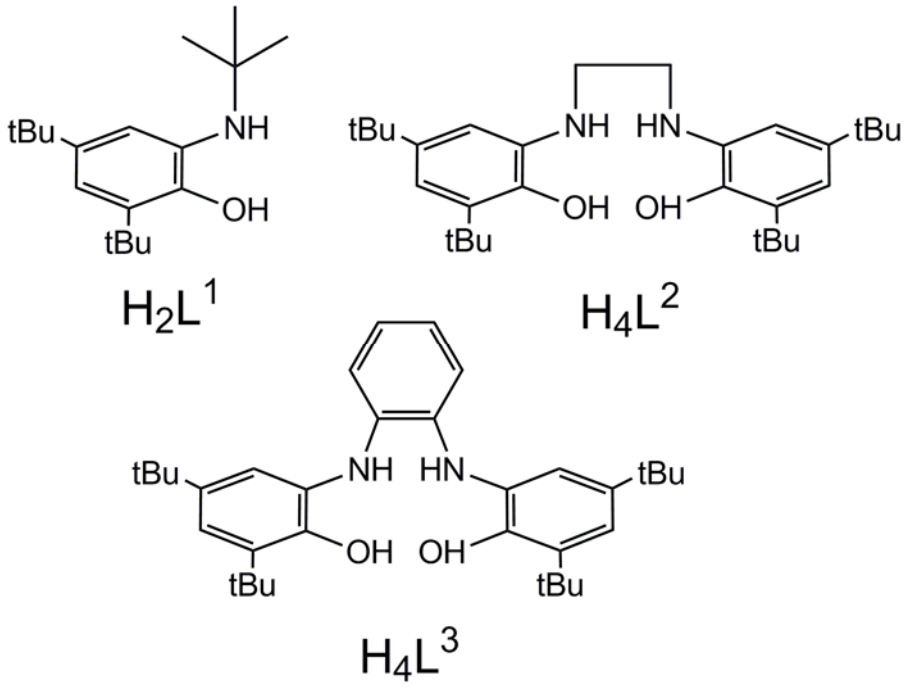

Scheme 6.1.

Other groups have looked at alternative amidophenol-derived ligands which do not contain the bulky N-phenyl substituents which lie orthogonal to the plane of the ligand. A few of them are highlighted in Scheme 6.1.[7,8] Ligand H_2L^1 contains a tertbutyl group on the nitrogen in the place of the phenyl group used in our $Co(ap^{Ar})_2$ system. A crystal structure obtained of $ZrCl_2(L^1)_2$ has a *cis* arrangement of the redox-active ligands using this analog.[7] While this complex demonstrates similar oxidative addition and cross-coupling reactivity, the reaction is still not efficient.[7,9] Some work has been done within our group with tetradentate, amidophenol-derived ligands as well. Attempts to metallate H_4L^2 with iron and cobalt all result in the loss of the ethyl backbone as determined by crystal structure analysis.[10] Coordination of cobalt with H_4L^3 is indicated by mass spectrometry and stability of the material to contain three ligands attached to two

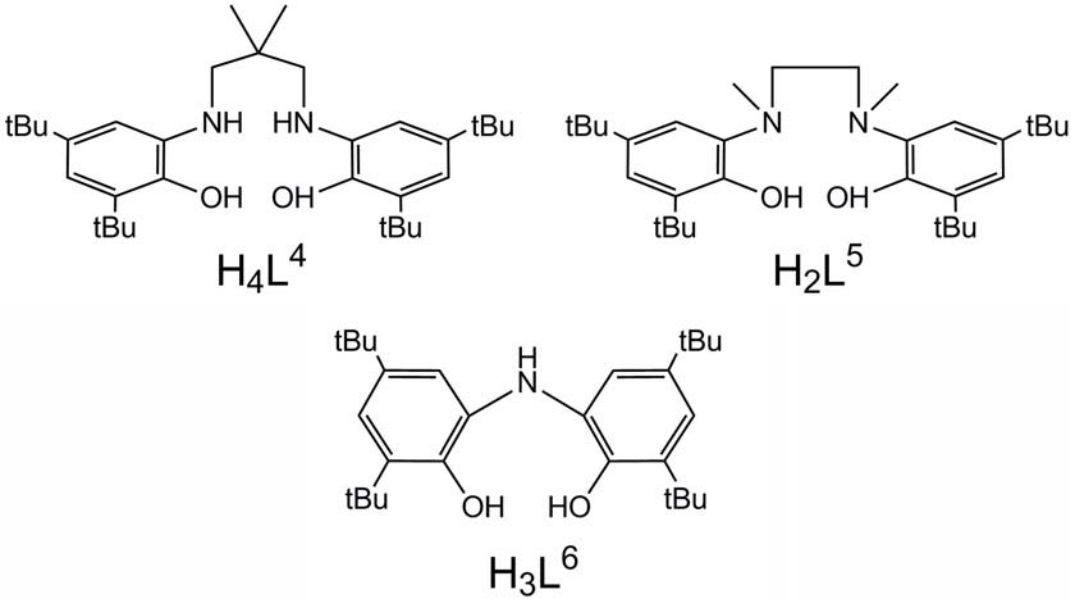

Scheme 6.2.

different metal centers making bimetallic, coordinatively saturated products.[11] This ligand also is potentially too rigid to allow the flexibility required for the tetradentate ligand to twist to allow the two open coordination sites to be *cis* to one another given the planar aryl rings throughout the ligand. These sites must be *cis* to facilitate successful coupling as we have demonstrated that the coupling occurs at the metal center in an innersphere reaction.

These issues may be addressed by other ligand scaffolds, which could simultaneously stabilize the low-coordinate environment, maintain the correct electronic overlap with the metal, and have the flexibility to rotate about the metal as required. For instance, H_4L^4 is a known ligand modification of the ethyl-backbone previously examined (H_4L^2).[12] The backbone of this ligand adds stability while remaining flexible and is significantly less sterically demanding as compared to the ligands containing N-phenyl

groups because they are in the plane of the ligand rather than orthogonal to the plane. This may decrease the steric encumbrance at the metal center. The ligand has already been shown to bind nickel, copper and palladium complexes in various oxidation states.[12] Similarly, H_2L^5 has been shown to coordinate tungsten in an octahedral arrangement and arrange such that two other monodentate ligands can be arranged *cis* to one another.[13] The redox-active nature of this ligand is not clearly established in the literature.[14] However, the ligand should be able to support oxidation state changes and further investigation is warranted.

A slightly different complex design may include use of the tridentate H_3L.[6,15] $Co(L^6)_2$ has been the focus of many years of study concerning the intramolecular valence tautamerism between the metal and ligand.[16,17] The binding of two of the redox active ligands makes the complex coordinatively saturated and unfavorable for facilitating reactivity at the cobalt center. These studies have, however, demonstrated that the molecular overlap is favorable for mixing of the metal and ligand electrons. One of these tridentate ligands has been shown on copper(II) to successfully arrange in combination with weakly coordinating ligands in square planar coordination leaving two open coordination sites.[15] Our goal moving forward would be to stabilize a cobalt complex with only one of these tridentate ligands. The use of a tridentate ligand opens up room around the metal center favoring successful reactivity. The tridentate nature of the ligand also allows open sites to exist *cis* to one another. This design may be more favorable than the square planar complexes for facilitation of coupling reactions as there is no isomerization issue to allow these cis coordination sites to be readily available. This combination has great potential to facilitate successful coupling at the metal center.

6.3. References

1. Diederich, F.; Stang, P. J.; Editors, *Metal-catalyzed Cross-coupling Reactions*. Wiley-VCH: 1998; p 517.

2. Liu, C.; Jin, L.; Lei, A., Transition-metal-catalyzed oxidative cross-coupling reactions. *Synlett* **2010**, 2527-2536.

3. Sherry, B. D.; Fuerstner, A., The Promise and Challenge of Iron-Catalyzed Cross Coupling. *Acc. Chem. Res.* **2008,** *41*, 1500-1511.

4. Gosmini, C.; Begouin, J.-M.; Moncomble, A., Cobalt-catalyzed cross-coupling reactions. *Chem. Comm.* **2008**, 3221-3233.

5. Bayless, M.; Soper, J. D., unpublished results.

6. Rolle, C. J.; Soper, J. D., unpublished results.

7. Blackmore, K. J.; Ziller, J. W.; Heyduk, A. F., "Oxidative Addition" to a Zirconium(IV) Redox-Active Ligand Complex. *Inorg. Chem.* **2005,** *44*, 5559-5561.

8. Carter, S. M.; Sia, A.; Shaw, M. J.; Heyduk, A. F., Isolation and Characterization of a Neutral Imino-semiquinone Radical. *J. Am. Chem. Soc.* **2008,** *130*, 5838-5839.

9. Haneline, M. R.; Heyduk, A. F., C-C Bond-Forming Reductive Elimination from a Zirconium(IV) Redox-Active Ligand Complex. *J. Am. Chem. Soc.* **2006,** *128*, 8410-8411.

10. Clapp, L. A.; Soper, J. D., unpublished results.

11. Smith, A. L.; Soper, J. D., unpublished results.

12. Min, K. S.; Weyhermueller, T.; Bothe, E.; Wieghardt, K., Tetradentate Bis(o-iminobenzosemiquinonate(1-)) π Radical Ligands and Their o-Aminophenolate(1-) Derivatives in Complexes of Nickel(II), Palladium(II), and Copper(II). *Inorg. Chem.* **2004,** *43*, 2922-2931.

13. Wong, Y.-L.; Ma, J.-F.; Law, W.-F.; Yan, Y.; Wong, W.-T.; Zhang, Z.-Y.; Mak, T. C. W.; Ng, D. K. P., Synthesis, electrochemistry, and oxygen-atom transfer reactions of dioxotungsten(VI) and -molybdenum(VI) complexes with N2O2 and N2S2 tetradentate ligands. *Eur. J. Inorg. Chem.* **1999**, 313-321.

14. Whiteoak, C. J.; Martin, d. R. R. T.; White, A. J. P.; Britovsek, G. J. P., Iron(II) Complexes with Tetradentate Bis(aminophenolate) Ligands: Synthesis and Characterization, Solution Behavior, and Reactivity with O2. *Inorg. Chem.* **2010,** *49*, 11106-11117.

15. Chaudhuri, P.; Hess, M.; Mueller, J.; Hildenbrand, K.; Bill, E.; Weyhermueller, T.; Wieghardt, K., Aerobic Oxidation of Primary Alcohols (Including Methanol) by Copper(II)- and Zinc(II)-Phenoxyl Radical Catalysts. *J. Am. Chem. Soc.* **1999,** *121*, 9599-9610.

16. Caneschi, A.; Cornia, A.; Dei, A., Valence Tautomerism in a Cobalt Complex of a Schiff Base Diquinone Ligand. *Inorg. Chem.* **1998,** *37*, 3419-3421.

17. Ruiz-Molina, D.; Veciana, J.; Wurst, K.; Hendrickson, D. N.; Rovira, C., Redox-Tunable Valence Tautomerism in a Cobalt Schiff Base Complex. *Inorg. Chem.* **2000,** *39*, 617-619.

VITA

Aubrey L. Smith

Aubrey L. Smith was born in Lincolnton, North Carolina. She received a B.S. in chemistry with a minor in biology from Wake Forest University in Winston-Salem, North Carolina in 2004. She obtained her Ph.D. in chemistry from Georgia Institute of Technology in 2011.